STATUS REPORTS

to the

RECYCLE

and

SURFACE AND COLLOID SCIENCE

PROJECT ADVISORY COMMITTEE

March 23, 1998

INSTITUTE OF PAPER SCIENCE AND TECHNOLOGY

Atlanta, Georgia

ANNUAL PROGRAM REVIEW

RECYCLE

and

SURFACE AND COLLOID SCIENCE

March 23, 1998

February 16, 1998

TO: MEMBERS OF THE RECYCLED PAPER AND SURFACE AND COLLOID SCIENCE PROJECT ADVISORY COMMITTEES

Attached for your review are the Status Reports for the projects to be discussed at the Recycled Paper and Surface Colloid Science Project Advisory Committee meeting being held at the Institute of Paper Science and Technology. The Program Review is scheduled for Monday, March 23, 1998, from 8:00 a.m. - 12:00 p.m. and the PAC Committee Meeting will meet on Tuesday, March 24, from 8:00 a.m. to 12:00 p.m.

We look forward to seeing you at this time.

Sincerely,

David I. Orloff, Ph.D.
Professor of Engineering & Director
Engineering and Paper Materials Division

DIO/map

Attachments

Institute of Paper Science and Technology, Inc.

500 10th Street, N.W.
Atlanta, GA 30318-5794

Telephone 404-894-5700
FAX# 404-894-IPST (4778)

RECYCLE/SURFACE AND COLLOID SCIENCE
PROJECT ADVISORY COMMITTEE

IPST Liaison: Dr. David Orloff (404) 894-6649; FAX (404) 894-1496
RAC Liaison: Mr. Ben Thorp (404) 652-4618; FAX (404) 584-1466
Alternate: Mr. David South (804) 843-5252; FAX (404) 843-5409

Mr. Scott B. Auger *(2001)
Technical Marketing Manager
EKA Chemicals Inc.
1519 Johnson Ferry Road
Suite 200
Marietta, GA 30062
(770) 578-0858
(770) 973-6474 FAX
sbauger@aol.com

Dr. Giancarlo A. Cavagna *(1997)
Research Associate
Westvaco Corporation
11101 Johns Hopkins Road
Laurel, MD 20723
(301) 497-1347
(301) 497-1309 FAX

Mr. Anil Dewan *(1999)
Director, Mechanical Pulping /Recycle Fiber
Champion International Corporation
West Nyack Road
West Nyack, NY 10994-1738
(914) 578-7240
(914) 578-7175 FAX

Mr. Pierre Gagnon *(1998)
St. Laurent Paperboard Inc.
Research Center
15400 Cherbrooke East
Montreal, CANADA H1A 3S2
(514) 642-9251
(514) 498-8614 FAX

Mr. Danny Haynes *(Alternate)
EKA Chemicals Inc.
1519 Johnson Ferry Road
Suite 200
Marietta, GA 30062

Dr. Gregory J. Hollod *(1996)
Vice President of Health, Safety
and Environmental
Riverwood International Corporation
3350 Cumberland Circle
Suite 1600
Atlanta, GA 30339
(770) 644-3223
(770) 644-2914 FAX

Dr. Kyle J. Bottorff *(1999)
Sr. Research Scientist
Hercules Incorporated
500 Hercules Road
Research Center-Lancaster Pike
Wilmington, DE 19808-1599
(302) 995-3704
(302) 995-4565 FAX
kbottorff@herc.com

Mr. Robert De Jong *(1999)
Fort James Corporation
1915 Marathon Avenue
Post Office Box 899
Neenah, WI 54957-0899
(920) 729-8555
(920) 729-8161 FAX

Ms. Sue Freeland *(1999)
Research Scientist
Weyerhaeuser Company
Fiber Chemistry Team
WTC 2B22
Tacoma, WA 98477
(253) 924-6414
(253) 924-6324 FAX

Mr. David Grimes *(1998) (Vice Chairman)
Senior Research Engineer
Beloit Corporation
Pittsfield Research Center
448 Hubbard Avenue
Pittsfield, MA 01201-3822
(413) 445-3266
(413) 499-3155 FAX

Mr. Herbert Holik *(1999)
Dipl.-Ing.
Voith Sulzer Stoffaufbereitung GmbH & Co. KG
Escher-Wyss-StraBe 25
Ravensburg, D-88212 GERMANY
4 9 751832402
4 9 751833030 FAX

Mr. Howard Jersild *(Alternate)
Wisconsin Tissue Mills
Post Office Box 489
Menasha, WI 54952
(920) 725-3703
(920) 727-8803 FAX

* The dates in ( ) indicate the final year of the appointment.

Revised 02/03/98:at

Recycle/Surface and Colloid Science PAC (cont.)

Mr. Stuart Johns *(2001)
Technical Specialist
The Mead Corporation/Chilpaco Division
Bridge and Eastern
Chillicothe, OH 45601
(614) 772-3062
(614) 772-3035 FAX

Mr. James Lynn Jonakin *(1999)
Director of Technology
MacMillan Bloedel Inc.
Post Office Box 336
Pine Hill, AL 36769-0336
(334) 963-4391
(334) 963-4220 FAX

Mr. Kasy King *(1998)
Manager, Pulp & Paper Technology
Appleton Papers Inc.
Post Office Box 359
Appleton, WI 54912-0359
(920) 991-8878
(920) 991-7243 FAX

Mr. G.R. Mannar *(2001)
Group Leader, Chemical Pulping
and Recycling
Beloit Corporation
Pittsfield Research Center
448 Hubbard Avenue
Pittsfield, MA 01201-3822
(413) 445-3313
(413) 499-3155 FAX

Mr. Kenneth R. McCumsey *(2001)
Product Technology Team Leader
Asten, Inc.
6480 West College Road
Appleton, WI 54913
(920) 734-2607
(920) 734-4229 FAX

Dr. Robert Moran *(1999)
Vice President, Manufacturing Services
Bowater Incorporated
55 East Camperdown Way
Post Office Box 1028
Greenville, SC 29602
(864) 282-9371
(864) 282-9570 FAX

Dr. Charles W. Neal *(2000)
Procter & Gamble Company
6105 Center Hill Avenue
Cincinnati, OH 45224
(513) 634-5126
(513) 634-7669 FAX

Mr. Jason R. Panek *(2001)
Technical Director
Manistique Papers
453 S. Mackinac Avenue
Manistique, MI 49854
(906) 341-2175
(906) 341-5635 FAX

Mr. Thomas D. Parish *(2000)
Research Engineer
Potlatch Corporation
20 North 22nd Street
Cloquet, MN 55720
(218) 879-2382
(218) 879-2375 FAX

Mr. Christopher D. Perry *(1998)
Technical Specialist
Buckman Laboratories International, Inc.
1256 N. McLean Blvd.
Memphis, TN 38108
(901) 272-6473
(901) 274-7991 FAX

Mr. Michael A. Pikulin *(2000)
Group Leader
Union Camp Corporation
R&D Division
Post Office Box 3301
Princeton, NJ 08543-3301
(609) 844-7224
(609) 844-7323 FAX

Mr. Erland C. Porter, Jr. *(1998)
Technical Manager
InterLake Papers, Inc.
433 North Main Street
Kimberly, WI 54136-1490
(920) 788-8330
(920) 788-8330 FAX

* The dates in ( ) indicate the final year of the appointment.

Revised 02/03/98:at

Recycle/Surface and Colloid Science PAC (cont.)

Dr. Paul W. Resler *(1999)
Research Specialist
3M Company
3M Specialty Chemicals Division
367 Grove Street
St. Paul, MN 55144-1000
(612) 778-5975
(612) 778-7691 FAX

Mr. Walter Rew *(1999)
Technical Director
Blandin Paper Company
115 First Street, SW
Grand Rapids, MN 55744-3407
(218) 327-6272
(218) 327-6392 FAX

Dr. Nigel Sanders *(1998) (Chairman)
Project Manager
Specialty Minerals Inc.
Surface and Colloid Science
9 Highland Avenue
Bethlehem, PA 18017
(610) 861-3457
(610) 861-3412 FAX

Dr. Steven J. Severtson *(1998)
Senior Chemist
Nalco Chemical Company
One Nalco Center
Naperville, IL 60563-1198
(630) 305-2029
(630) 305-2982 FAX

Dr. Michael R. St. John *(1999)
Research Associate
Nalco Chemical Company
One Nalco Center
Naperville, IL 60563-1198
(630) 305-2349
(630) 305-2982 FAX

Mr. Thomas K. Toothman *(2001)
Paper Operations Technical Manager
Wisconsin Tissue Mills Inc.
Third & Tayco Streets
Post Office Box 489
Menasha, WI 54952
(920) 725-2431
(920) 727-2940 FAX

Dr. David White *(1998)
Fort James Corporation
1915 Marathon Avenue
Neenah, WI 54957-0899
(920) 729-8466
(920) 729-8023 FAX

Mr. Louis K. Wilhelm *(1999)
Corporate Recycling Manager
P.H. Glatfelter Co.
1655 Bergstrom Road
Neenah, WI 54957-0488
(920) 727-2200
(920) 727-2305 FAX

* The dates in ( ) indicate the final year of the appointment.

Revised 02/03/98:at

RECYCLE & SURFACE AND COLLOID SCIENCE PROJECT ADVISORY COMMITTEE MEETING

March 23, 1998

Institute of Paper Science and Technology
Atlanta, Georgia

PROGRAM REVIEW AGENDA

Seminar Room (Room 114)

8:00 a.m. - 8:15 a.m.	Opening Remarks Antitrust Statement Confidentiality Statement		Nigel Sanders
8:15 a.m. - 8:30 a.m.	Welcome by Vice President of Research		Gary Baum
8:30 a.m. - 8:40 a.m.	Overview of IPST Recycle/Surface Science Research		David Orloff
8:40 a.m. - 9:30 a.m.	Project F00903	Flotation Deinking Fluid Mechanics	Ted Heindel
9:30 a.m. - 10:00 a.m.	Project E010	Engineering and Recovery Exploratory Research	Zunyong Zhu
10:00 a.m. - 10:15 a.m.	Break		
10:15 a.m. - 10:55 a.m.	Project F00904	Fiber Carry Over Reduction in Flotation Deinking	Yulin Deng
10:55 a.m. - 11:40 a.m.	Project F00902	Shear-Induced Agglomeration of Stickies	Sujit Banerjee
11:40 a.m. - 12:00 p.m.	Wet End Chemistry Control Advisor (WECCA)		Bill Scott

RECYCLE & SURFACE AND COLLOID SCIENCE PROJECT ADVISORY COMMITTEE MEETING

March 24, 1998

Institute of Paper Science and Technology
Atlanta, Georgia

COMMITTEE DISCUSSIONS AGENDA

Seminar Room (Room 173)

8:00 a.m.- 8:10 a.m.	Convene - Antitrust Statement - Confidentiality Statement - New Members - Acceptance of Fall, 1997 Agenda - Review of Agenda	Nigel Sanders
8:10 a.m. - 8:30 a.m.	Ph.D. Student's presentation: Fracture of Xerographic Toner on a Swelling Substrate	Joel Panek
8:30 a.m. - 10:00 a.m.	Subcommittee discussion of projects	By committee
10:00 a.m. - 10:15 a.m.	Break	
10:15 a.m.- 11:15 a.m.	Re-Convene and Summary of Reviews (including WECCA Proposal)	Review Leaders
11:15 a.m. - 12:00 p.m.	Other Business Summary of Research Roadmap Brainstorming Meeting Date for Fall Meeting Adjourn	Nigel Sanders

TABLE OF CONTENTS

SHEAR-INDUCED AGGLOMERATION OF STICKIES

STATUS REPORT

FOR

PROJECT F00902

Sujit Banerjee
Tom Merchant

March 23-24, 1998

Institute of Paper Science and Technology
500 10th Street, N.W.
Atlanta, Georgia

DUES-FUNDED PROJECT SUMMARY

Project Title:	Shear-Induced Agglomeration of Stickies
Project Code:	Stickies
Project Number:	F00902
PAC:	Recycle
Division:	Engineering
Project Staff	
Faculty/Senior Staff:	Sujit Banerjee
Staff:	Tom Merchant
FY 98-99 Budget:	$94,000
Allocated as Matching Funds:	
Time Allocation	
Faculty/Senior Staff:	15%
Support:	90%
Supporting Research	
M.S. Students:	Dave Wilhelm, Steve Makris
Ph.D. Students:	Howard Corcoran
External:	

RESEARCH LINE/ROADMAP: Reduce and/or control contaminants in recycled-fiber pulp using breakthrough technologies to allow complete interchange of recycled pulp with virgin pulp of similar fiber make-up at economical cost.

PROJECT OBJECTIVE: Develop methodology to reduce the impact of stickies

SUMMARY OF RESULTS: The rate of agglomeration of stickies in water or whitewater increases with increasing shear and decreasing pH. The mechanism through which additives such as talc, PEI, and DETAC detackify stickies was studied. It was found that although talc increases the rate of agglomeration somewhat, its principal action seems to be through detackifying the agglomerated material. In contrast, the chemical additives appear to act on the colloidal stickies by making the zeta potential of the particles less negative. Talc could have the added benefit of keeping machine surfaces free of stickies. However, mills may be using much more talc than is necessary. In related work, introducing a temperature difference between forward and reverse cleaners should greatly increase separation efficiency.

The principal purpose of the work described here is to develop and apply a method for *reproducibly* agglomerating stickies in an aqueous suspension. The main application of the technique is to screen chemicals and additives used for stickies control for their efficiency and mode of action, and to optimize their dosage. Shear is used to agglomerate stickies. When two stickie particles collide with a force strong enough to overcome their mutual repulsion, agglomeration occurs, the stickies grow to the point where they destabilize, and the water clarifies. If the turbidity of the water is followed over time, the clarification can be quantified. Zeta potential and particle size are also tracked. These values, when considered together with the kinetic data, offer insight into the mechanism of stickies control, some of which can be used to select additives, and optimize dosage.

Experimental

Our apparatus consists of a mixing chamber where temperature and stirrer speed is computer-controlled, and gas or liquid can be automatically introduced. The equipment (New Brunswick Bioflow 3000, illustrated in Figure 1) was originally acquired for fermentation in connection with a biotechnology project. The glass tank has a total volume of 5L, and a working volume of 2.5L. Inserted into the center of the tank is a

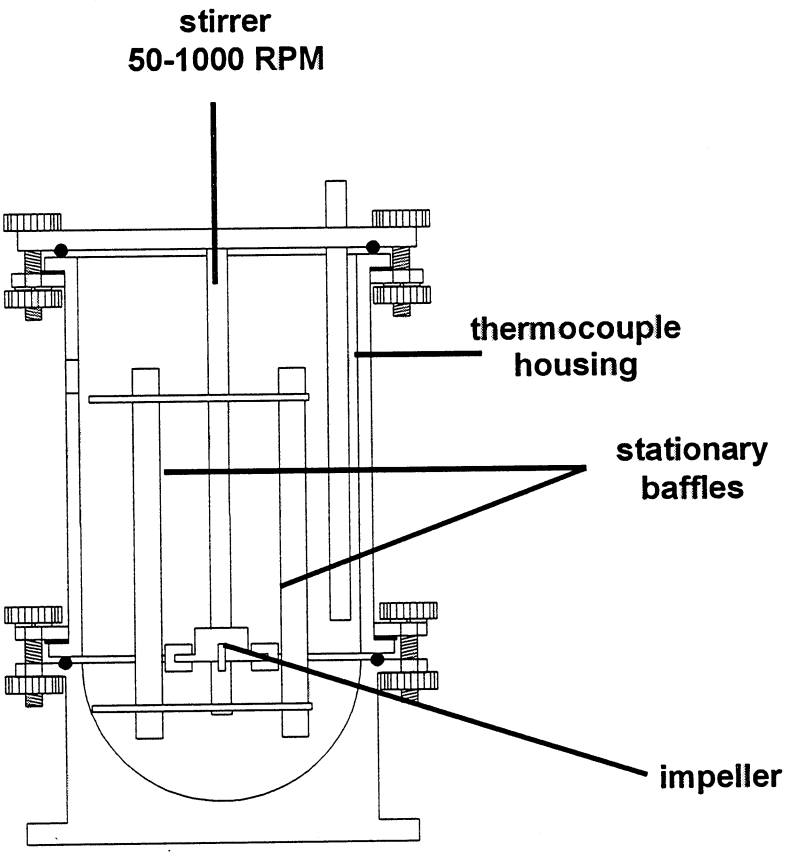

Figure 1: Schematic of the Bioflow 3000 fermenter.

metal shaft stirrer with a radial flow impeller that can be controlled between 50-1000 rpm. Four removable metal baffles are placed to reduce solid body rotation and minimize vortex formation. The bottom of the tank is jacketed with a controlled temperature water bath. A probe placed into the liquid in the tank monitors the temperature, which is regulated by a microprocessor. The chamber also accommodates a pH probe. Air can be introduced through a ring-shaped sparger placed directly beneath the impeller.

Agglomeration kinetics were measured under acidic conditions, since agglomeration either did not occur, or occurred very slowly at pH>4. Measurements were usually made at 50°C and at 1,000 rpm by periodically removing samples and measuring their optical density at 650 nm, the wavelength typically used to measure turbidity. In late 1997, we acquired a Malvern Zetasizer 3000, which allowed us to measure zeta potential and particle size. The machine utilizes a laser to measure Z-average particle size and zeta potential through dynamic light scattering. The method assumes the particles to be spherical, and between 0.05-5μ, averaged over the entire population. Polydispersivity, a measure of the population distribution of the particles, is also reported. Samples containing talc (whose particle size of >1.0μ exceeded that of the acrylates) were allowed to settle for a day prior to the zeta measurement.

Acrylates were obtained from B.F.Goodrich (Carbotac latex). Two batches were used, one of which was fresh, while the other had been in storage for a few months prior to use. The particle size of the fresh latex was 0.28μ; that of the other was 0.33μ. The higher value probably reflected agglomeration during storage. Preparing a stable suspension of cured acrylate was quite difficult and the following technique was devised after much trial and error. A smooth glass plate was cleaned thoroughly and dried to remove any residual surfactants. The latex (10 mL) was painted as a narrow strip near the edge of the plate. A wound wire Meyer draw-down rod was then used to spread the latex evenly across the glass plate, care being taken to avoid the formation of either thick pools or thin areas of broken film of latex. A stream of hot air from a hair dryer was then used to dry the latex. The appearance of the material changed from bluish-white to a clear film that was sticky to the touch, but did not transfer away from the glass. This film was allowed to further cure overnight before being collected and resuspended. Polyvinyl acetate (PVAc) of molecular weight 12,800 was obtained from Aldrich.

The cured latex film was then removed as rolls from the glass by scraping off with a razor blade. These rolls were then added to 600 mL of hot deionized water on a stir-plate with 1mL 1.0N KOH and 50μL BRD surfactant (a blend of fatty acids and a nonionic surfactant), whereupon the rolls loosened and partially unwound, forming sheets of solid latex in the hot water. The suspension was then chopped into smaller particles with a high-speed homogenizer. Most of the particles are quite large and settle to the bottom of the beaker, and the yield of dispersed fine material is quite small. After cooling to room temperature the solids were further homogenized to produce a milky suspension, from which some further settling occurred. The decanted liquid was then used for kinetic work.

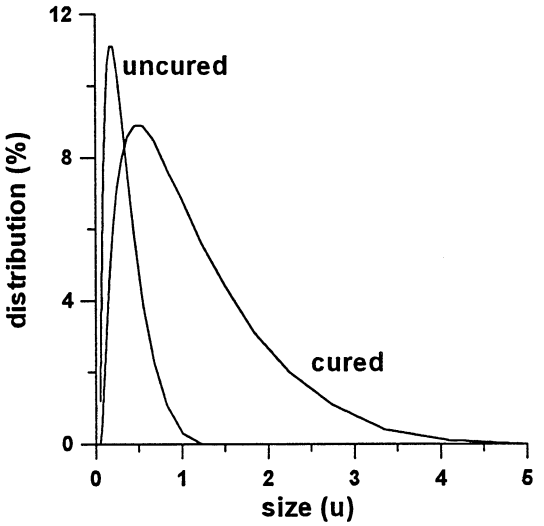

Figure 2: Comparison of particle size and dispersion for uncured and cured stickies.

A target initial optical density of 0.3 or more was chosen, and the amount of resuspended cured latex needed for this target OD was calculated. The reaction chamber was charged with deionized water (or whitewater), such that the total volume (after the subsequent addition of resuspended cured latex) would be 2 L. The water was then stirred at 100 rpm until it reached 50°C, whereupon the impeller speed was reduced to 50 rpm, and the resuspended cured latex added. The pH was then stabilized to a target value with 1N HCl or KOH. The impeller speed was then increased to 1,000 rpm, and the kinetic run begun. Initially, samples were collected every 15 seconds, but the interval was lengthened as the run progressed. Runs were generally continued to about 1-3 half-lives.

As mentioned above, two batches of acrylate were used. One had an average size of 0.33μ, whereas the particles in the other averaged 0.28μ. Both suspensions were fairly monodispersed, having a very narrow range of particle sizes. However, suspensions of the cured acrylates contained particles of both much larger Z-average size (>0.5μ), and of a wider size distribution. Furthermore, both size and range varied greatly between batches. A typical illustration is provided in Figure 2.

Clarification kinetics were usually of the first-order, although second-order or mixed-order behavior was frequently encountered. The uncertainty in rate constants was about 20% for the uncured stickies, but were much higher (at about 100%) for the cured material, probably because of its higher size distribution.

If the kinetics followed the scheme

$$\text{stickie} + \text{stickie} \rightarrow \text{agglomerate} \qquad (1)$$

Table 1: Effect of rpm on the agglomeration of PVAc (MW: 12,800, uncured)[1]			
ID	rpm	k (min^{-1})	r^2
TM4	50		< 0.8
TM5	100		<0.8
TM6	200		<0.8
TM7	300	5.5E-04	0.85
TM8	400	3.9E-03	0.993
TM9	500	9.8E-03	0.997
TM10	600	1.6E-02	0.998
TM11	700	2.0E-02	0.9991
TM12	800	2.1E-02	0.999
TM13	900	2.8E-02	0.9993
TM14	1000	4.4E-02	0.9993

[1]20 mL of PVAc in MeOH at 9.9% (w/v) added to 2 L of pH 2.62 water

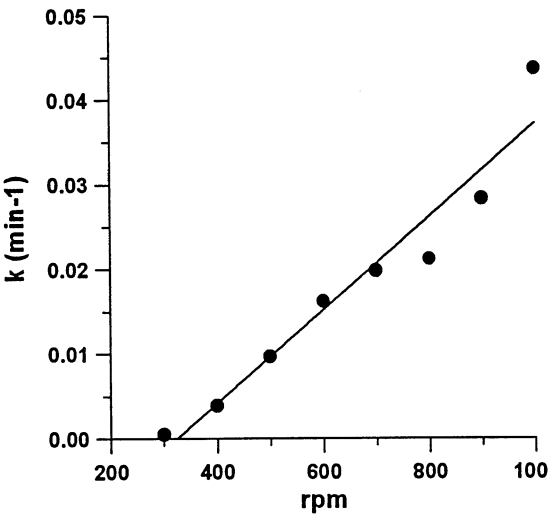

Figure 3: Dependence of agglomeration rate on rpm

where the agglomerate was removed from the process, then the agglomeration should be of the second-order. On the other hand, if the properties of the agglomerate were similar to that of the initial stickie, i.e., the process

$$\text{stickie} + \text{agglomerate} \rightarrow \text{re-agglomerate} \qquad (2)$$

had the same rate constant as process (1), then the reaction would be first-order. Since the stickie will grow and fall out of suspension at some point, mixed-order kinetics are anticipated, with the process being initially first-order, and then becoming more complex. Another complication is that the initial "stickie" is not just a single entity, but probably reflects a distribution of properties. If a subset of this distribution of stickies agglomerates faster than the remainder, then the kinetics will be complex, since multiple processes will be underway.

Effect of shear on agglomeration

The rate of agglomeration increases with increasing shear since the force of collision is more easily able to overcome inter-particle repulsive forces and induce agglomeration. If shear can be used to reproducibly agglomerate stickies, then the effect of other variables such as chemicals and additives that influence agglomeration can be evaluated. In order to determine the effect of shear on the agglomeration rate, PVAc (MW: 12,800) was added as a 9.9% solution in methanol, to water at pH 2.6. The dependence of the agglomeration kinetics on rpm was measured by collecting data at a given rpm, and then progressively increasing the rpm, with the rate being measured at

Table 2: Effect of turbulence on the agglomeration of acrylate[1]			
ID	pH	k (min^{-1})	r^2
without baffles			
TM130	1.17	1.1E-01	0.999
TM131	1.87	6.4E-02	0.9997
TM132	2.24	5.3E-02	0.9995
TM133	2.28	5.9E-02	0.9995
TM134	2.42	5.4E-02	0.9992
TM135	2.54	5.0E-02	0.9990
TM136	2.77	4.5E-02	0.998
TM137	2.97	4.4E-02	0.999
TM138	3.47	1.1E-02	0.98
TM139	4.00	2.8E-03	0.94
with baffles			
TM140	1.90	1.6E-01	0.999
TM141	1.94	1.6E-01	0.9993
TM142	1.98	1.6E-01	0.9991
TM143	2.03	1.3E-01	0.9992
TM144	2.13	1.4E-01	0.9995
TM145	2.34	1.7E-01	0.997
TM146	2.44	1.2E-01	0.9995
TM147	2.53	1.6E-01	0.9991
TM148	2.60	1.5E-01	0.9996
TM149	2.79	1.2E-01	0.998
[1]5 mL of a 50% acrylate suspension (0.33μ) added to 2 L of water at 1,000 rpm			

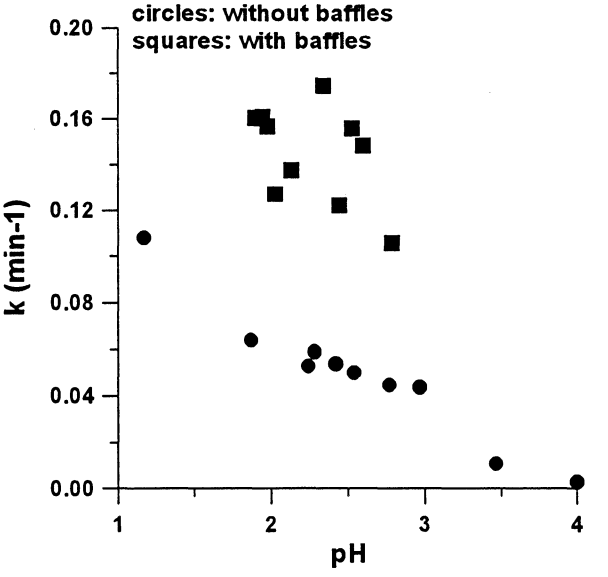

Figure 4: Effect of baffles on acrylate agglomeration

each step. The influence of other variables was therefore minimized. The results, presented in Table 1 and illustrated in Figure 3, show that agglomeration increases linearly with shear. Agglomeration was too slow below 300 rpm, and reproducible rates could not be measured.

The Figure 3 relationship is linear only because the data were acquired over a single run. Rates measured across different runs were highly variable, probably because the size range of PVAc particles in suspension varied with each batch. As will be emphasized later, reproducibility deteriorates if the characteristics of the suspension are not kept constant.

Table 3: Effect of pH on the agglomeration of acrylate[1]			
ID	pH	k (min^{-1})	r^2
TM15	4.75	1.5E-03	0.91
TM16	4.80	5.5E-03	0.95
TM17	3.95	9.1E-02	0.9997
TM18	3.38	1.3E-01	0.9996
TM19	3.04	1.4E-01	0.9997
TM20	2.81	1.4E-01	0.9997
TM21	2.76	1.5E-01	0.995
TM22	2.45	1.5E-01	0.9990
TM23	2.16	1.6E-01	0.9990

[1]5 mL of a 50% acrylate suspension (0.33μ) added to 2 L of water at 1,000 rpm

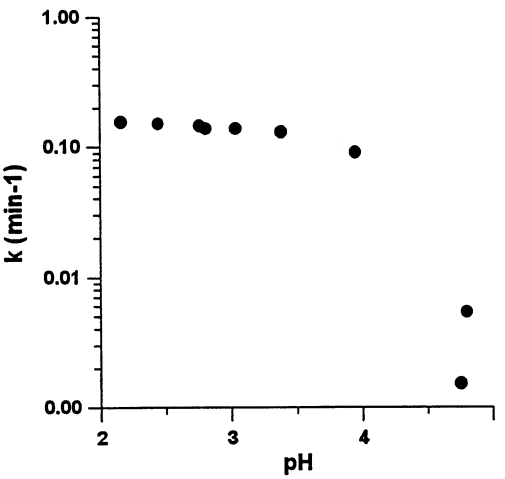

Figure 5: Dependence of acrylate agglomeration on pH

Removing the baffles in our mixing chamber can reduce shear. Although experiments were usually run with the baffles in place, comparative measurements were made with acrylate latex (0.33μ) with and without the baffles. The agglomeration rates listed in Table 2 and illustrated in Figure 4 demonstrate that the baffles lead to a pronounced increase in rate, confirming the effect of shear on agglomeration. Finally, experiments were made with and without injection of 1 lpm air under the conditions used to generate the Table 2 data with the baffles attached. Inclusion of air increased the rates by almost an order of magnitude. These results demonstrate that increasing shear by any means, whether by increasing impeller rpm, installing baffles, or injecting air, increases the agglomeration rate of both PVAc and acrylate.

Effect of pH on agglomeration

The dependence of the agglomeration rate on pH is illustrated in Figure 5 for acrylates, and the data are provided in Table 3. The break at a pH of about 4 indicates that stickies will resist agglomeration at higher pH. The likely reason is that zeta is reduced under acidic conditions. Mills that deliver acid shocks to remove stickies, should, therefore, target a pH of slightly less than 4. Unlike the acrylates, there is no clear relationship between pH and agglomeration rate for PVAc as illustrated by the data in Table 4 and Figure 6. Particle size variability of the stickie suspension in water is probably responsible. Since the acrylate is introduced as a stable suspension, it will tend to monodisperse in water. However, PVAc is introduced in a methanol carrier, and the stickies will fall out of solution in a variety of particle sizes. Since particle size affects the rate of agglomeration (as we will show later), the Figure 6 plot is affected by two variables, and the effect of pH alone is obscured.

Table 4: Effect of pH on the agglomeration of MW 12,800 PVAc[1]			
ID	pH	k (min^{-1})	r^2
TM24	3.30	1.8E-01	0.998
TM25	7.68	1.2E-01	0.994
TM26	3.99	6.4E-02	0.99
TM27	2.75	1.3E-01	0.98
TM28	3.40	1.0E-01	0.997
TM29	2.62	1.6E-01	0.91
TM30	2.88	6.4E-01	0.97
TM31	10.77	1.8E-01	0.98
TM32	2.82	6.6E-01	0.97
TM33	2.45	1.8E-01	0.999
TM34	2.24	6.7E-01	0.96
TM35	4.54	7.9E-02	0.99
TM36	2.94	5.7E-01	0.98
TM37	2.29	5.0E-01	0.981
TM30	5.27	4.3E-01	0.992
TM38	2.42	7.3E-02	0.99
TM39	2.43	6.2E-01	0.99
TM40	2 .62	5.9E-01	0.99
TM41	2.96	5.4E-01	0.99
TM42	2.61	5.0E-02	0.99
TM43	4.62	3.5E-02	0.996
TM44	4.01	2.1E-01	0.99
TM45	3.59	6.6E-01	0.98
TM46	3.05	4.0E-02	0.997
TM47	4.09	1.9E-01	0.9999
TM48	4.02	2.2E-02	0.996
[1]10-30 mL of 10-14% PVAc in MeOH was added to 2 L of water at 1,000 rpm			

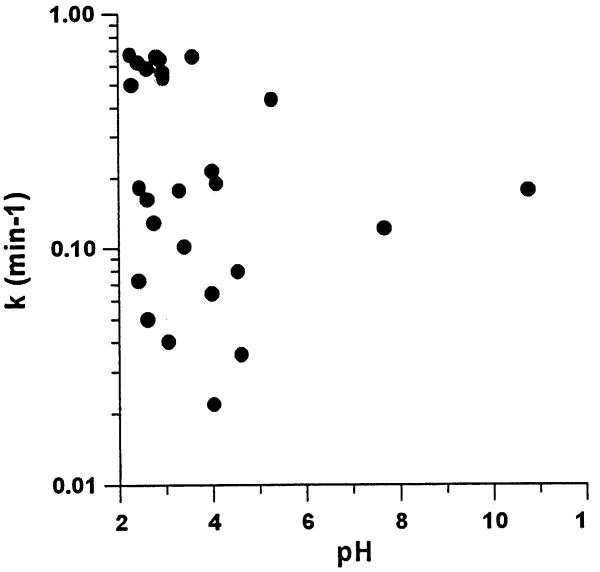

Figure 6: Dependence of PVAc agglomeration on pH

Table 5: Comparison of agglomeration of acrylate in distilled water and whitewater					
ID	pH	white-water	k (min^{-1})	r^2	absolute difference (%)
TM92	4.89	Y	6.3E-03	0.95	15
TM16	4.80	N	5.5E-03	0.95	
TM93	3.05	Y	2.0E-01	0.995	
TM109	3.01	Y	3.7E-01	0.99	100
TM19	3.04	N	1.4E-01	0.9997	
TM94	2.51	Y	1.9E-01	0.97	36
TM64	2.47	N	1.3E-01	0.999	
TM32	2.45	N	1.5E-01	0.990	
[1]0.5-5 mL of a 50% acrylate suspension (0.33μ) added to 2 L of water at 1,000 rpm					

Table 6: Agglomeration of cured/resuspended acrylate[1]	
pH	k (r^2)
3.5-3.7	0.15 (0.997)
2.5	0.063 (0.999)
2.5	0.0033 (0.986)
3.0	0.0016 (0.993)
2.7-3.0	0.19 (0.9992)
4.1-4.5	0.15 (0.99)
[1]in water except for the last entry which refers to whitewater	

Agglomeration in whitewater

Whitewater obtained from Bowater's GNN Millinocket mill was stored cold prior to use. We are grateful to Bob Moran, Dave Walsh, and Harry Bard for arranging for periodic shipments of whitewater. Agglomeration rates of acrylate (0.33μ) in distilled water and whitewater are compared in Table 5. While the whitewater rates are slightly faster than those in distilled water, the differences are not large. We conclude that conclusions reached for distilled water will mostly apply to whitewater, and that the additional constituents of whitewater do not materially influence the rates.

Agglomeration of cured/resuspended stickies

The agglomeration rates of cured and resuspended acrylates listed in Table 6 display a much higher variability than those in Table 5 for the uncured material. However, the median range of 0.06 to 0.15 min^{-1} is roughly comparable to the rates in Table 5 for uncured acrylate, suggesting that there are no order-of-magnitude differences in behavior. The high variability of the rates appears to be principally associated with differences in particle size. A large drop in particle size tracks a similar decrease in optical density occurs during early agglomeration as shown in Figure 7. The zeta potential, however, is relatively stable. The variability in Table 7 can now be understood on the basis of particle size, since the size distribution is not constant across different preparations of the cured stickies.

Effect of additives on acrylate (uncured) agglomeration

Talc

Since talc is used to deactivate stickies, its mechanism of action was probed by adding it to GNN whitewater and measuring its rate of agglomeration. Talc (Mistron-400) is typically used at 0.4% (ODT) of a 0.9 lb/gallon formulation. Whitewater was spiked with 0.6 mL of a 50% suspension of acrylate (0.33μ), and data were taken at various impeller speeds. Only the 750 and 1,000 rpm conditions led to first-order kinetics; agglomeration was too slow at lower rates. The kinetic data summarized in Table 7 show that the rates are unaffected by the presence of talc. Although some of the values in Table 7 are flagged as zero-talc, the whitewater is paper machine whitewater returned from PM #6 to the whitewater tower, and contains some residual talc. Major differences occurred in the appearance of the agglomerated stickie. Without talc, the agglomerate was compact and tacky, and attached to the sides of the chamber. In

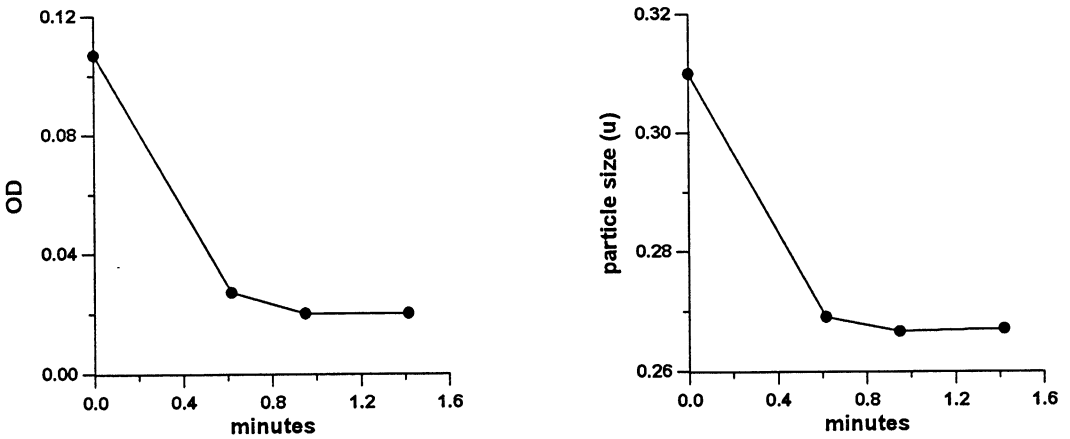

Figure 7: Optical density and particle size changes during cured PSA agglomeration in water at pH 3.3.

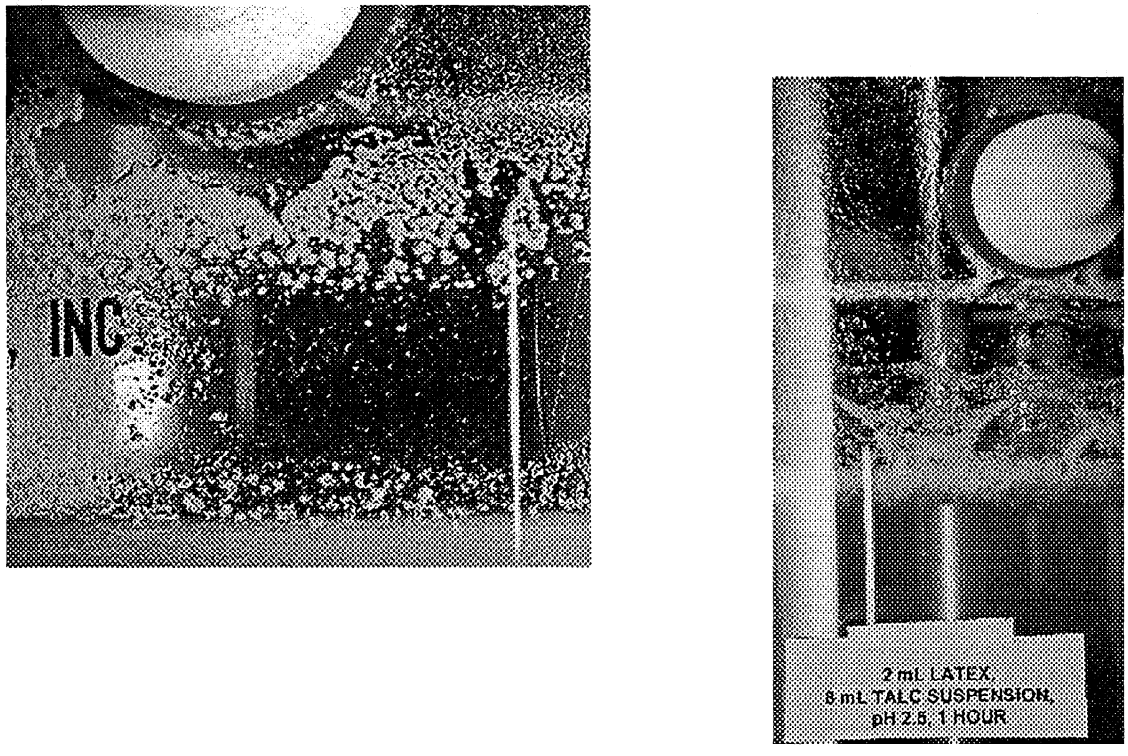

Figure 8: Appearance of the mixer walls with (right) and without (left) talc addition.

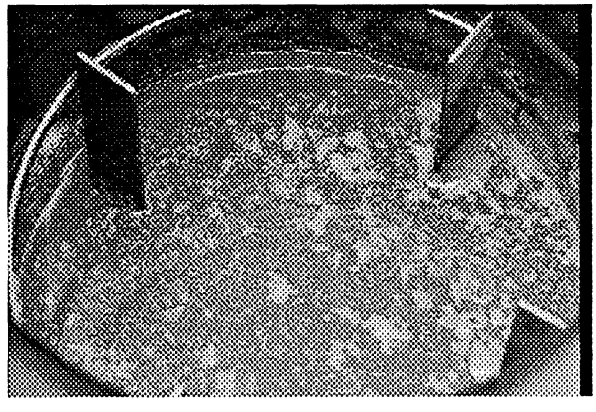

Figure 9: Appearance of stickies in the presence of talc.

the presence of talc, the agglomerated stickie was feathery, and remained in the water layer, and the walls were relatively clean, as shown in Figure 8. Figure 9 demonstrates that the bulk of the agglomerated stickie floated on the water. Clearly, talc detackified the stickie, but the result was visibly the same at all doses. The levels of talc applied were lower than the 0.4% conventionally used by GNN, and since no differences were observed at concentrations exceeding 0.03%, it appears that the mill should be able to reduce its talc dosage without suffering adverse effects. The level of stickies used in these experiments far exceeds levels likely to be encountered in the mill, and there should be a sufficient reserve of talc even under reduced dosage to handle stickie surges.

In order to determine whether stickie particle size influenced agglomeration in the presence of talc, the 0.28μ latex was suspended in water of pH 2.7-2.8 and agitated at 1,000 rpm. The rates along with the initial zeta potentials (which did not change during agglomeration) are recorded in Table 8. The smaller particles agglomerate very much more slowly, demonstrating that a relatively small difference in size has an enormous effect on the rate. The 0.28μ material does not agglomerate at all on our time scale, whereas appreciable agglomeration occurs with the 0.33μ suspension. For 0.03-0.05% talc, the difference in rate is about thirtyfold. Clearly, agglomeration is inordinately sensitive to particle size. In contrast to the Table 7 data for the 0.33μ stickies, the rate for the smaller particles are linear with talc level. The reason for the difference is not known. However, the increase is less than an order of magnitude, and as will be shown later, much greater increases are obtained with the chemical additives.

We conclude that talc affects the agglomeration rate to at best a small extent, and that its principal benefit is to detackify the agglomerated material. The benefits of talc can be realized at dosages much lower than is currently used, and we suggest that mills that presently use talc progressively lower their application rate. The GNN mill is currently following our recommendation.

Table 7: Effect of talc on acrylate agglomeration (0.33μ acrylate)

1,000 rpm					750 rpm				
ID	pH	talc (%)[1]	k (min^{-1})	r^2	ID	pH	talc (%)[1]	k (min^{-1})	r^2
TM109	3.01	0	3.7E-1	0.987	TM108	3.08	0	6.7E-2	0.99
TM104	2.97	0.03	2.1E-1	0.987	TM103	2.98	0.03	6.6E-2	0.996
		0.12			TM98	3.08	0.12	7.1E-2	0.993
TM114	3.09	0.24	4.4E-1	0.985	TM113	3.09	0.24	6.3E-2	0.94

[1]of the talc concentrate (1 lb/gallon); the mill dosage is 0.4%

Table 8: Effect of talc on acrylate agglomeration (0.28μ acrylate)			
talc (%)[1]	k (min^{-1})	r^2	zeta (mV)
0		≈0	-42
0.05	0.0065	0.87	-41
0.15	0.014	0.83	-32
0.5	0.041	0.97	-29
[1]of the talc concentrate (1 lb/gallon) in 2L of whitewater; the mill dosage is 0.4%; pH:2.7-2.8			

EXPN-3405/ACCURAC-181

The GNN mill uses a combination of EXPN-3405 and ACCURAC-181 at their #6 paper machine. EXPN-3405, a mixture of polyethyleneimine and a mixed polyamide polyamine polymer, is applied at 3 lb/ton. The ACCURAC is cationic polyacrylamide, and is applied at 2.5 lb/ton. The effect of the combination of agglomeration is compared to corresponding data for EXPN alone and to a control in Figure 10 with 0.28μ acrylate. The rate enhancement is sizeable. As before, the stickie alone does not agglomerate, whereas the combination rapidly removes the stickie from suspension. The kinetics are neither first- nor second-order, suggesting the involvement of more than one process. The zeta potential of the control and of the EXPN stickies remained at about –50 mV and about –45 mV throughout. In the presence of the combination, the zeta potential started at about –38 mV and decreased to about –50 mV. This suggests that the combination reduces zeta, and that the stickies that remain towards the end of the run bear a high surface charge and resist agglomeration. Only minor differences in particle size were observed among the three sets.

DETAC-DI283

First-order agglomeration rate constants of acrylate added to GNN whitewater containing DETAC are reported in Table 9. The mill applies the additive at 4 lb/ODT. Clearly, the rate increases dramatically in the presence of DETAC, and appears to be linear with DETAC concentration, although this is based on only two points. DETAC has a definite effect on the initial zeta potential as shown in Figure 11. The control remains at about –44 mV throughout. In the presence of 50 ppm DETAC, the zeta begins at roughly the same level, but decreases somewhat throughout the run. At 200 ppm, the starting zeta is much lower, and increases a little during agglomeration. The mode of action appears to be similar to that of EXPN-3405/ACCURAC-181.

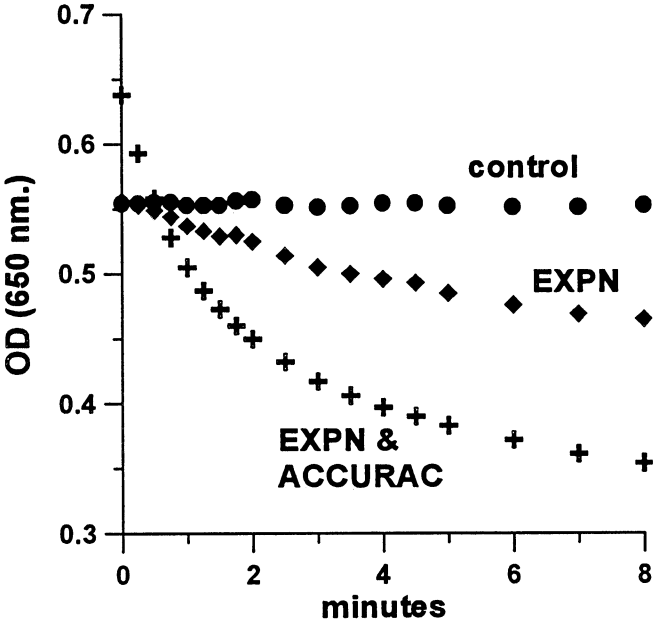

Figure 10: Agglomeration rates in the presence of EXPN and ACCURAC

Table 9: Acrylate agglomerate in the presence of DETAC		
ppm	percent of mill dosage[1]	1st-order k(r^2)
0	0	0.0039 (0.97)
50	25	0.032 (0.99)
200	100	0.12 (0.998)
[1]200 ppm		

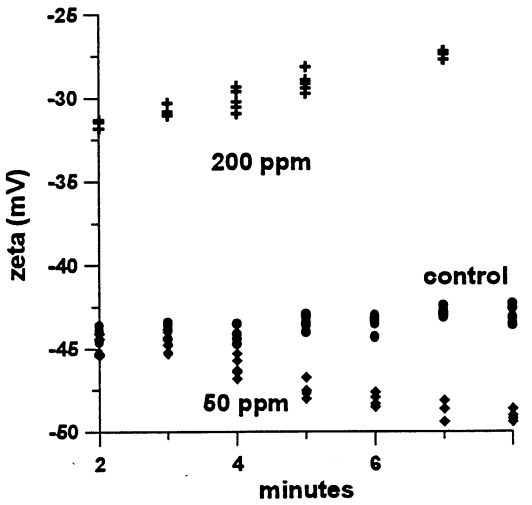

Figure 11: DETAC-induced changes in acrylate zeta potential

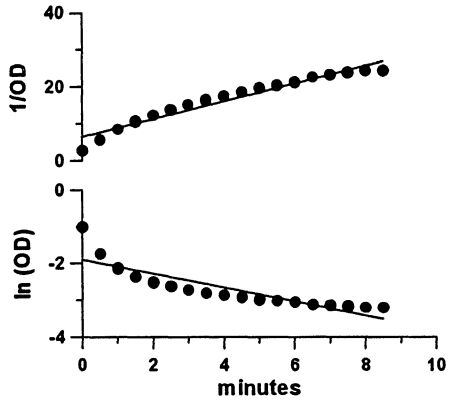

Figure 12: First- (bottom) and second-order (bottom) of the agglomeration kinetics of uncured acrylate.

Both additives increase the rate of agglomeration by reducing zeta. However, zeta progressively decreases in the presence of DETAC, whereas the opposite seems to be true for EXPN-3405/AC-CURAC-181, for reasons that are unclear.

Effect of additives on acrylate (cured) agglomeration

DETAC-DI283

The effect of DETAC-DI283 upon cured/resuspended acrylic latex was measured against controls. The levels of DETAC-DI283 used for these experiments were 10, 50, 100, 200, and 500 ppm, which correspond to 5, 25, 50, 100 and 250% of mill use dosage, respectively. Three separate batches of cured/resuspended acrylic latex were prepared. Given the differences among batches, the results should be compared within each batch, and not across batches.

The agglomeration rate for the controls were intermediate between first and second order, as shown in Figure 12. Although second-order plots provide a slightly better fit, first-order rates are used for comparison in order to maintain consistency with the remainder of the report. A major point of difference between the suspensions from the cured and uncured material is that agglomeration is quite fast for the cured material, whereas no agglomeration was observed with the 0.28μ material. This suggests that the cured material contains some easily removable components that rapidly fall out. The implication is that the more recalcitrant material will remain in suspension. This could explain the complex kinetics since the nature of the stickie changes during the run.

The rates *within* each batch vary by less than a factor of two, as shown in Table 10. Particle size decreases during agglomeration, but DETAC does not seem to influence the trend. The only significant difference is the change in zeta at 500 ppm (batch 2). The zeta potential was constant during agglomeration for all three batches. DETAC begins to lower zeta at 500 ppm, whereas the threshold for the uncured stickie was 200

Table 10: Effect of DETAC on the properties of stickies					
DETAC (ppm)	k (r^2) 1st order	k (r^2) 2nd order	zeta (mV)	size (μ) initial	size (μ) final
batch 1, pH 2.8					
0	0.20 (0.75)	2.4 (0.95)	-59	0.48	0.3
10	0.22 (0.79)	3.6 (0.98)	-59	0.41	0.3
batch 2, pH 3.8					
0	0.11 (0.72)	1.1 (0.86)	-47	0.41	0.31
50	0.26(0.85)	6.3 (0.997)	-42	0.43	0.31
500	0.20 (0.78)	3.2 (0.94)	-17	0.45	0.43
batch 3, pH 4.0					
0	0.068 (0.84)	0.25 (0.90)		0.37	0.34
100	0.078 (0.93)	0.30 (0.97)		0.38	0.34
200	0.072 (0.94)	0.25 (0.97)		0.39	0.36

ppm. We consider the agreement to be good in light of the wider distribution in particle characteristics in the cured suspension. The large increase in agglomeration rate induced by DETAC for the uncured stickies (Table 9) is not apparent in Table 10, again, probably because the suspension from the cured material is not monodispersed, and the larger particles are removed with shear, masking the benefit of DETAC.

Comparison of stickies control additives

It is risky to make any kind of a recommendation from limited laboratory data. Hence, rather than rank the performance of the addditives studied, we will highlight the advantages of each. The rate enhancement observed in the presence of talc is smaller than those induced by the chemical additives, and the change in zeta is somewhat less pronounced. This suggests that while talc does interact with the stickies at the colloidal level, the interaction is stronger with the chemical additives. Talc has one unique attribute not shared by the other additives. For talc, the agglomerated material at the end of the run was found in water as non-tacky feathery streaks. Agglomerates in the presence of other additives were attached to the blade or to the walls. This suggests that talc may be able to keep machine surfaces free of stickies. Our results suggest that the dosage used by the mill may be unnecessarily high.

Future efforts

At this stage of the program, we understand many of the interactions among stickies, fiber, and water and are able to screen and recommend additives for stickies control. We recommend that this aspect be completed in the following year through studies in non-newsprint mills. Also, some fundamental aspects of the work, namely the

effect of pH on zeta and particle size need to be better understood. We have observed that the effect is quite variable, and are unable to predict it. Finally, we could complete the study by select additive combinations (e.g., talc and DETAC), or designing new additives for optimum effectiveness.

The work described in the Appendix may greatly increase cleaner efficiency, and is probably the most important result from this year's activities. IPST is filing for a patent on this. The work was funded outside the PAC, and follow-on efforts in non-newsprint mills is strongly recommended.

Our recommended time allocations to these activities are as follows:

- Complete fundamental aspects of the stickie-water interactions (40%).
- Extend to non-newsprint mills (40%).
- Start work on improving cleaner efficiency in non-newsprint mills (20%).

PAC input will be sought on these proposed allocations.

In related work, Howard Corcoran will start doctoral work on determining what causes stickies to attach to surfaces, and will develop means to disrupt them. This effort will be in collaboration with MacMillan Bloedel through the courtesy of Lynn Jonakin. Both corporate and the Henderson, KY, mill will be involved.

APPENDIX

An Option for Better Stickies Removal Through Cleaner Optimization

David K. Wilhelm, Stephen Makris, Sujit Banerjee

The work reported here was conducted by Dave Wilhelm and Steve Makris as a part of their MS research, with Sujit Banerjee serving as their advisor. Although the work lies outside the purview of the PAC, it relates to the general subject of stickies control, and is, therefore, offered as an Appendix. The purpose of the study was to collect contaminants from various unit operations from two mills (Bowater, GNN and Augusta Newsprint) and to track their composition as they moved downstream. Approximately 5-10 contaminants were analyzed from each location. A variety of contaminants were found at the front end of both mills. However, the contaminants present after the final cleaning stage at both mills had a high proportion of a mixture of an acrylate and a hot melt, suggesting that this combination resisted screening and cleaning.

Some of the contaminants from Augusta Newsprint were placed in cold water, and the water was slowly heated. The stickies sank initially, but floated at a "transition temperature." The transition was quite sharp, and occurred over a 1-2°F range. It was also reversible, i.e. the same transition temperature was obtained when the floating stickie sank as the water was cooled. Results obtained from two locations are listed in Table A-1, along with the temperature of the process water at that location. Note that with one exception, the contaminants at the fine screen accepts have a higher transition temperature than those at the front end, the magazine repulper. If the 91°F value is omitted, then the average transition temperature rises from 109°F to 114°F. At the transition temperature, the stickie would have a specific gravity (ρ) of one, at which point the cleaners would be transparent. Hence, the greater the difference between the transition temperature and the process water temperature, the more efficient will be the centrifugal separation.

The cleaners are run at a temperature of 123°F, so the stickies that survive cleaning and screening will have ρ of slightly less than one. These are the troublesome stickies, the ones most apt to be found in whitewater. Improving cleaner technology target stickies whose specific gravities are very close to one, but there will always be a window centered at ρ=1 that will defy separation. We offer an alternative.

Consider a situation where two reverse cleaners are operated at different temperatures. A stickie of ρ=1 in one cleaner must have a different specific gravity in the other, *since the coefficient of thermal expansion of a stickie is much greater than that of water*. Hence, by mismatching temperatures, the ρ=1 window will be breached, and all stickies can be potentially removed. The two-cleaner scenario is only provided as an illustration; similar results will follow if the temperatures of the forward and reverse cleaners are mismatched. There are several other possible configurations. Mismatching temperatures is central to the process, and there are several ways in which this can be achieved. The easiest way would be to relocate one set of cleaners to a location

Table A-1: Transition temperatures (°F) of stickies	
fine screen accepts	magazine repulper
91	91
109	95
108	99
118	104
119	104
average: 109	**99**
clnr temp: 123	

where the temperature difference between cleaners is maximized.

Mill descriptions

GNN Millinocket

Great Northern Paper's East Millinocket recycle mill produces 100% recycle DIP from a furnish of 75% ONP and 25% OMG. The stock preparation line consists of an alkaline loop and an acid loop for deinking and contaminant removal. Each loop has separate white water circuits and clarification. The alkaline loop consists of coarse and fine screens, multiple pressurized flotation cells, forward cleaners, thickener/washers and refiners. The acid loop includes pressurized flotation cells, forward and through cleaners, and thickener/washers. The white water is diluted with paper mill whitewater to the desired consistency and pH for high-density storage.

Pulping is done under alkaline conditions in a continuous drum pulper, which is followed by a high density cleaner, swelling chest, 0.050" coarse screens, and 0.004" wedge slotted fine screens. The screens are followed by pressurized flotation cells for deinking. Forward cleaners are then employed for "heavy" contaminant removal. The pulp is then washed in a double nip thickener followed by a screw press. A refiner used for dispersion completes the alkaline loop. The stock is subsequently diluted with acid and acid loop whitewater, and then sent to flotation cells. Cleaning is accomplished through forward and through hydrocyclones arranged in series. Again the stock is washed with double nip thickener washers and screw pressed. The pulp is finally diluted with paper mill white water for high density storage.

Augusta Newsprint

Augusta Newsprint has a flotation deinking plant that produces 370 metric tons per day. The recycle furnish consists of an 80/20 mix of ONP to OMG. The newsprint and magazine are pulped separately in alkaline conditions (approx. pH=10.2, consist. 9.0%). They go through a high density cleaning stage, and are then blended together prior to coarse screening. After the coarse screens, the pulp is sent through floatation cells, reverse cleaners, an alkaline disk filter (thickener) and alkaline screw press (thickener). The pulp is then acid shocked to a pH of approximately 5 and sent through the forward cleaners and fines screens before it is thickened to go to the blend chest of the paper machine. The paper mill has two Valmet Sym-Formers that produce recycled content newsprint with a capacity of 1,045 metric tons per day, and uses 10 million gallons per day of water.

FLOTATION DEINKING FLUID MECHANICS

STATUS REPORT

FOR

PROJECT F00903

Ted Heindel

March 23-24, 1998

Institute of Paper Science and Technology
500 10th Street, N.W.
Atlanta, Georgia

DUES-FUNDED PROJECT SUMMARY

Project Title:	**FLOTATION DEINKING FLUID MECHANICS**
Project Code:	DEINKFLOW
Project Number:	F00903
PAC:	Recycle and Surface and Colloid Science
Division:	Engineering
Project Staff	
Faculty/Senior Staff:	Ted Heindel
Staff:	Adele Emery, Krishna Maruvada, Fred Bloom (consultant)
FY 98-99 Budget:	$155,445
Allocated as Matching Funds:	
Time Allocation	
Faculty/Senior Staff:	Heindel - 40%
Support:	Emery - 70%; Maruvada - 100% (1-15-98); Bloom - 10%
Supporting Research	
M.S. Students:	3 IPST students
Ph.D. Students:	
External:	1 AF&PA

1 RESEARCH LINE/ROADMAP:

Reduce and/or control contaminants (e.g., stickies, dyes, toners) in recycled fiber pulp using break-through technologies to allow the interchange of recycled pulp with virgin pulp of similar fiber make up at economical cost.

2 PROJECT OBJECTIVE:

The objective of this project is to increase flotation efficiency by maximizing contaminant removal from wastepaper while minimizing fiber loss. This objective will be realized by developing a better understanding of the fundamental fluid mechanic processes involved in flotation separation.

3 PROJECT SUMMARY:

This report summarizes the progress of this study over the past year in the areas of modeling the overall flotation separation process and measuring the bubble size distribution in a pulp suspension.

Accurate microprocess probabilities are important to effectively model the overall flotation macroprocess. During the past year, the flotation microprocess of collision has been revisited and an exact expression for the probability of collision (P_c) has been developed. Details of this research can be found in Member Company Report 4 of this project [1]. Our exact expression for P_c only assumes that the bubble and particle are spherical and that $R_p < R_B$. The expression developed here removes the additional assumptions that are typically invoked in the literature (i.e., $R_p + R_B \approx R_B$ and $(R_p/R_B)^3 << (R_p/R_B)^2$). In addition to removing these restrictions from the expression for P_c, we also include the possibility that the particle settling velocity may also influence the collision probability.

The expression for P_c developed in this research is a function of three dimensionless groups: (i) the magnitude of the dimensionless particle settling velocity, $|G|$; (ii) the bubble Reynolds number, Re_B; and (iii) the ratio of particle-to-bubble size, R_p/R_B. This expression was then used to predict P_c for selected parametric ranges of $0 \le |G| \le 5$, $0 \le Re_B \le 500$, and $0.001 \le R_p/R_B \le 1$.

In general, P_c is independent of Re_B when $R_p/R_B \lesssim 0.05$ for all values of $|G|$. Conversely, P_c is not significantly influenced by $|G|$ as $R_p/R_B \rightarrow 1$ for all values of Re_B. The additional assumptions

typically employed in the literature (i.e., $R_p + R_B \approx R_B$ and $(R_p/R_B)^3 << (R_p/R_B)^2$) are valid only when $R_p/R_B \lesssim 0.05$-0.1, depending on the values of $|G|$ and Re_B.

Finally, the new prediction for P_c developed during the past year was compared to available experimental P_c data from the mineral processing industry. This new expression does a very good job at predicting measured P_c values. The inclusion of the particle settling velocity is very important, particularly when the particles have a density much higher than that of water. Additionally, the form of P_c derived from basic principles in this report is much simpler than that recently proposed by another researcher and it is just as accurate at predicting experimental results.

The flotation microprocess of attachment by sliding has also been improved during the past year. A closed-form approximation has been developed for the probability of attachment by sliding (P_{asl}). This new expression is an improvement in the P_{asl} expression previously used, and is a function of the various system parameters (e.g., bubble size, particle size and density, fluid properties, etc.) and the liquid film thickness between the bubble and particle. This phase of the research is detailed in Member Company Report 6 of this project [2]. Preliminary results reveal that P_{asl} is influenced by bubble and particle size and there may be a particular bubble/particle size combination that maximizes P_{asl}.

In the area of bubble size measurements, a large amount of qualitative and quantitative data has been acquired concerning bubble size in a quiescent bubble column with four different experimental systems: (1) ONP systems with various chemistries and chemistry concentrations; (2) NBSK systems with various consistencies but no added chemistry; (3) a copy paper system with no added chemistry; and (4) an ONP system with no added chemistry but a higher gas flow rate. Details of this research effort have recently been presented in Member Company Report 5 of this project [3].

For the specific chemistries addressed here and added to an air/water system or an air/water/1% ONP (unprinted) system, the following general conclusions are realized:

- Increasing the BRD 2360 concentration (a fatty acid) results in negligible changes in average bubble size, except for the 1% ONP with gasket air injection. It is hypothesized that this change may be more a result of differences in the fiber network structure, and not BRD 2360 concentration.
- Increasing the BRD 2342 concentration (a nonionic surfactant) in the presence of 1% ONP results in an increase in the average bubble diameter, with the sparger injection technique producing larger bubbles than the gasket at Position 2. Clear trends are difficult to discern for the 0% data.
- Increasing the BRD 2363 concentration (a fatty acid/nonionic surfactant blend) results in a general increase in the average bubble size in all systems addressed here, except the 1% ONP sparger data.
- BRD 2342 produced the most foam of all three chemistries.
- By comparing the three different chemistries at fixed concentrations of 1.7 and 3.3 ml/kg, the BRD 2342 produces the smallest average bubble diameter for all systems addressed here, except the 1% ONP sparger system, where the BRD 2342 produces the largest average bubble diameter.
- Surface tension did not correlate the bubble results recorded in this study.

The northern bleached softwood kraft (NBSK) had a much longer fiber length than the ONP used in this study. The longer fibers promoted fiber network formation and bubble coalescence. The few, but large, bubbles recorded when the air flow rate is 0.25 slpm prevented statistically significant results from being realized except at the very low fiber consistency of 0.1%. Additional experiments were completed at an air flow rate of 2 slpm. General conclusions from these results are:

- The higher gas flow rate promotes backmixed flow conditions where small bubbles descend along the column sides and are eventually reentrained in the bulk rising column of air.
- The sparger air injection technique results in a higher gas holdup when the air injection rate is held constant at 2 slpm.

- The average bubble size increases with NBSK fiber consistency.
- The gasket air injection technique produces larger average bubble diameters at Position 2 and does not keep the fiber suspension well-mixed, which may lead to fiber network nonuniformities and larger variations in the average bubble size and bubble size distribution.
- The sparger air injection technique produces a bimodal bubble size distribution, with the majority of the bubbles in the size range less than 10 mm in diameter and a peak in the 2-3 mm range. The bubbles in this range all have the same average bubble size (~3 mm) for all NBSK fiber consistencies addressed here, but the relative frequency decreases with increasing consistency. Few bubbles are greater than 10 mm in diameter, but those that are, are typically larger than 25 mm. The number of bubbles that fall in this category increases with increasing NBSK consistency. These larger bubbles also play an important role by acting as mobile mixers, which keep the smaller bubbles uniform and the fiber suspension well-mixed and homogeneous.

The 1% copy paper system produced similar results to those obtained with 1% NBSK, implying that the NBSK results are representative of those obtained with typical copy paper found in recycling office-type printing and writing grade papers for the conditions of this study.

Flow patterns observed with the 1% ONP system with an air injection rate of 2 slpm are similar to those produced by the 1% NBSK system. However, the average bubble size was smaller with the ONP system. The bimodal bubble size distribution is also observed with the 1% ONP and sparger system with the air injection rate of 2 slpm, but the number of bubbles larger than 10 mm is much smaller than that produced with 1% NBSK.

This status report will highlight the results from this research effort during the past year. Specific details can be found in the three Member Company Reports mentioned above [1-3].

4 PROJECT BACKGROUND and DISCUSSION:

4.1 Flotation Modeling

The flotation separation macroprocess is composed of a series of four microprocesses that must take place in sequence for the successful removal of a contaminant particle by an air bubble. These microprocesses include: (i) capture or collision of the ink particle by an air bubble; (ii) adhesion of the ink particle to the air bubble as it slides over the bubble surface; (iii) extension of a three-phase contact at the bubble/particle/liquid interface; and (iv) stabilization/ destabilization of the bubble/particle aggregate. Member Company Report 1 of this project [4] summarized the microprocesses in great detail and presented available probability equations for each microprocess. These microprocess probabilities were used to develop a first-generation kinetic-type model of the overall flotation process, which was also elaborated upon in Member Company Report 1 [4]. The model is governed by two kinetic constants that are functions of the various microprocess probabilities, and was used in Member Company Report 2 of this research effort to predict flotation efficiency and other flotation performance parameters for selected parametric ranges [5]. Work during the past year in the flotation modeling aspect of this project included refinement of the microprocess probabilities of the collision (P_c) and adhesion by sliding (P_{asl}), and the initiation of model validation studies. This work is summarized in the following sections.

4.1.1 Probability of Collision Improvements

Improvements to the probability of collision (P_c) model have recently been summarized in Member Company Report 4 of this project [1]. Material highlights will be presented here.

The probability of collision is typically modeled by assuming a particular fluid flow field a particle is in as it flows toward a bubble. The particle is generally assumed to follow potential flow conditions, Stokes flow conditions, or an intermediate flow condition between potential and Stokes flow. The intermediate flow field is typically assumed to follow that proposed by Yoon and Luttrell [6]. The influence these flows have on P_c is shown in Fig. 1. Stokes flow corresponds to the intermediate flow of Yoon and Luttrell [6] when $Re_B = 0$ and this flow predicts the lowest value for P_c for all $R_p/R_B \leq 1$, with P_c increasing as R_p/R_B increases. The

values of P_c predicted for intermediate flow are a function of Re_B and selected Re_B values are shown in Fig. 1 for $Re_B \leq 500$. The applicability of these results at $Re_B = 500$ is questionable because they were developed for $0 \leq Re_B \leq 100$; however, Yoon and Luttrell [6] state that it "may be applicable for $Re_B > 100$, although no experimental (streamline) data [were] available in the present work." This figure also reveals that P_c increases as Re_B increases for a fixed R_p/R_B, and these values run parallel to those predicted for Stokes flow. Potential flow predictions are also shown in Fig. 1 for completeness. Potential flow predicts the highest values for P_c when $R_p/R_B \lesssim 0.1$. One interesting result from this figure is that all three flow conditions predict values for $P_c > 1$ as $R_p/R_B \rightarrow 1$. This is the result of two assumptions that have been applied in these derivations, but not emphasized. These assumptions are

$$R_p + R_B \approx R_B \tag{1}$$

$$\left(\frac{R_p}{R_B}\right)^3 << \left(\frac{R_p}{R_B}\right)^2 \tag{2}$$

Using the intermediate flow of Yoon and Luttrell [6], we have removed these two assumptions to yield results presented in Fig. 2. The exact and approximate solutions follow closely to one another for small values of R_p/R_B, and at $R_p/R_B = 0.1$, the approximate solution presented by Yoon and Luttrell [6] over predicts P_c by approximately 25% when $Re_B = 0$ and by more than 35% when $Re_B = 500$. Increasing R_p/R_B further toward 1 increases this difference. By employing the flow of Yoon and Luttrell [6] in the development of the exact solution for P_c, the predictions are valid for $Re_B \leq 100$, but their utility is again suspect for $Re_B > 100$. However, calculations are shown for $Re_B = 500$ to reveal that the same trends are followed and unrealistic predictions ($P_c > 1$) result only when $R_p/R_B \gtrsim 0.3$ and $Re_B = 500$. This result will be further discussed below.

Another parameter that is typically neglected in modeling the collision process between a particle and bubble is the particle settling velocity due to the inertial force. We have included this force in our improved model for P_c, to yield an exact result of [1]

$$P_c = \frac{1}{1+|G|}\left\{\frac{1}{2\left[\left(\frac{R_p}{R_B}\right)+1\right]^3}\left[2\left(\frac{R_p}{R_B}\right)^3 + 3\left(\frac{R_p}{R_B}\right)^2\right] + \frac{\frac{2}{15}Re_B^{0.72}}{\left[\left(\frac{R_p}{R_B}\right)+1\right]^4}\left[\left(\frac{R_p}{R_B}\right)^3 + 2\left(\frac{R_p}{R_B}\right)^2\right]\right\} + \frac{|G|}{1+|G|} \tag{3}$$

where $|G|$ is the magnitude of the dimensionless particle settling velocity and Re_B is the bubble Reynolds number. This model does not assume Eqs. (1) and (2) are valid. The parameters in Eq. (3) are described by

$$G = \lambda \frac{\tilde{v}_{ps}}{v_B} \tag{4}$$

$$\tilde{\upsilon}_{ps} = -2\frac{R_p^2(\rho_p - \rho_\ell)g}{9\mu_\ell} \tag{5}$$

$$\lambda = 18\frac{Re_p}{Ar} \tag{6}$$

$$\begin{aligned} Re_p &= \frac{\upsilon_{ps}(2R_p)}{\nu_\ell} \\ &= \frac{Ar}{18}; && Re_p < 2 \\ &= 0.152Ar^{0.715}; && 2 \le Re_p < 500 \end{aligned} \tag{7}$$

$$Ar = \frac{\rho_p - \rho_\ell}{\rho_\ell}\frac{(2R_p)^3 g}{\nu_\ell^2} \tag{8}$$

$$Re_B = \frac{\upsilon_B(2R_B)}{\nu_\ell} \tag{9}$$

with Ar = Archimedes number
g = acceleration due to gravity
Re_B = bubble Reynolds number
Re_p = particle Reynolds number
R_B = bubble radius
R_p = particle radius
υ_{ps} = particle settling velocity ($= \lambda\tilde{\upsilon}_{ps}$)
$\tilde{\upsilon}_{ps}$ = particle settling velocity in Stokes flow
υ_B = bubble rise velocity
λ = dimensionless friction factor representing the deviation from Stokes flow
μ_ℓ = dynamic viscosity
ν_ℓ = kinematic viscosity
ρ_ℓ = fluid density
ρ_p = particle density

Hence, Figs. 1 and 2 correspond to the exact solution for P_c with $|G| = 0$.

The effect Re_B has on P_c is shown in Fig. 3 for $|G| = 0.1$. This figure represents the general trends observed when Re_B is varied with different values of $|G|$. The bubble Reynolds number has a negligible effect on the P_c predictions when $R_p/R_B \lesssim 0.05$, and P_c is constant for a given value of $|G|$, with a higher constant value of P_c corresponding to larger values of $|G|$ [1]. When $R_p/R_B \gtrsim 0.05$, P_c increases exponentially with increasing R_p/R_B. Additionally, the increase in P_c is more abrupt as Re_B increases. When $R_p/R_B = 1$, $P_c \le 1$ for $Re_B \le 100$. As previously stated, these predictions are questionable when $Re_B > 100$ because the stream function used to generate this prediction included data only up to $Re_B = 100$ [6]. In our predictions, when $Re_B = 500$ and $R_p/R_B \gtrsim 0.3$, $P_c > 1$, but P_c is independent of Re_B when $R_p/R_B \lesssim 0.05$ and Eq. (3) can be used outside its given Re_B range under these specific conditions.

Figure 4 shows the effect $|G|$ has on P_c for $Re_B = 10$ and represents general trends. The approximate solution assumes Eqs. (1) and (2) are valid, which is the result found in Yoon and

Luttrell [6], with the inclusion of the particle settling velocity (|G|). This figure reveals that particle settling velocity is important, and Eqs. (1) and (2) are valid at small values of R_p/R_B. Conversely, as $R_p/R_B \rightarrow 1$, Eqs. (1) and (2) are not applicable and the inclusion of |G| has only a secondary effect.

Additional calculations have been performed for fixed values of R_p/R_B when both |G| and Re_B are varied. A sample of the resultant contour plots is shown in Fig. 5 for $R_p/R_B = 0.1$, where the contour lines represent P_c values with logarithmic increments. For small Re_B, P_c is a strong function of |G|. As Re_B increases, P_c is independent of |G| when |G| is small. At large |G|, P_c is independent of Re_B for all values.

Direct experimental observations of the collision process are very complicated because it is difficult to isolate this microprocess from the other microprocesses in actual flotation separation. However, attempts to experimentally record P_c have been made by a few researchers addressing mineral flotation [6-11]. We compared our predictions for P_c with this available experimental data in [1]. Figure 6 shows one such comparison with the quartz data of Nguyen-Van [9]. Nguyen-Van [9] also developed a rather complicated expression for P_c, which is summarized in [1] and is also shown in Fig. 6. Our P_c prediction has a much simpler form and does a good job at following the experimental data. The largest discrepancy is at the largest R_B values, but this is still within ~25% of the experimental data. This deviation between our predictions and the experimental data may be due to the collision angle having an effect at these conditions. Predictions of P_c assuming Eqs. (1) and (2) are valid, but $|G| \neq 0$, are also shown in Fig. 6. This result does not significantly differ from that of the exact solution because the experimental conditions satisfy the assumptions incorporated into the approximations. The predictions of Yoon and Luttrell [6] are also shown in Fig. 6 and do not predict the experimental results very well, indicating that |G| has a significant effect for these experimental conditions.

4.1.2 Probability of Adhesion Improvements

Particle attachment by sliding over the bubble surface is probably the single most important microprocess in the overall flotation macroprocess, and it is also possibly the most complicated. We have recently developed a closed-form approximation for P_{asl}, the probability of attachment by sliding, which is a function of the various system parameters and the liquid film thickness between the bubble and particle. Details of this expression can be found in Member Company Report 6 of this research [2], and a summary will only be provided here. The expression for P_{asl} has the form

$$P_{asl} = \exp\left[-2\left(\frac{\lambda}{C_B}\right)\left(\frac{R_p}{R_B + R_p}\right)\left|\frac{G + g(R_B + R_p)}{k(R_B + R_p)}\right|\left(\frac{h_0}{h_{crit}} - 1\right)\right] \tag{10}$$

where λ represents the deviation of the particle friction factor from that corresponding to Stokes flow; C_B gauges the mobility of the bubble surface; R_p and R_B are the particle and bubble radii, respectively; G is the dimensionless particle settling velocity; $g(R_B + R_p)$ and $k(R_B + R_p)$ are functions of $(R_B + R_p)$ and correspond to intermediate flow of Yoon and Luttrell [6]; and h_0/h_{crit} is the ratio of initial-to-critical film thickness of the fluid separating the particle and bubble. The equations for λ and G have been presented above, the remaining values are expressed by

$$\begin{aligned} C_B &= 1; \quad \text{rigid bubble surface} \\ &= 4; \quad \text{mobile bubble surface} \end{aligned} \tag{11}$$

$$g(R_B + R_p) = \left[1 - \frac{3}{4}\left(\frac{R_B}{R_B + R_p}\right) - \frac{1}{4}\left(\frac{R_B}{R_B + R_p}\right)^3\right] + \frac{Re_B^{0.72}}{15}\left[\left(\frac{R_B}{R_B + R_p}\right) + \left(\frac{R_B}{R_B + R_p}\right)^3 - 2\left(\frac{R_B}{R_B + R_p}\right)^4\right] \quad (12)$$

$$k(R_B + R_p) = -\left\{\left[1 - \frac{3}{2}\left(\frac{R_B}{R_B + R_p}\right) + \frac{1}{2}\left(\frac{R_B}{R_B + R_p}\right)^3\right] + 2\frac{Re_B^{0.72}}{15}\left[\left(\frac{R_B}{R_B + R_p}\right)^4 - \left(\frac{R_B}{R_B + R_p}\right)^3 - \left(\frac{R_B}{R_B + R_p}\right)^2 + \left(\frac{R_B}{R_B + R_p}\right)\right]\right\} \quad (13)$$

Using Eq. (10), P_{asl} has been calculated for a variety of conditions. In these calculations, the bubble rise velocity has been determined by curve-fitting the data presented by Clift et al. [12] for contaminated water systems to generate a relationship for υ_B as a function of R_B (see, for example, [5], Fig. 2), C_B was fixed to correspond to a rigid bubble surface (C_B = 1) since the system typically contains surfactants, and the fluid properties correspond to those of water. Hence, P_{asl} is only a function of R_B, R_p, ρ_p, and h_0/h_{crit}. However, Schulze [13] has indicated that h_0 is a function of particle diameter, viscosity, particle settling velocity, surface tension, and surface mobility, and it depends on the specific system of interest. In the preliminary calculations shown here, we have assumed that h_0 is independent of these variables. More details are presented in [2].

Figure 7 displays P_{asl} as a function of bubble radius for selected particle radii and fixed conditions of h_0/h_{crit} = 5 and ρ_p = 1.3 g/cm^3. The large filled circles on the R_p = 200, 300, and 500 μm curves represent conditions when $R_p = R_B$, values where calculations are terminated (i.e., the model is valid for $R_p < R_B$). As shown, P_{asl} covers over four orders of magnitude, depending on R_p, with smaller P_{asl} corresponding to smaller R_p. Also, P_{asl} decreases with increasing R_B, with the largest decline at $R_p \approx 100$ μm. Additionally, for very small or very large R_p, P_{asl} is not a strong function of R_B.

The latter trend is apparent in Fig. 8, where P_{asl} is shown as a function of R_p for selected R_B and fixed h_0/h_{crit} = 5 and ρ_p = 1.3 g/cm^3. Again, the large filled circles represent conditions when $R_p = R_B$. For a fixed particle radius, P_{asl} increases with decreasing R_B. However, when R_p is very small, P_{asl} is almost independent of R_B with $P_{asl} \approx 0.00033$ at R_p = 1 μm and the other conditions as given. P_{asl} does not increase substantially until R_p > 10 μm for R_B = 0.1 mm and R_p > 100 μm for R_B = 5 mm.

Figure 9 shows the influence particle density has on P_{asl} for fixed R_B = 0.5 mm, R_p = 50 μm, and h_0/h_{crit} = 5. As the particle density increases, P_{asl} increases. This is expected since increasing the particle density will increase the particle settling velocity and allow the inertia force to bring the particle closer to the bubble, promoting attachment by sliding.

At the time of this status report writing (February 9, 1998), additional P_{asl} figures were being generated and parametric influences on h_0 and/or h_{crit} were being researched. Details can be found in Member Company Report 6 of this project [2].

4.1.3 Model Validation Status

Dr. Krishna Maruvada joined our research group as a Post Doc on January 15, 1998 and has a charge to conduct model validation experiments for our first-generation flotation model. The

model is a two parameter population balance-type kinetic model for the removal of contaminant particles from waste paper. The formation of a bubble-particle aggregate has been modeled as a first order reversible reaction with two rate constants, k_1 and k_2 of the forward and reverse reactions, respectively. These two constants depend upon the physical properties of the system, as well as on various other parameters such as bubble size, particle size, particle density and the hydrodynamic conditions in the flotation cell [4, 5]. To validate this model, we propose to conduct experiments under carefully controlled conditions so that the dependence of the two parameters can be studied as a function of various system variables.

As a preliminary step, we have analyzed available flotation deinking data in light of our model. Vidotti et al. [14] have recently published experimental results for the deinking of office paper. Four different paper samples containing the same number of printed characters were repulped under defined standard conditions. The four experiments differ from each other in the way the paper was printed. Two were printed using laser printers (HP-3LP and HP-4LP) and the remaining two were printed using copy machines (Cannon and Toshiba). Flotation experiments were conducted in a pilot plant for each of these samples. Handsheets of the feed stock and flotation accepts were analyzed by image analysis to determine the particle size distribution.

The following procedure is adopted for our analysis of the Vidotti et al. [14] data. For each size range, Vidotti et al. [14] tabulated the number of free ink particles (n_p^f) per 10 cm^2 in the flotation accepts as a function of time (t). Since the original number of particles in each size range are known from the feed concentration, the number density which is given by the following equation can be calculated and is plotted as a function of time.

$$\gamma(t) = \frac{n_p^f(t)}{n_p^f(t=0)} \tag{14}$$

Our theoretical model predicts that the rate of change of particle number density depends on the two model parameters as given by [5, 15]

$$\frac{d\gamma}{dt} = -k_1 n_p \gamma^2(t) + \left[k_1\left(n_p - n_B\right) - k_2\right]\gamma(t) + k_2 \tag{15}$$

Hence from the experimental data, the rate of change of particle number density is plotted as a function of the number density γ and a second degree polynomial is fitted to the resulting curve. From the coefficients of the fitted polynomial the values for the model parameters (k_1 and k_2) are obtained for each size range.

The results from this analysis of the four samples are plotted and given below. Figure 10 presents the dependence of k_1, the kinetic constant representing particle removal, on the particle size. Since k_1 and k_2 are obtained by quadratic regression, the experimental data is statistically insufficient to draw any quantitative conclusions regarding their dependence on the size of the ink particle. However, the following qualitative observations can be made:

(i) k_1 is positive indicating that the formation of the bubble particle aggregate is favored for all particle sizes presented above.

(ii) k_1 is small when the particle diameter is small and increases with the particle size.

These observations are qualitatively in agreement with the predictions of our model. According to the model, k_1 is a product of the probabilities of various microprocesses. The probability of capture indicates that for a given bubble size the probability increases with the particle size. Accordingly, for small particles the probability is low and consequently k_1 is small. Hence, for small particles, the model agrees with the experimental observations. As a next step, the model predictions for k_1 will be generated for the given experimental conditions so that a quantitative comparison can be made.

Figure 11 indicates the dependence of k_2 on particle diameter. Although the data appear to be scattered, it may be observed that most of the values for k_2 in the figure are negative. However, in our model k_2 is a kinetic constant representing the destruction of bubble/particle aggregates

and is a positive number. The negative value physically implies that $k_2 = 0$ and the bubble/particle aggregate is very stable for the flotation conditions of Vidotti et al. [14]. Considering that the size of the bubble in their experiments is of the order of 2 mm, we may expect that bubble/particle aggregate to remain stable for small particle diameters.

At the time of this report writing, an experimental plan was being developed in which a series of controlled experiments will be conducted in our laboratory to systematically study the dependence of various variables on the model parameters and overall flotation efficiency. One possible approach is to identify a material that has similar physical and surface properties to that of toner particles, but can be obtained in various uniform sizes in the particle size range applicable to flotation deinking. This material would then be added to a clean fiber slurry and flotation experiments will be performed to determine removal efficiencies. Alternatively, real recycled office paper will be repulped using standard TAPPI procedures, which will then be used for the flotation experiments. Handsheets will be prepared from the flotation accepts and number of ink particles present will be counted using image analysis. This latter approach is more realistic, but initial particle size is more difficult to control.

As a first step in our experimental program, we plan to investigate the influence of bubble size on the overall flotation efficiency and compare the experimental results with our model predictions. One of the ways to study the dependence of bubble size is by using different kinds of surfactants. Each surfactant has a specific critical micelle concentration which uniquely determines the corresponding surface tension. The equilibrium surface tension can be measured by the DCA (Dynamic contact angle analyzer) which is available at IPST. By using an appropriate constant gas injection rate and impeller speed, such that the air bubbles formed will remain in equilibrium with the bulk solution, bubbles of different sizes can be created by changing the surfactants. Flotation efficiencies will be plotted as a function of bubble size while keeping all other parameters constant and compared to model predictions.

4.1.4 Modeling Summary

Research during the past year in flotation modeling has focused on improving the microprocess probability predictions of capture (P_c) and adhesion by sliding (P_{asl}), as well as model validation experiments. Member Company Reports 4 and 6 [1, 2] of this research detail the efforts in the P_c and P_{asl} improvements, respectively. The model validation experiments were delayed until late January. However, with the arrival of Dr. Maruvada in January, the model validation experiments are currently underway.

4.2 Bubble Size Measurements

Bubble size is important for effective flotation deinking. Member Company Report 3 of this project [16] summarized a method to visualize bubble dynamics and measure bubble size distributions in a fiber suspension at consistencies typical of flotation deinking. Initial results were also presented for bubble size measurements in an ONP system without added system chemistry. During the past year, experiments were performed to determine the bubble size in a quiescent bubble column with four different experimental systems: (1) ONP systems with various chemistries and chemistry concentrations; (2) NBSK systems with various consistencies but no added chemistry; (3) a copy paper system with no added chemistry; and (4) an ONP system with no added chemistry but a higher gas flow rate. Table 1 summarizes all experimental conditions addressed during this time. Specific details of this portion of the project have recently been reported in Member Company Report 5 of this project [3]. This section will highlight the conclusions of this report.

Table 1: Experimental conditions addressed in Member Company Report 5.

System	Consistency	Air Flow Rate (slpm)	System Chemistry
Water only	0%	0.25	None added
Water only	0%	0.25	BRD 2360 - 1.7 ml/kg
Water only	0%	0.25	BRD 2360 - 3.3 ml/kg
Water only	0%	0.25	BRD 2360 - 6.7 ml/kg
Water only	0%	0.25	BRD 2342 - 1.7 ml/kg
Water only	0%	0.25	BRD 2342 - 3.3 ml/kg
Water only	0%	0.25	BRD 2363 - 1.7 ml/kg
Water only	0%	0.25	BRD 2363 - 3.3 ml/kg
Water only	0%	2.0	None added
ONP	1%	0.25	None added
ONP	1%	0.25	BRD 2360 - 1.7 ml/kg
ONP	1%	0.25	BRD 2360 - 3.3 ml/kg
ONP	1%	0.25	BRD 2360 - 6.7 ml/kg
ONP	1%	0.25	BRD 2342 - 1.7 ml/kg
ONP	1%	0.25	BRD 2342 - 3.3 ml/kg
ONP	1%	0.25	BRD 2363 - 1.7 ml/kg
ONP	1%	0.25	BRD 2363 - 3.3 ml/kg
ONP	1%	2.0	None added
NBSK	0.1%	0.25	None added
NBSK	0.5%	0.25	None added
NBSK	0.5%	2.0	None added
NBSK	1.0%	2.0	None added
NBSK	1.5%	2.0	None added
Copy Paper	1%	2.0	None added

4.2.1 Effect of System Chemistry

The effect of system chemistry conditions on bubble size in an ONP suspension was addressed by modifying an air/water/1% ONP fiber system with three different deinking chemistries: (i) BRD 2360, a fatty acid; (ii) BRD 2342, a nonionic surfactant; and (iii) BRD 2363, a fatty acid/nonionic surfactant blend. All system chemistry variations were investigated in 0 and 1% ONP consistency systems. The 0% consistency system corresponds to an air/water system, where the chemical concentration is based on the mass of dry fiber in the 1% ONP system. Additionally, all tests were conducted at a constant air flow rate of 0.25 slpm, and both the gasket and sparger air injection techniques were investigated. Specific experimental details can be found in [3].

The average bubble diameters at Position 2 in our bubble column are summarized in Fig. 12 as a function of BRD 2360 concentration (the fatty acid). The typical chemical concentration of 3.3

ml/kg (6 lbs/ton) is recommended by the chemical supplier (Buckman Laboratories) for ONP deinking, and this concentration is identified for reference. It appears that only the gasket at 1% ONP consistency is significantly affected by the BRD 2360 concentration. This may be more of a function of the physical system than chemical concentration. In the air/water system, the average bubble diameter is not significantly affected by the BRD 2360 concentration for either air injection method because the bubbles are free to disperse and coalescence is limited. When 1% ONP is added to the system, the average bubble diameter increases, but it is relatively unaffected by BRD 2360 concentration when the sparger air injection technique is used. This is because the sparger head allows air into the system over a relatively large surface area. The bubbles require a sufficient buoyant force to rise through the fiber network, resulting in the increased bubble diameter. Since they enter the system at different locations along the sparger head, depending on the path of lowest pressure drop, the 1% fiber suspension remains fairly well-mixed and the bubble diameters remain uniform for each system chemical concentration. In contrast, for the gasket air injection technique, air enters the system through a single port. The air bubbles again must have a sufficient buoyant force to rise through the fiber network. If the system does not remain well-mixed, a fiber network slightly different from the previous test condition may form, which may require larger (or smaller) bubbles to break through this network. It is hypothesized that this type of system was present at 3.3 ml/kg of BRD 2360 with the gasket air injection, resulting in a significant change in average bubble diameter.

Figure 13 shows the average bubble diameters as a function of BRD 2342 concentration (the nonionic surfactant). As expected, the 1% ONP results yield larger average bubble diameters than the air/water systems (0% consistency) for all test conditions. In the air/water system, the sparger results show a slight increase in bubble size when the BRD 2342 concentration increases. The gasket data do not follow this trend. When 1% ONP is added to the system, the average bubble size reveals an increasing trend with increasing BRD 2342 concentration for both air injection techniques. Additionally, on average, the sparger produces larger bubbles than the gasket at Position 2.

A plot of average bubble size as a function of BRD 2363 concentration (the fatty acid/ nonionic surfactant blend) is shown in Fig. 14. Although there are significant standard deviations associated with each average bubble size measurement, as shown in the figures associated with [3], a general trend of increasing average bubble size with increasing BRD 2363 concentration is revealed for all test conditions, except the 1% ONP sparger data.

Figure 15 shows the average bubble diameters for the three different chemistries at a concentration of 1.7 ml/kg. Focusing on the gasket results, the average bubble size trends for the 0 and 1% ONP consistency systems coincide when the chemistry type is altered. In contrast, when the sparger is used as the air injection technique, the average bubble size trends for the 0 and 1% ONP systems counter one another when the system chemistry changes. The results reveal that BRD 2342 produced the largest average bubble diameters at 1% ONP with the sparger air injection technique. For all other systems, this trend is reversed and BRD 2342 results in the smallest average bubble size. Similar trends are revealed when the chemical concentration is 3.3 ml/kg (Fig. 16).

It was suggested by various PAC members that surface tension may be a significant parameter and may make it difficult to determine specific chemistry effects. This was not recorded for the specific samples utilized in these experiments (but will be recorded for all future experiments). To determine what effect, if any, surface tension has on the bubble size in the air/water system, the various chemicals addressed in this study were individually added to deionized water in the specified concentration. The surface tension was measured with a Wilhelmy plate balance. In general, the higher the chemical concentration, the lower the surface tension, indicating that the CMC (critical micelle concentration) was not reached [17].

Figure 17 is a plot of average bubble size obtained in our experiments as a function of surface tension and shows no significant trends. In bubble size studies in air/water systems by other researchers, the effect of surfactants is not clear. Kim et al. [18] cite prior work they completed where increasing the surface tension increased the bubble size only by a small amount. Nicol and Davidson [19] state that surfactants stabilize the bubble surface and hinder

bubble coalescence, so their presence should reduce the mean bubble size, assuming considerable bubble coalescence would occur without the added surfactant. This type of system was not observed in our quiescent bubble column. Additionally, Schulze [20] provides a relationship between bubble size, surface tension, fluid density, and mixing intensity which would indicate bubble size should decrease with decreasing surface tension. In contrast, Lin et al. [21] conclude that bubble diameter is a complex function of surface tension, fluid density, bubble contact diameter at the injection port, and contact angle at the bubble-fluid-solid interface (i.e., the injector location). They further remark that the dominant factor influencing the bubble size in their system is the contact angle, measured in the fluid at the orifice surface. Therefore, bubble size is influenced strongly by the surface energy of the injection port. Based on this literature, and as shown in this study, bubble size is not a simple function of surface tension.

It was also suggested by PAC members that viscosity may also play a significant role and should be measured for each system. However, fluid viscosity measurements in dilute fiber systems (~1%) are difficult with common viscometers because these devices require the medium to be continuous at dimensions similar to those of individual fibers. The 1% ONP system used in this study does not satisfy this requirement. Additionally, Chase et al. [22] have indicated that using rotational viscometers, such as the cup and bob, cone and plate, or spindle types, resulted in apparent viscosity measurements approaching that of water when testing pulp suspensions at consistencies as high as 1.5%. They also record viscosities close to that of water for hardwood pulps with consistencies less than 3% and a freeness of 300-400 ml CSF. These measurements were recorded in a rotating viscometer they developed. Therefore, viscosity may not be the most appropriate measure to determine the effect the fibers have on bubble formation. The crowding factor [23-26] may be a better measure of fiber-fiber interactions and their effect on bubble size. Research in this area will commence during 1998-1999.

4.2.2 Effect of Fiber Type

Experiments in a quiescent bubble column using northern bleached softwood kraft (NBSK), copy paper, and ONP have also been completed to determine if various fiber types have a significant influence on the recorded bubble diameters. The weight-weighted average fiber length and ash content of the fibers used in this portion of the study are summarized in Table 2. Deionized water was used as the fiber suspending fluid and no additional chemistry was added to the various systems.

Table 2: Fiber length and ash content of the fiber types used in this study.

	Average Fiber Length (mm)	Ash Content (%)
ONP	1.4	0.7
NBSK	2.8	0.3
Copy Paper	2.0	6.6

Experiments were first conducted in NBSK with an air flow rate of 0.25 slpm. These longer fibers produced large, infrequent bubbles at this air flow rate. Therefore, a series of experiments were completed in which an air flow rate of 2 slpm was used in the quiescent bubble column. This air flow rate will be used to compare fiber type effects. Detailed results can be found in [3].

Flash x-rays were taken of a NBSK system at consistencies of 0, 0.5, 1.0 and 1.5% and an air flow rate of 2 slpm. Both the gasket and sparger air injection technique were used in these experiments. Figure 18 shows the x-ray composite for the air/water system at 2 slpm with the sparger air injection. The Tygon tubing used as the air line is clearly visible on the left-hand side of the column. Many bubbles are observed with this type of air injection, as indicated by the many dark regions on the radiographs. These bubbles are rather small and rise in a turbulent fashion and encompass the entire column width. The many rising bubbles carry small amounts of fluid in their wakes as they rise, moving the fluid from the column bottom to the top. Due to continuity considerations, this fluid is replaced by fluid descending along the column sides. This

general phenomenon is typically termed backmixing and results in the many small bubbles recorded on the left-hand side of Position 1 in Fig. 18. The many small bubbles that descend in the backmixed flow are eventually entrained in the bulk rising column of air. The large number of bubbles and backmixing have a visible effect on the gas holdup of the system, defined as the percent gas by volume, and results in a considerable increase in the height at the air/liquid interface. The increase in fluid height to approximately 84 cm results in a gas holdup of almost 5% for these conditions.

Adding 1.0% NBSK into the system with sparger air injection results in a significant change in flow conditions (Fig. 19). Many small bubbles are still present, but periodically very large bubbles develop near the sparger head and rise through the system. The bulk rising air flow oscillates in a serpentine fashion, and the larger bubbles follow this pattern. Some of the smaller bubbles are caught in the backmixed flow, but are eventually entrained in the bulk flow. The increase in gas holdup is clearly visible, but its value is difficult to determine due to the waviness at the air/liquid interface. This is caused by the large bubbles breaking through the surface, which is just about to happen in Fig. 19 at Position 4 as three large bubbles are just about to disrupt the air/liquid interface and exit the system.

Figure 20 shows the bubble size distributions acquired with the sparger air injector at Position 2 in the bubble column. The average bubble size and standard deviation increase with increasing NBSK consistency, but this is primarily the result of the increase in the number of very large bubbles as the consistency increases. Most of the large bubbles have an equivalent diameter greater than 25 mm. Since the column thickness is only 20 mm, these bubbles can span the entire column depth if they are spherical and the equivalent bubble diameter for these large bubbles is not the appropriate term. (Recall, by definition, the equivalent bubble diameter is the diameter of the circle whose area equals that of the bubble area recorded on the x-ray film.) Although the number of these bubbles is rather small compared to the entire bubble population, the number clearly increases with increasing consistency. One very apparent feature of Fig. 20 is that the bubble size distribution is bimodal; there is a range of small bubbles and a range of very large bubbles, but few bubbles in the intermediate size range. The distribution of small bubbles (bubble diameters less than approximately 10 mm) is similar as NBSK consistency increases, with a peak in all cases in the 2-3 mm range. The main difference is that the magnitude of the peak decreases as NBSK consistency increases, and is due to the increase in the number of bubbles greater than 25 mm as consistency increases. Focusing on bubble diameters that are less than 10 mm and neglecting those that are greater, averages can be generated. For each test condition, the average is 3.0, 3.0, 3.0, and 3.3 mm for the 0, 0.5, 1.0, and 1.5% consistency systems, respectively, indicating the uniformity in this region.

Although the sparger produces few very large bubbles, which increase in number as the NBSK consistency increases, these large bubbles serve a very important function. They act as "mobile mixers" in this fiber suspension and maintain a uniform system throughout the bubble column. This allows for the majority of the bubbles to remain relatively small and free to move through the system. In terms of flotation deinking cells, the small bubbles would capture ink particles, and the large bubbles would keep the suspension homogeneous by preventing fiber network and air channel formation.

The average bubble size as a function of fiber consistency is shown in Fig. 21 for the NBSK results. The ONP results reported in [16] with no added system chemistry are also included for reference, although they correspond to an air injection rate of 0.25 slpm. Focusing on the NBSK results, the gasket injection technique produces a larger average bubble diameter for all consistencies addressed. The large average bubble diameter at 1% NBSK from the gasket injection is hypothesized to be the result of nonuniform fiber networks between the various consistencies. There is, however, a general trend of increasing bubble diameter with increasing consistency. This trend is more apparent with the sparger air injection technique. As discussed above, the increase in average bubble diameter for the sparger with increasing consistency is due to the increase in the number of large bubbles, but constitutes a small percentage of the overall bubble population.

Additional bubble size measurements were obtained in a 1% unprinted copy paper (Union Camp Yorktown xerographic paper as supplied to IPST) and ONP system with a 2 slpm air injection rate and compared to the 1% NBSK system. The bubble size distributions for the NBSK and copy paper system are very comparable when the gasket air injection is used (Fig. 22). The ONP system produces a smaller average bubble size and the bubble size distribution is shifted to much smaller bubble sizes.

Figure 23 reveals the bubble size distributions when the sparger air injection is used. Again, the NBSK and copy paper system reveal similar distributions and average bubble diameters. Additionally, the ONP system produces a similar distribution, that is, most of the bubbles for all systems are confined to bubble diameters less than approximately 10 mm. The differences between the ONP and chemical pulp systems are found outside this range, where a few bubbles are found. The ONP system has approximately 1% of its bubble population with a diameter greater than 10 mm, but these few bubbles are spread out over a variety of diameters. In contrast, the NBSK system has approximately 5% of its bubble population with diameters greater than 10 mm, with 3% greater than 25 mm. The few, but very large, bubbles in the NBSK system cause the average bubble diameter to be larger than that recorded for the ONP system. One significant feature Fig. 23 displays is the importance of these few large bubbles; they create a uniform system that helps maintain the majority of the bubbles in a relatively narrow bubble size distribution, regardless of fiber type.

4.2.3 Bubble Size Measurements Summary

A large amount of bubble size data have been obtained over the past year and details are provided in [3]. For the specific chemistries addressed here and added to an air/water system or an air/water/1% ONP system, clear trends were difficult to ascertain due to the variations in the fiber network structure for the different test conditions. However, in general, the nonionic surfactant produced smaller average bubble diameters, but variations in the general trends were observed.

The northern bleached softwood kraft (NBSK) studies were conducted at an air flow rate of 2 slpm, which produced severe backmixing. This resulted in the sparger air injection technique yielding a higher gas holdup and a bimodal bubble size distribution, with the majority of the bubbles in the size range less than 10 mm in diameter and a peak in the 2-3 mm range. The bubbles in this range all have the same average bubble size (~3 mm) for all NBSK fiber consistencies addressed here, but the relative frequency decreases with increasing consistency. Few bubbles are greater than 10 mm in diameter, but there are those that are typically larger than 25 mm. The number of bubbles that fall in this category increases with increasing NBSK consistency. These larger bubbles play an important role by acting as mobile mixers, which keeps the smaller bubbles uniform and the fiber suspension well-mixed and homogeneous. Also, the average bubble size increases with NBSK fiber consistency.

Results for 1% copy paper and 1% ONP systems with an air injection rate of 2 slpm were also obtained and compared to those from 1% NBSK. The most significant difference was that the ONP system produced the smallest average bubble size.

4.2.4 FXR Flow Loop Status

Future bubble size measurement work utilizing the flash x-ray equipment will focus on cocurrent bubble columns, where the gas and fiber slurry is rising through the test section. This will be accomplished with a recently completed flow loop, schematically shown in Fig. 24. The flow loop consists of two baffled holding tanks to allow any gas in the system to escape, a pump, a flow meter, associated plumbing, and a bubble column. The bubble column consists of two 1 m sections attached end-to-end with interior dimensions 10 cm $\times$ 2 cm. A fiber slurry will travel from the column bottom to the top, and air will be injected at the column base. The flow loop will ensure that a uniform fiber suspension is maintained because of the continuous mixing. The cocurrent flow loop is designed such that countercurrent flow could be produced, or, with slight modifications to the framing, the column could be orientated horizontally. Tests will be

conducted to determine the effect of stock flow rate on bubble size. The fiber crowding factor will also be addressed, and surface tension will be recorded for all experimental conditions. X-rays will be taken at selected locations, and image analysis will be performed to determine the equivalent bubble diameters.

4.3 NEW DEINKING TECHNOLOGIES

I have been asked to summarize the latest deinking technologies (N. Sanders November 24, 1997 memo) for the PAC. Of specific interest was the Regenex and packed column technologies. However, information pertaining to packed column deinking technology was not available in the open literature. Regenex provided a packet of product literature, which also included a video of the process [27].

The Regenex technology is termed a Continuous Batch Fiber Recovery System (CBFRS) and was adapted from industrial textile and linen laundering operations. The system consists of a series of interconnected cylindrical modules which oscillate in synchronization. Material is transferred from module to module during processing (i.e., each module is one batch, but is processed in series producing a continuous operation). Each individual module can be likened to a small reaction vessel where temperature, chemistry, and consistency can be well-controlled. Any required water is also controlled and flows counter to the material flow.

With a modular design, the Regenex product literature states that paper recycling systems can be designed for as small as 3 tpd or as large as 200-300 tpd. The modular design also allows for greater flexibility so that one system can be configured to process multiple recovered paper grades at different times. Regenex claims that the system has been especially effective in deinking mixed office paper, milk carton stock, aseptic packaging, and old newspapers. According to Regenex, the benefits of this system over traditional technologies include:

- A much lower paper demand over conventional deinking systems (approximately 150 kW/hour/ton).
- Lower engineering, construction, and maintenance costs due to the modular design and skid-mounted system.
- Capacity is easily increased by installing additional modules or processing lines.
- Stock transfer is simplified, eliminating piping, values, pumps, and storage tanks.
- Bleaching is easily integrated into the modular system.

Overall, the Regenex system would work well to recover fiber from very specialized recovered paper stocks which may be highly contaminated. Alternatively, it could also be considered if an incremental increase in recycling capacity is required.

In addition to the Regenex technology, a search of recent patents in the area of deinking equipment has identified two additional technologies that are typically not found in traditional recycling operations. Extraction technology was utilized by Walker [28] to remove soluble ink (i.e., water-based) from newsprint. This is an extension of screw-press technology. Marwah and Gold [29, 30] indicate that magnetic separation may be used to remove ink and stickie particles from recovered paper. An agglomerator and magnetic material are added to the fiber suspension and the contaminant particles (inks and/or stickies) coalesce onto the magnetic particles. The aggregate is then removed through a magnetic separator, leaving clean fiber behind. Owen [31] also has a recent patent addressing deinking by magnetic forces. In this patent, it is claimed that given a strong enough magnetic force, most toner particles could be removed from recovered paper.

This brief review is not a comprehensive summary of all new technologies that may be applicable to contaminant removal in fiber streams. Additional input from PAC members is encouraged.

4.4 RELATED PUBLICATIONS

The following documents authored (or co-authored) by this principal investigator and related to flotation deinking fluid mechanics have been published since March 1997:

- Bose, F., Ghiaasiaan, S.M., and Heindel, T.J., "Hydrodynamics of Dispersed Liquid Droplets in Agitated Synthetic Fibrous Slurries," *Industrial and Engineering Chemistry Research*, **36**:11 5028-5036 (1997). (IPST Technical Paper Series Number 678.)
- Bloom, F., and Heindel, T.J., "A Theoretical Model of Flotation Deinking Efficiency," *Journal of Colloid and Interface Science*, **190**: 182-197 (1997). (IPST Technical Paper Series Number 646.)
- Bloom, F., and Heindel, T.J., "Mathematical Modelling of the Flotation Deinking Process," *Mathematical and Computer Modelling*, **25**(5): 13-58 (1997). (IPST Technical Paper Series Number 634.)
- Heindel, T.J., and Monefeldt, J.L., "Flash X-ray Radiography for Visualizing Gas Flows in Opaque Liquid/Fiber Suspensions," *6th International Symposium on Gas-Liquid Two-Phase Flows*, Vancouver, BC, June 22-26, 1997. (IPST Technical Paper Series Number 639.)
- Heindel, T.J., "The Fundamentals of Flotation Deinking," *1997 TAPPI Pulping Conference*, TAPPI Press, Atlanta, GA, 521-533 (1997). (IPST Technical Paper Series Number 656.)
- Heindel, T.J., and Monefeldt, J.L., "Observations of the Bubble Dynamics in a Pulp Suspension Using Flash X-ray Radiography," *1997 TAPPI Engineering and Papermakers Conference*, TAPPI Press, Atlanta, GA, 1421-1433 (1997). (IPST Technical Paper Series Number 655.)
- Heindel, T.J., and Bloom, F., "New Measures for Maximizing Ink Particle Removal in a Flotation Cell," *1997 TAPPI Recycling Symposium*, Atlanta, GA, TAPPI Press, 101-113 (1997). (IPST Technical Paper Series Number 635.)
- Heindel, T.J., "FXR Throws 'Light' on the Obscure," *TAPPI Journal*, **80**(6): 20,22, (1997).
- Heindel, T.J., Banerjee, S., and Deng, Y., "Recycling Research at IPST," *PaperAge*, **113**(11): 23-24 (1997). (IPST Technical Paper Series Number 684.)

4.5 RELATED PROPOSALS

Various non-proprietary research proposals have been submitted during the past year to enhance the current flotation deinking fluid mechanics research program. The status of these and related proposals are summarized here.

- "Mixing in Gas/Liquid/Fiber Flows," by T.J. Heindel and submitted to TAPPI Research Foundation. ($32.8K, 1 year, unfunded)
- "Stickies Removal Through Shear-Induced Coalescence and Breakup," by T.J. Heindel, S. Banerjee, S.M. Ghiaasiaan, and S.I. Adbel-Khalik and submitted to the Agenda 2020 Recycling Task Group. ($540K, 3 years, unfunded)
- "An Analysis of Printing and Writing Recovered Paper Grade Specifications," by T.J. Heindel and W.P. Moore and submitted to the Agenda 2020 Recycling Task Group. ($70K, 1 year, unfunded)
- "Bubble Size Control to Improve Oxygen-Based Bleaching," by T.J. Heindel and T.J. McDonough and submitted to the Agenda 2020 Environmental Performance Task Group. ($682K, 3 years, pending)
- "Gas Flows in Fiber Suspensions," by T.J. Heindel and submitted to the NSF CAREER Program. ($200K, 4 years, pending)
- "Model Improvements and Model Validation to Improve Flotation Deinking Performance," by T.J. Heindel and submitted to the Agenda 2020 Capital Effectiveness Program. ($629.4K, 3 years, pending)

5 GOALS FOR FY 98-99:

Goals for the next period (March 1998 to March 1999) are grouped into two areas and are summarized below.

Flotation Modeling

1. Perform model validation experiments and compare the experimental results with model predictions.
2. Extend the theoretical flotation model to relax selected assumptions.
3. Summarize the modeling work in a Member Company Report.

Bubble Size Measurements

4. Determine the effect copy paper consistency has on bubble size in a cocurrent bubble column.
5. Determine the effect superficial gas velocity has on bubble size in a cocurrent bubble column filled with unprinted copy paper.
6. Determine the effect superficial liquid velocity has on bubble size in a cocurrent bubble column filled with unprinted copy paper.
7. Summarize the bubble size measurement work in a Member Company Report.

6 DELIVERABLES:

Two Member Company Reports will be completed during the next year addressing advances in the flotation model (including validation) and bubble size measurements in a cocurrent bubble column.

7 SCHEDULE:

The project is designed such that the two separate areas of flotation modeling and bubble size measurements can be addressed concurrently throughout the year. Specific task numbers refer to the goals stated above.

Task	Apr	May	Jun	Jul	Aug	Sep	Oct	Nov	Dec	Jan	Feb	Mar
1	X	X	X	X	X	X	X	X	X	X		
2				X	X	X	X	X	X	X		
3								X	X	X	X	
4	X	X	X	X								
5				X	X	X	X					
6						X	X	X	X	X		
7									X	X	X	X

8 REFERENCES

[1] Heindel, T.J., and Bloom, F., Mathematical Modeling of the Overall Flotation Deinking Process: Probability of Collision Improvements, Institute of Paper Science and Technology, Atlanta, GA, Member Company Report, Project F00903, Report 4, (January 15, 1998).

[2] Heindel, T.J., and Bloom, F., Mathematical Modeling of the Overall Flotation Deinking Process: Probability of Attachment by Sliding Improvements, Institute of Paper Science and Technology, Atlanta, GA, Member Company Report, Project F00903, Report 6, (In preparation, 1998).

[3] Heindel, T.J., and Emery, A.E., The Effect of ONP Chemistry and Fiber Type on Gas Bubble Size in a Quiescent Bubble Column, Institute of Paper Science and Technology, Atlanta, GA, Member Company Report, Project F00903, Report 5, (February 12, 1998).

[4] Heindel, T.J., and Bloom, F., Mathematical Modeling of the Overall Flotation Deinking Process, Institute of Paper Science and Technology, Atlanta, GA, Member Company Report, Project F00903, Report 1, (December 8, 1995).

[5] Heindel, T.J., and Bloom, F., Mathematical Modeling of the Overall Flotation Deinking Process: Predictions of Selected Performance Parameters, Institute of Paper Science and Technology, Atlanta, GA, Member Company Report, Project F00903, Report 2, (November 25, 1996).

[6] Yoon, R.H., and Luttrell, G.H., "The Effect of Bubble Size on Fine Particle Flotation," *Mineral Processing and Extractive Metallurgy Review*, **5**: 101-122 (1989).

[7] Luttrell, G.H., and Yoon, R.-H., "A Hydrodynamic Model for Bubble-Particle Attachment," *Journal of Colloid and Interface Science*, **154**(1): 129-137 (1992).

[8] Nguyen-Van, A., and Kmet, S., "Collision Efficiency for Fine Mineral Particles with Single Bubble in a Countercurrent Flow Regime," *International Journal of Mineral Processing*, **35**(3/4): 205-223 (1992).

[9] Nguyen-Van, A., "The Collision Between Fine Particles and Single Air Bubbles in Flotation," *Journal of Colloid and Interface Science*, **162**: 123-128 (1994).
[10] Anfruns, J.P., and Kitchener, J.A., "The Absolute Rate of Capture of Single Particles by Single Bubbles," *Flotation*, M.C. Fuerstenau, Ed., New York, American Institute of Mining, Metallurgical, and Petroleum Engineers, Inc., 625-637 (1976).
[11] Anfruns, J.P., and Kitchener, "Rate of Capture of Small Particles in Flotation," *Transactions of the Institution of Mining and Metallurgy - Section C*, **89**: C9-C15 (1977).
[12] Clift, R., Grace, J.R., and Weber, M.E., *Bubble, Drops, and Particles*, Academic Press, New York, 1978.
[13] Schulze, H.J., "Flotation as a Heterocoagulation Process: Possibilities of Calculating the Probability of Flotation," *Coagulation and Flocculation*, B. Dobias, Ed., 321-353 (1993).
[14] Vidotti, R.M., Johnson, D.A., and Thompson, E.V., "Repulping and Flotation Studies of Photocopied and Laser-Printed Office Paper: Part II: Flotation," *Progress in Paper Recycling*, 3(3): 39-49 (1994).
[15] Heindel, T.J., and Bloom, F., "New Measures for Maximizing Ink Particle Removal in a Flotation Cell," *1997 TAPPI Recycling Symposium*, Atlanta, GA, TAPPI Press, 101-113 (1997).
[16] Heindel, T.J., A Method to Visualize Gas Bubbles in a Pulp Suspension, Institute of Paper Science and Technology, Atlanta, GA, Member Company Report, Project F00903, Report 3, (February 3, 1997).
[17] Shaw, D.J., *Introduction to Colloid and Surface Chemistry*, 4th Ed., Butterworth-Heinemann, Oxford, 1992.
[18] Kim, S.D., Kim, H.S., and Han, J.H., "Axial Dispersion Characteristics in Three-Phase Fluidized Beds," *Chemical Engineering Science*, **47**(13/14): 3419-3426 (1992).
[19] Nicol, R.S., and Davidson, J.F., "Effect of Surfactants on the Gas Hold-up in Circulating Bubble Columns," *Chemical Engineering Research and Design*, **66**: 159-164 (1988).
[20] Schulze, H.J., "Zur Hydrodynamik der Flotations-Elementarvorgänge," *Wochenblatt Für Papierfabrikation*, **122**(5): 160, 162, 164-168 (1994).
[21] Lin, J.N., Banerji, S.K., and Yasuda, H., "Role of Interfacial Tension in the Formation and the Detachment of Air Bubbles: 1. A Single Hole on a Horizontal Plate Immersed in Water," *Langmuir*, **10**: 936-942 (1994).
[22] Chase, W.C., Donatelli, A.A., and Walkinshaw, J.W., "Effects of Freeness and Consistency on the Viscosity of Hardwood and Softwood Pulp Suspensions," *TAPPI Journal*, **72**(5): 199-204 (1989).
[23] Kerekes, R.J., and Schell, C.J., "Characterization of Fibre Flocculation Regimes by a Crowding Factor," *Journal of Pulp and Paper Science*, **18**(1): J32-J38 (1992).
[24] Kerekes, R.J., and Schell, C.J., "Effects of Fiber Length and Coarseness on Pulp Flocculation," *TAPPI Journal*, **78**(2): 133-139 (1995).
[25] Kerekes, R.J., "Characterizing Fibre Suspensions," *1996 Engineering Conference*, Chicago, TAPPI Press, 21-28 (September 16-19, 1996).
[26] Dodson, C.T., "Fiber Crowding, Fiber Contacts, and Fiber Flocculation," *TAPPI Journal*, **79**(9): 211-216 (1996).
[27] Regenex, Product Literature, Kenner, LA, (1997).
[28] Walker, D.R., "Method and Apparatus for Deinking Newsprint using Counterflow Extractor," United States, Patent Number 5,520,780, (May 28, 1996)
[29] Marwah, N., and Gold, A.A., "Magnetic Deinking of Waste Papers," United States, Patent Number 5,527,426, (June 18, 1996)
[30] Marwah, N., and Gold, A.A., "Magnetic Removal of 'Stickies' from Waste Papers," United States, Patent Number 5,639,346, (June 17, 1997)
[31] Owen, D.M., "Deinking of Paper Using Magnetic Forces," United States, Patent Number 5,685,952, (November 11, 1997).

9 FIGURES

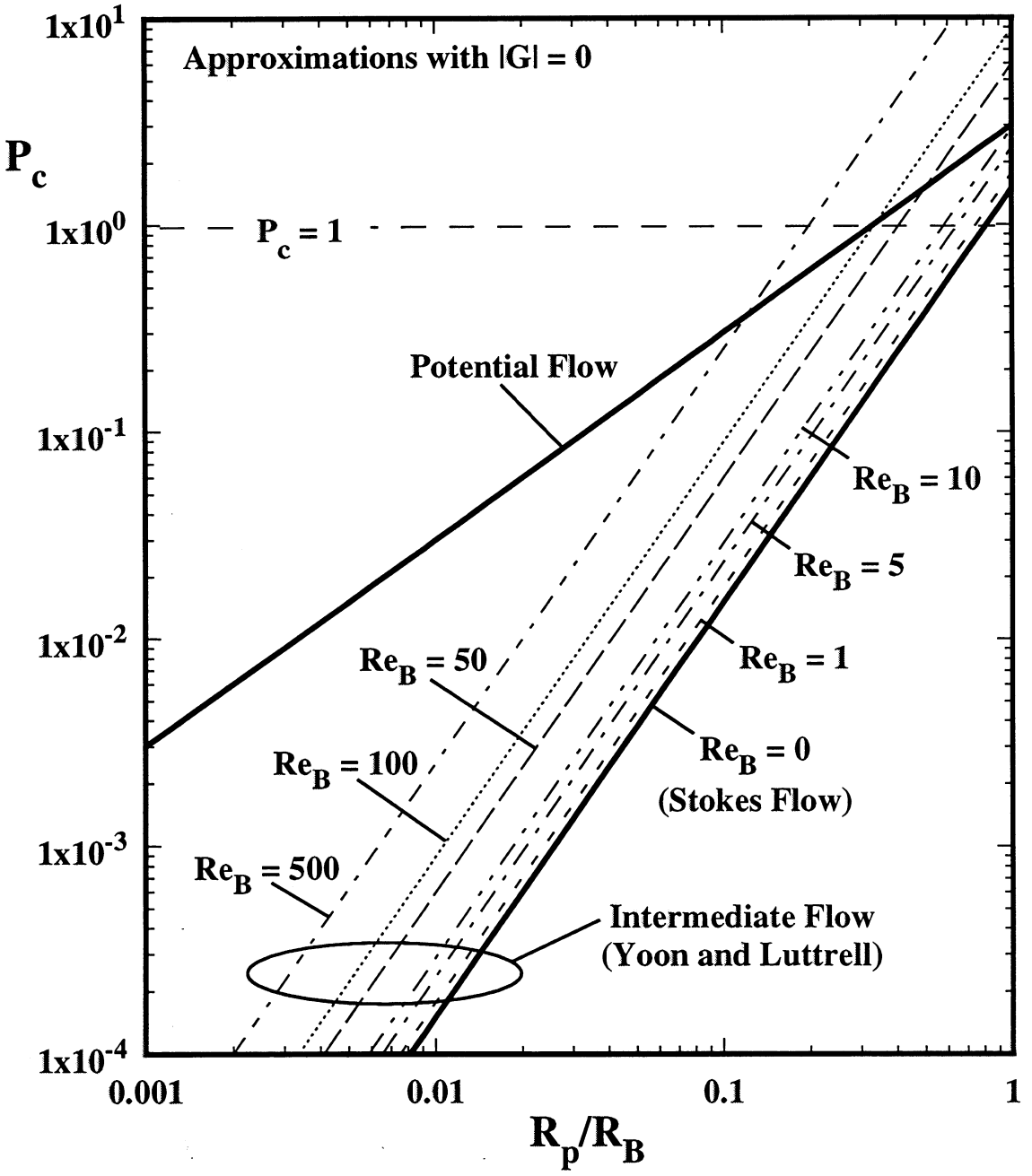

Figure 1: Probability of collision predictions based on potential flow, Stokes flow, and intermediate flow of Yoon and Luttrell [6].

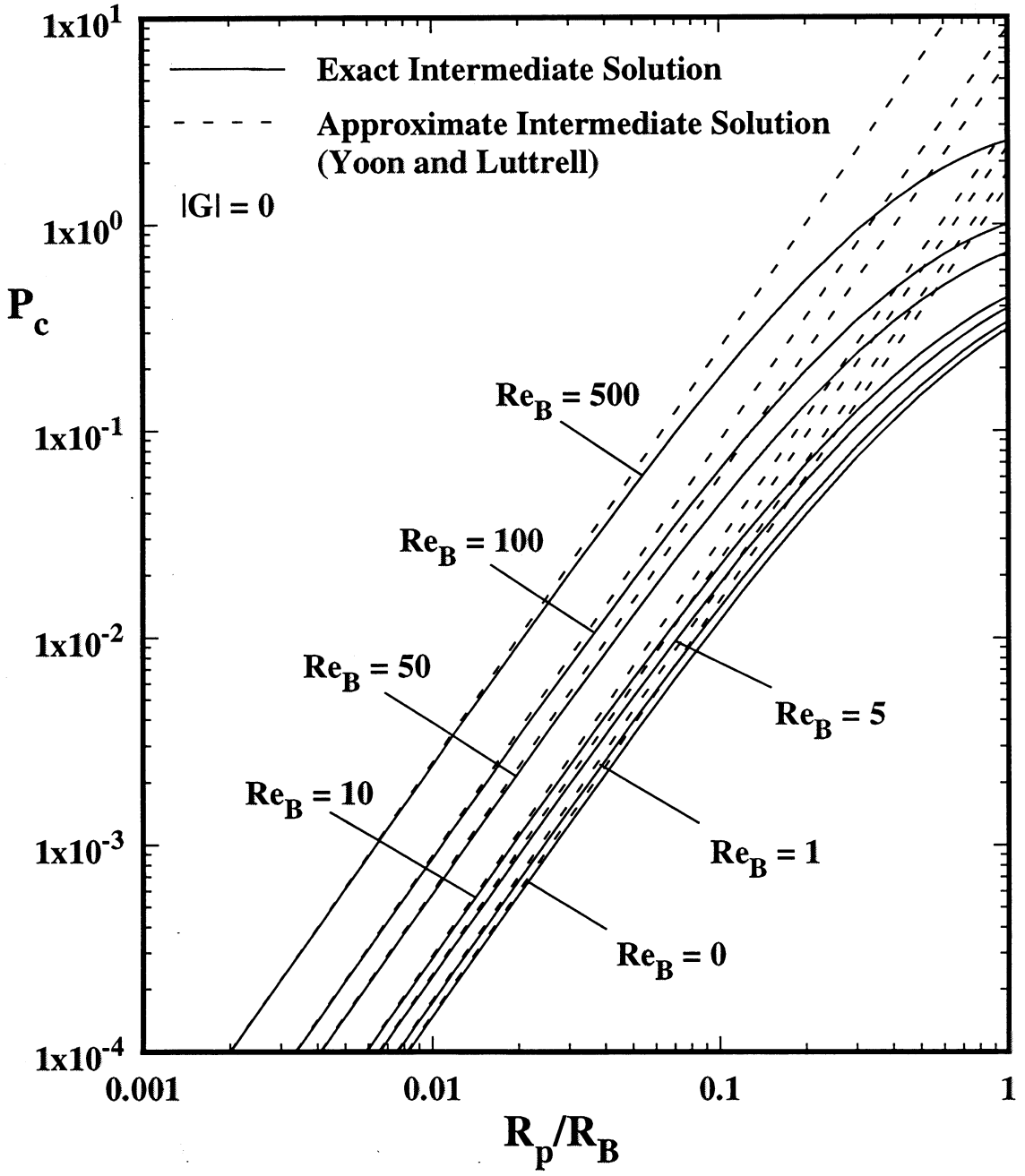

Figure 2: Exact and approximate P_c predictions for intermediate flow with $0 \leq Re_B \leq 500$ and $|G| = 0$.

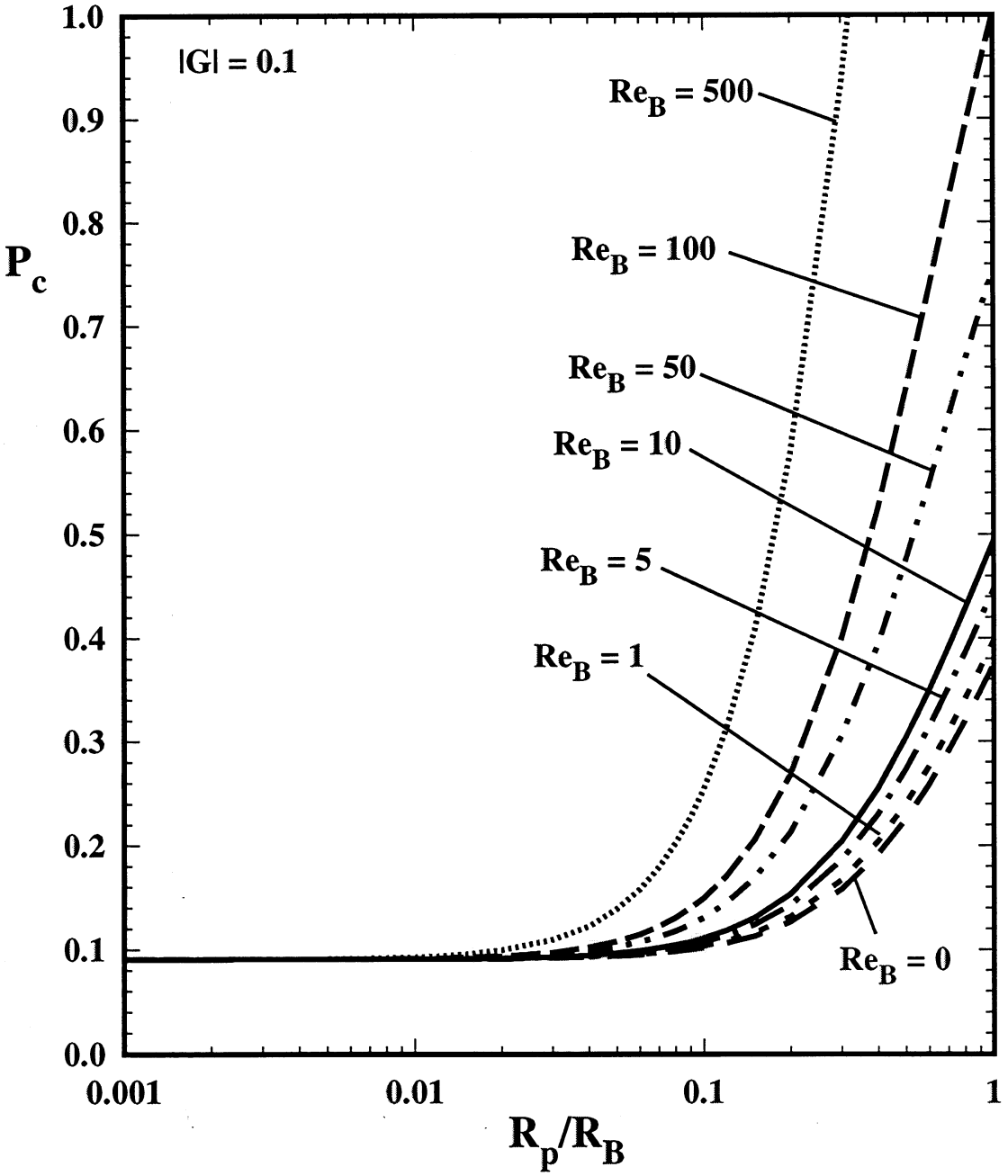

Figure 3: Exact P_c predictions for intermediate flow with $0 \leq Re_B \leq 500$ and $|G| = 0.1$.

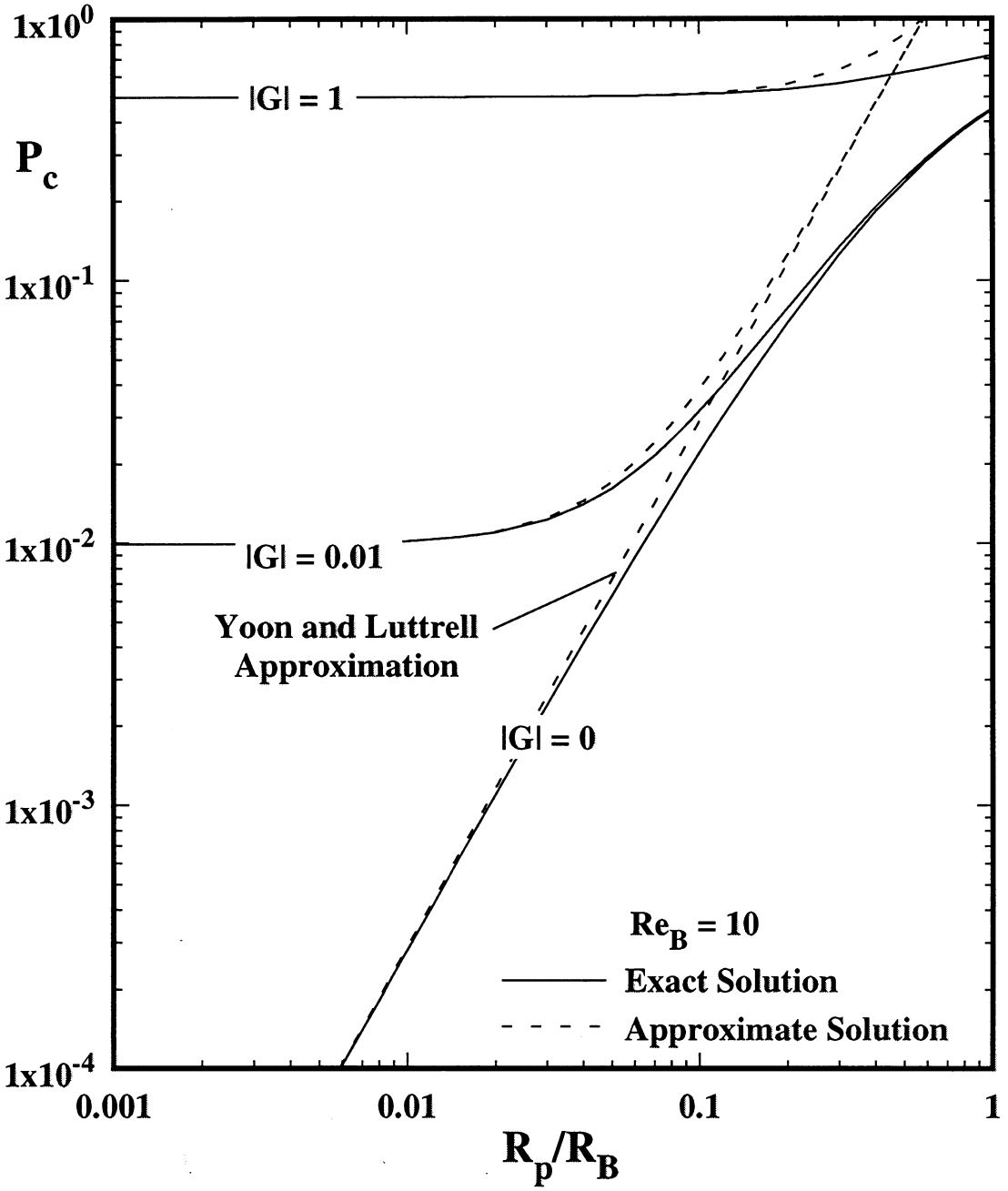

Figure 4: Exact and approximate P_c predictions for |G| = 0, 0.01, and 1 and Re_B = 10.

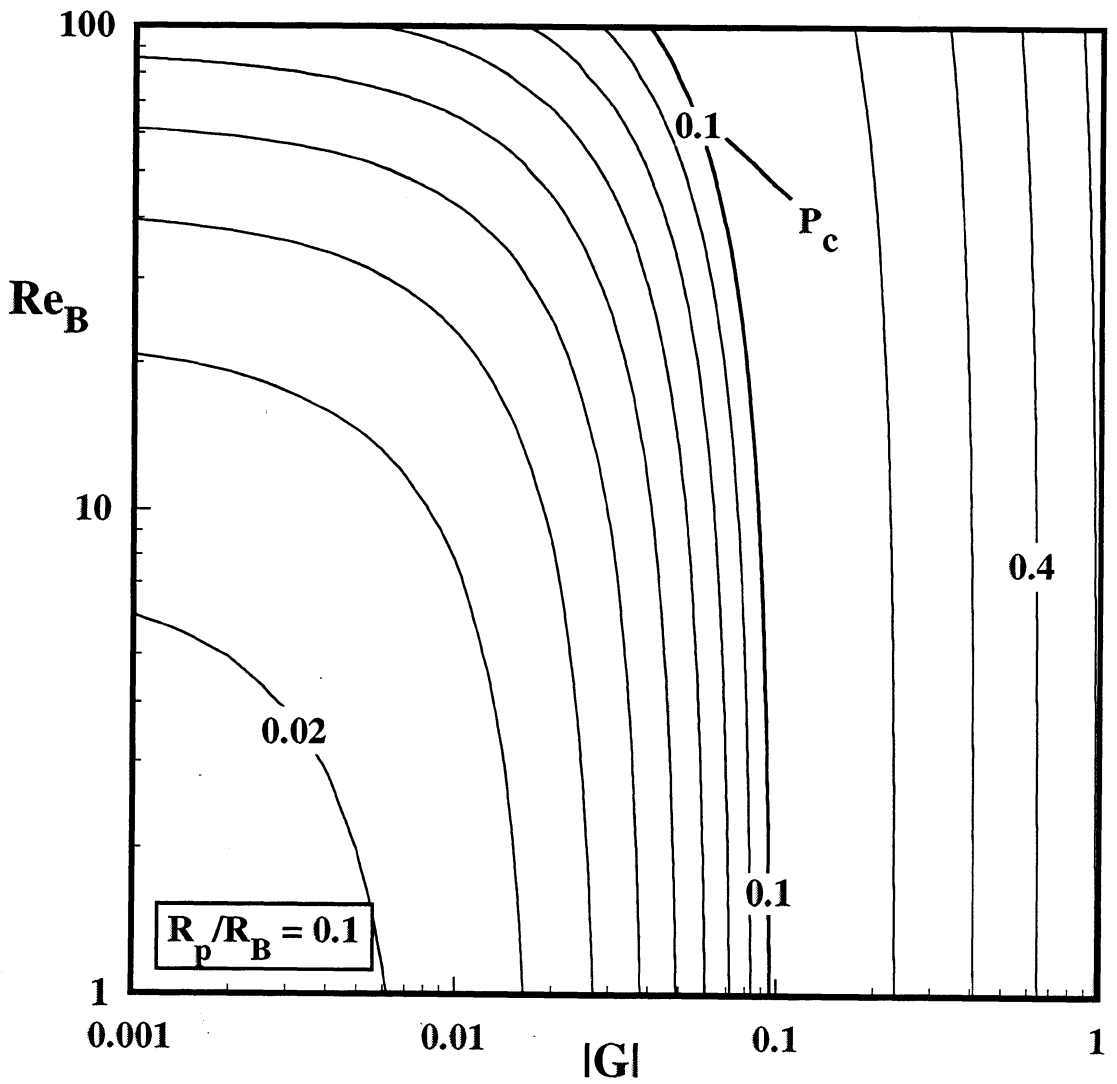

Figure 5: Contours of Pc when Rp/RB = 0.1. Note that the Pc scale is logarithmic.

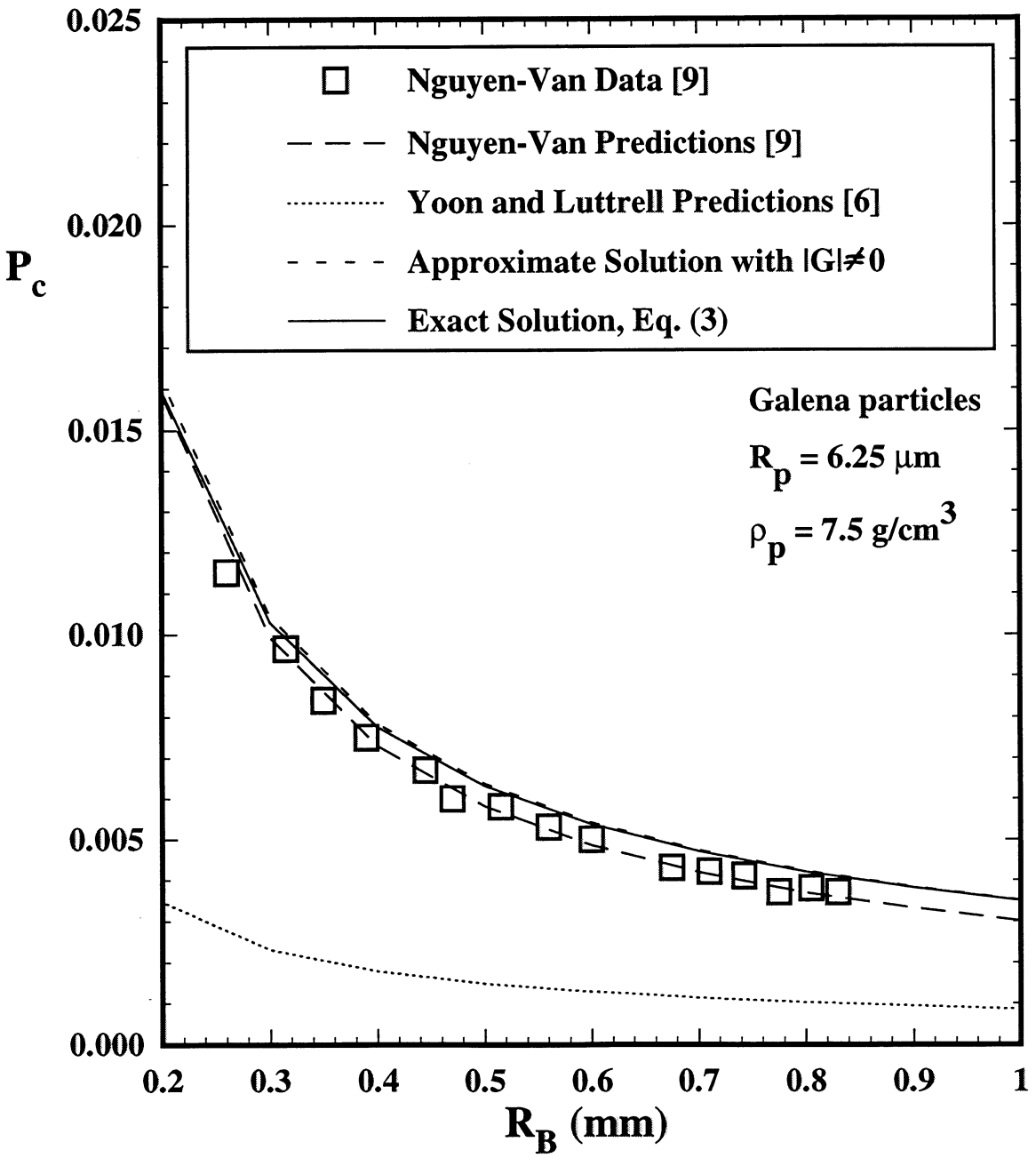

Figure 6: Comparisons between experimental and numerical values for P_c for galena particles with R_p = 6.25 μm.

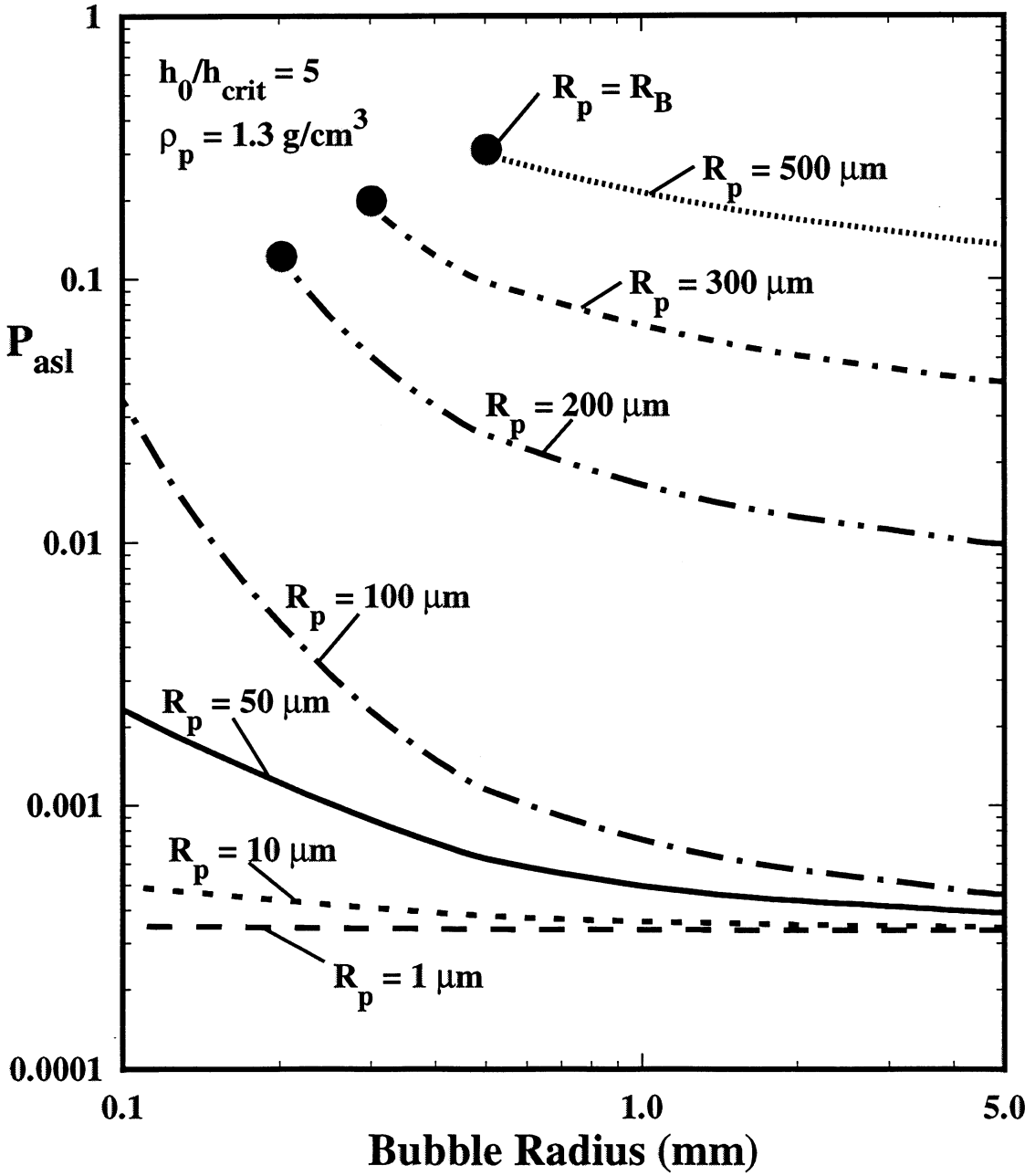

Figure 7: Probability of adhesion by sliding as a function of bubble radius for selected particle radii and $h_0/h_{crit} = 5$ and $\rho_p = 1.3$ g/cm^3.

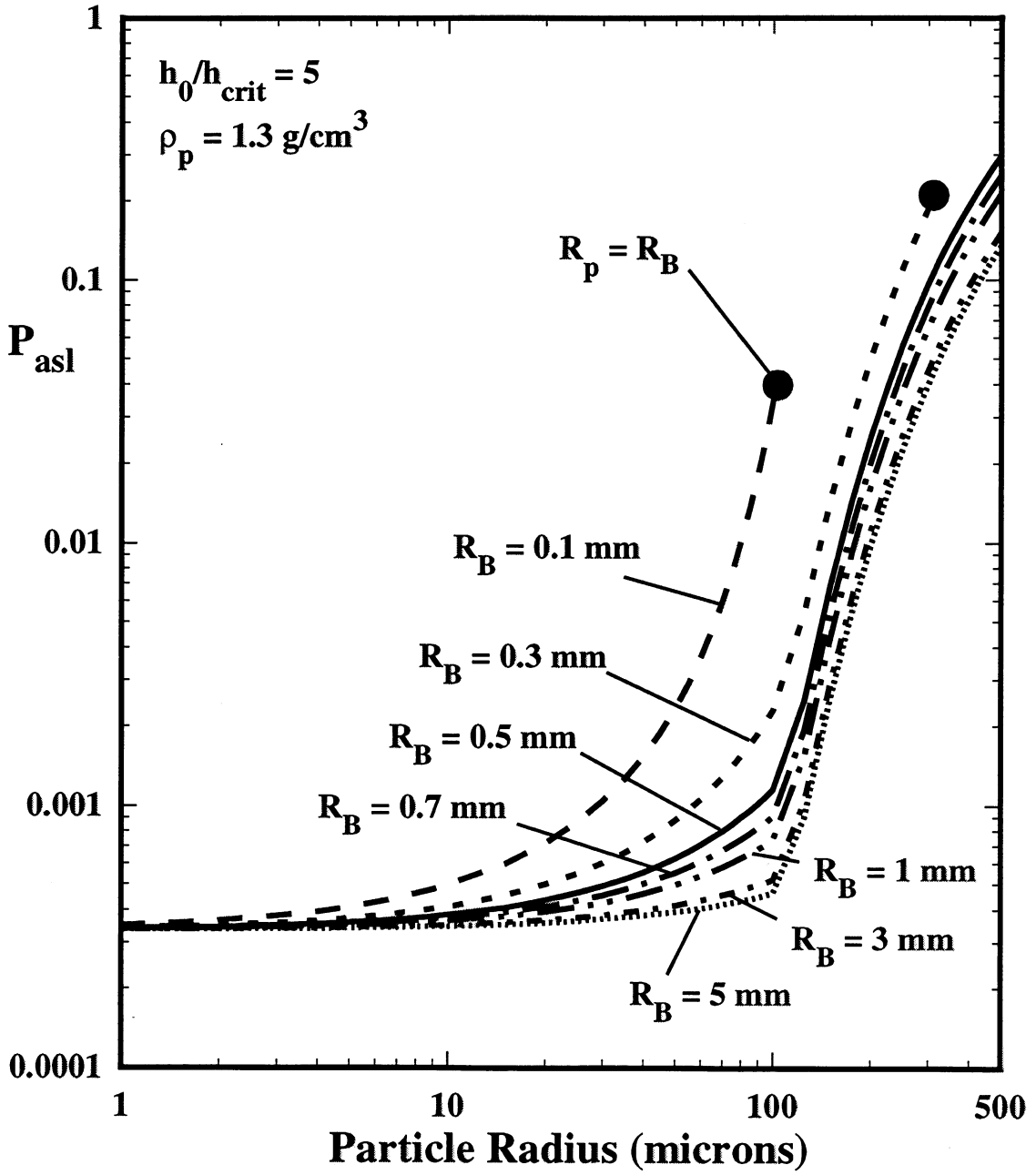

Figure 8: Probability of adhesion by sliding as a function of particle radius for selected bubble radii and $h_0/h_{crit} = 5$ and $\rho_p = 1.3$ g/cm^3.

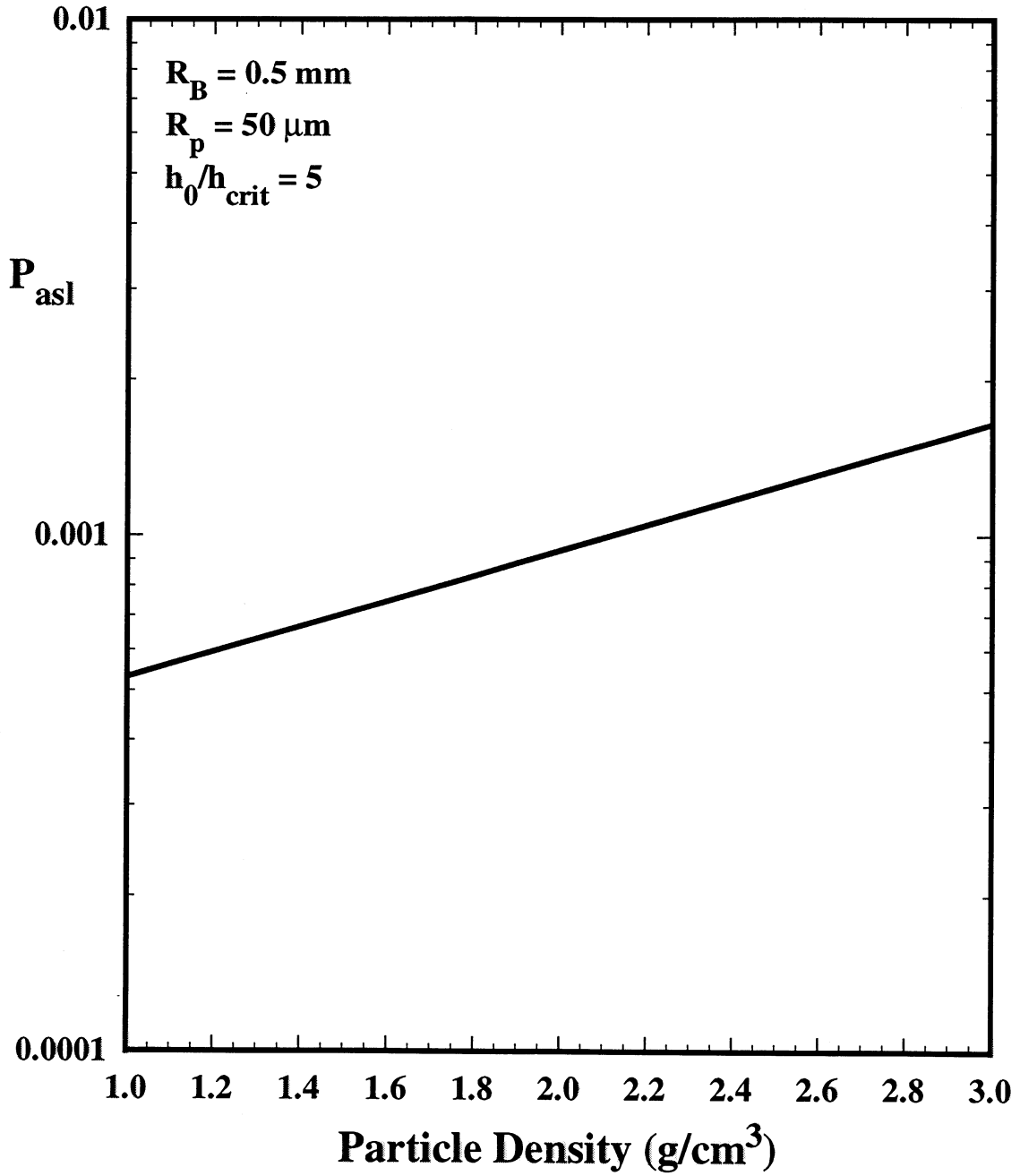

Figure 9: Probability of adhesion by sliding as a function of particle density for R_B = 0.5 mm, R_p = 50 μm, and h_0/h_{crit} = 5.

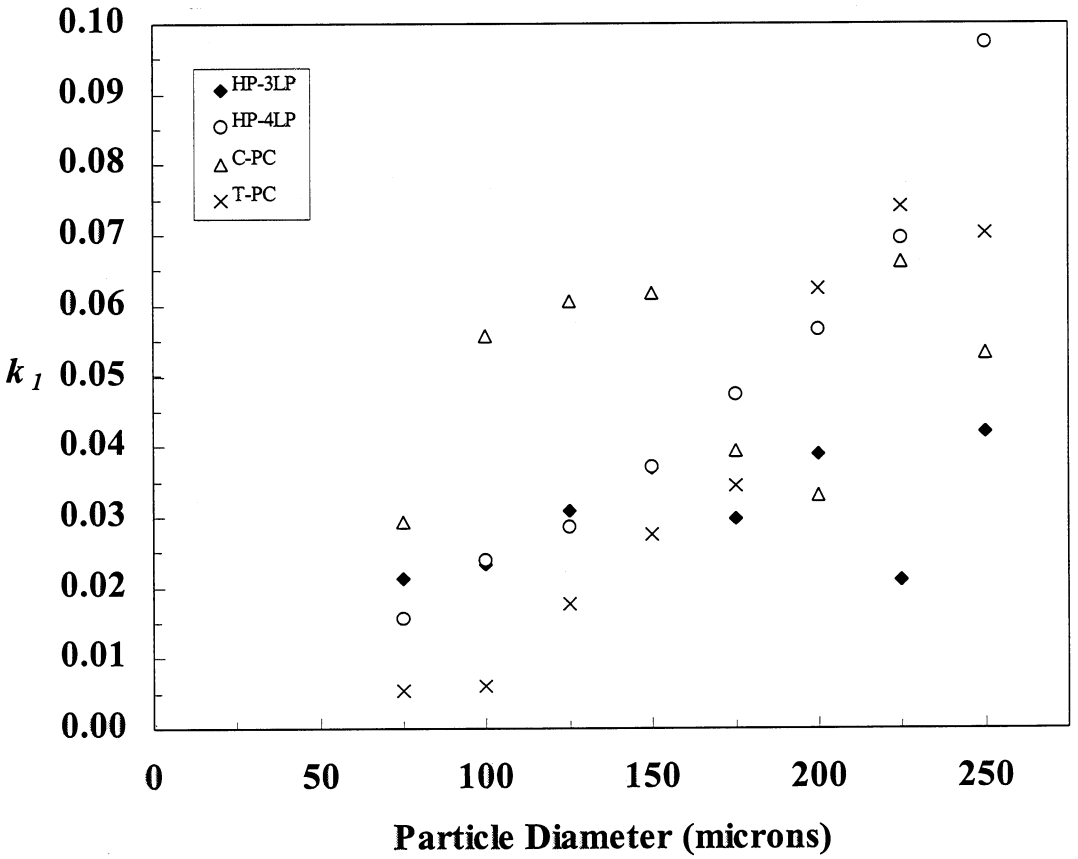

Figure 10: Effect on particle size on the model parameter k_1 using the experimental data of Vidotti et al. [14].

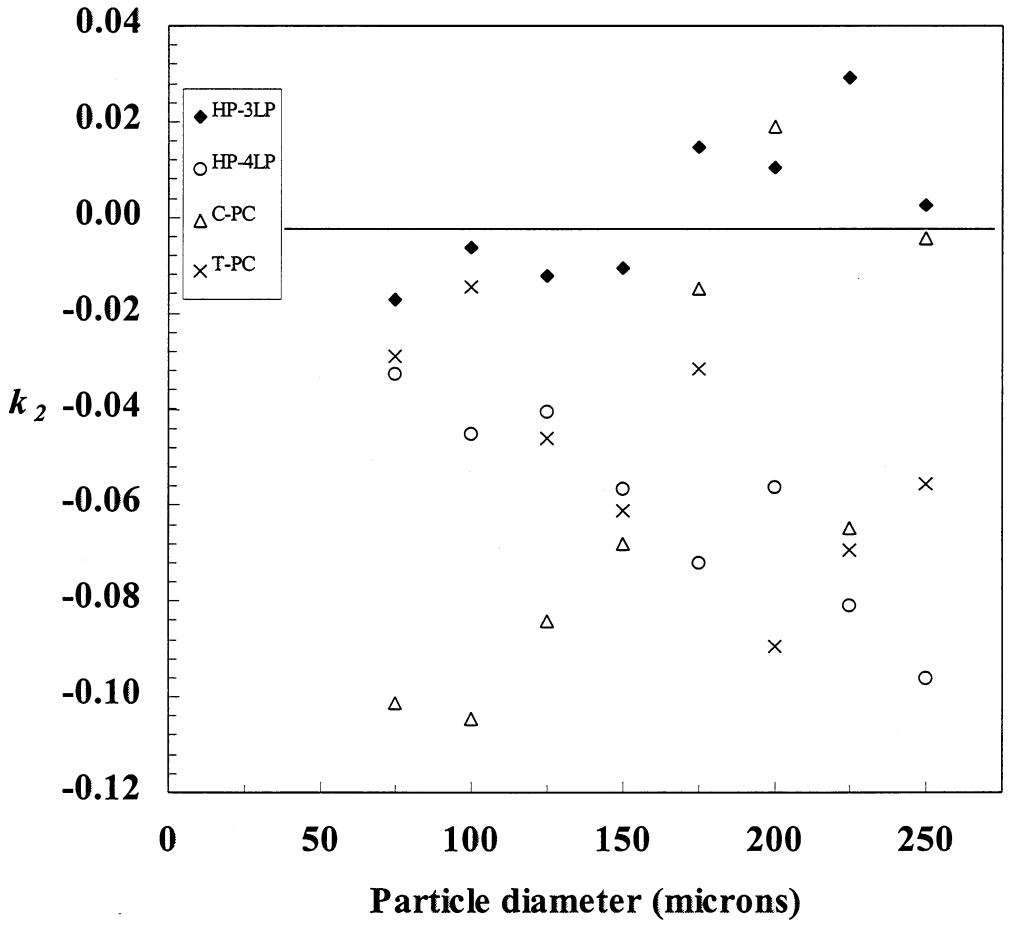

Figure 11: Effect on particle size on the model parameter k_2 using the experimental data of Vidotti et al. [14].

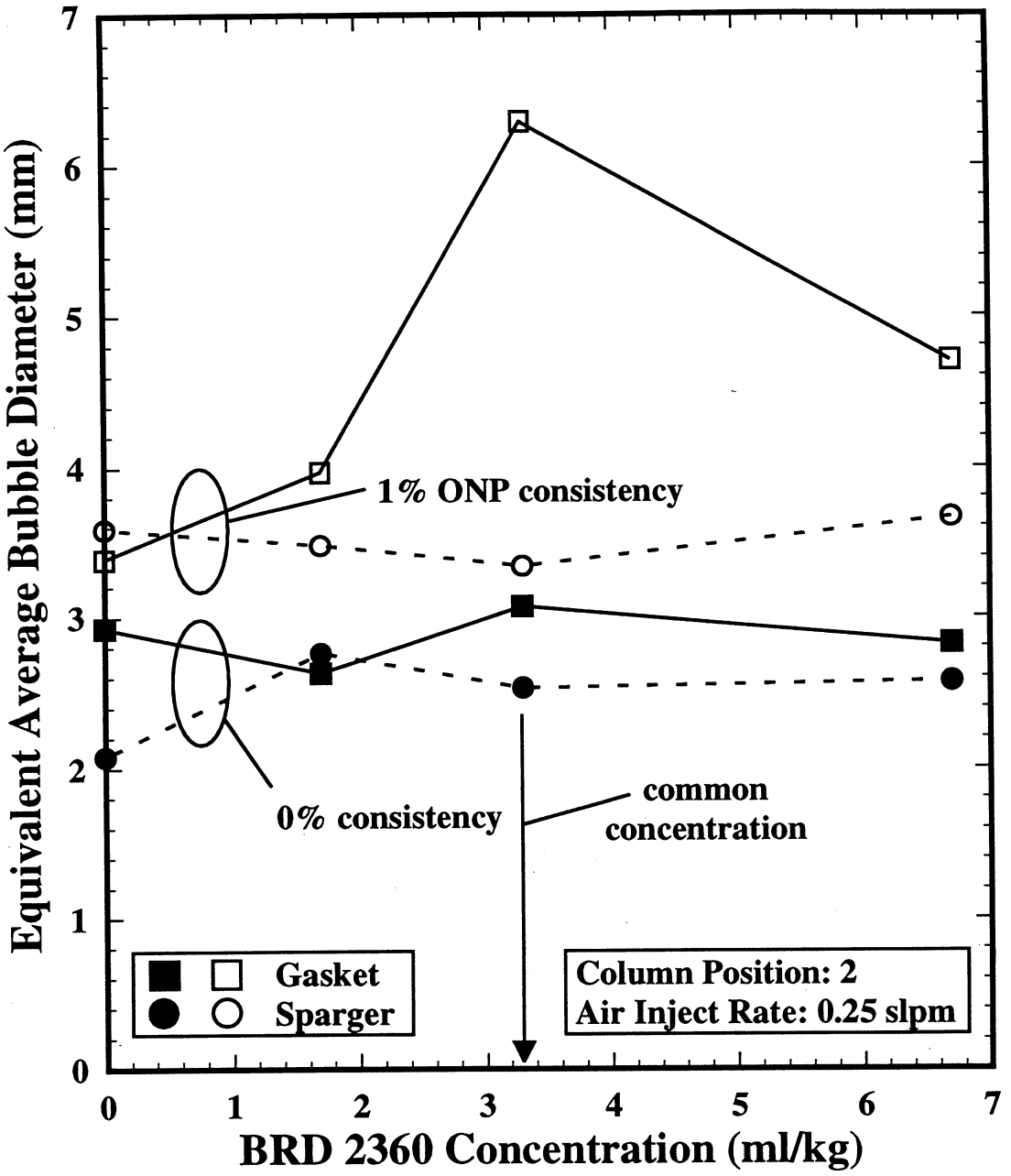

Figure 12: Effect of BRD 2360 concentration on the average bubble size.

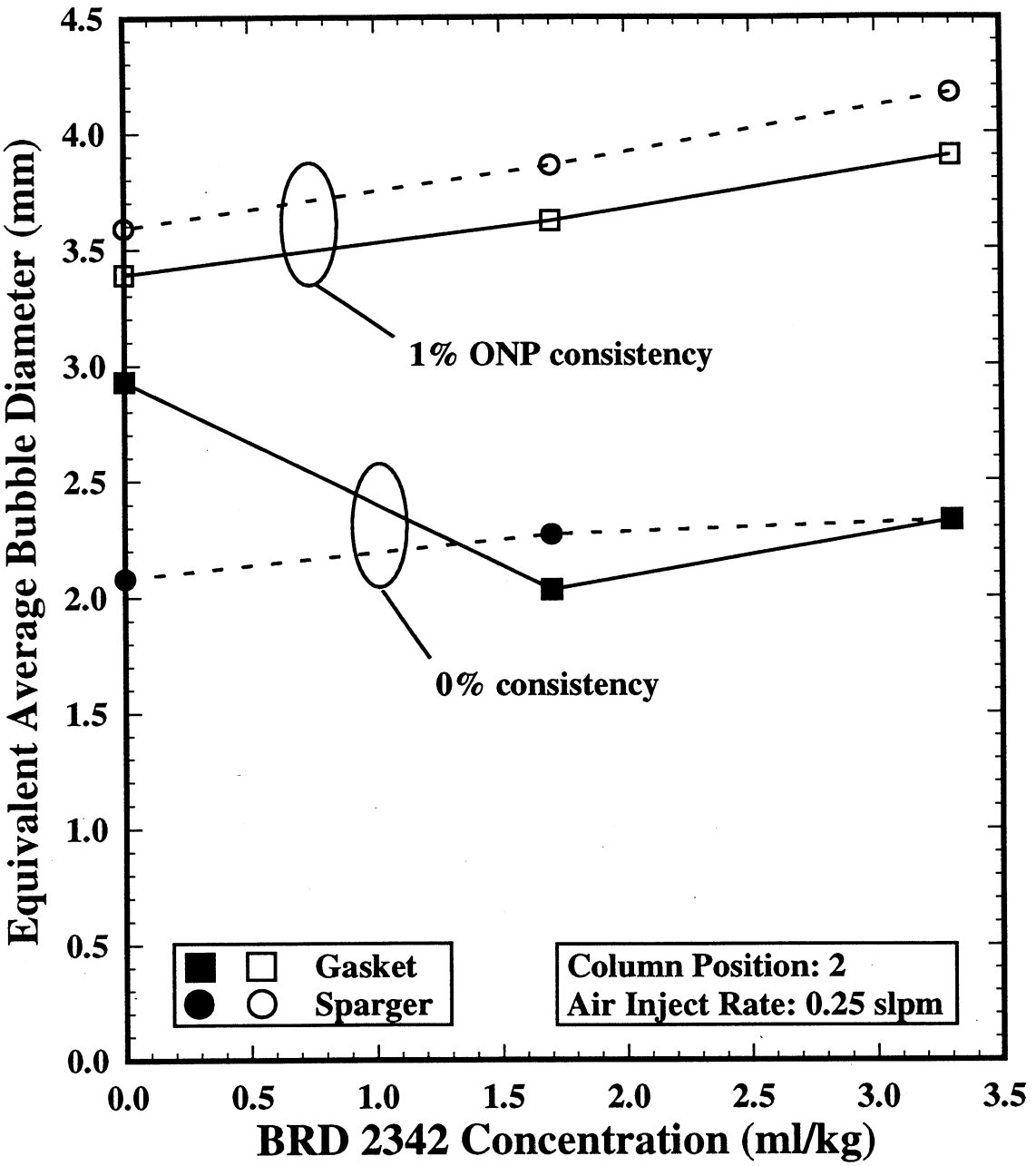

Figure 13: Effect of BRD 2342 concentration on the average bubble size.

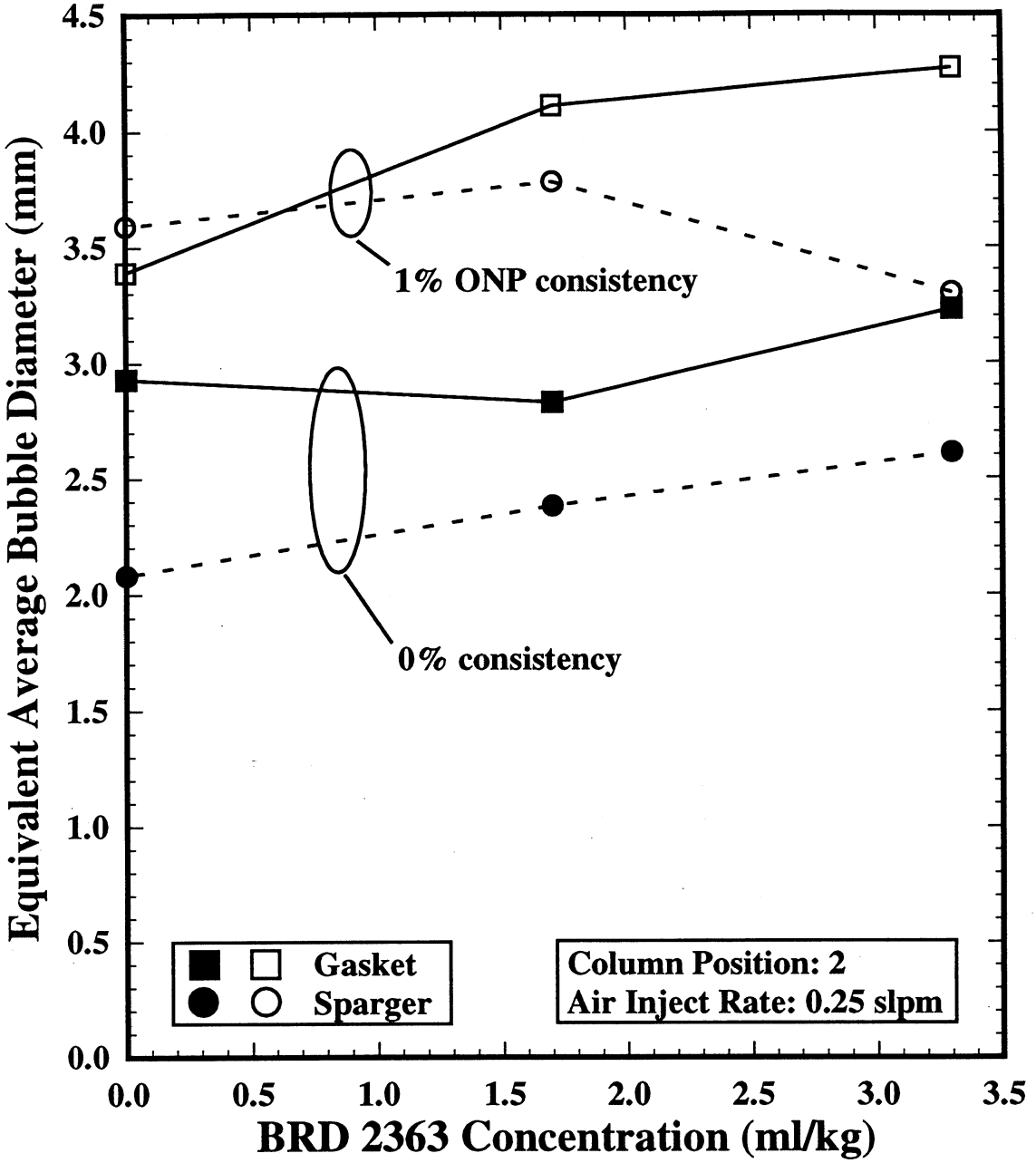

Figure 14: Effect of BRD 2363 concentration on the average bubble size.

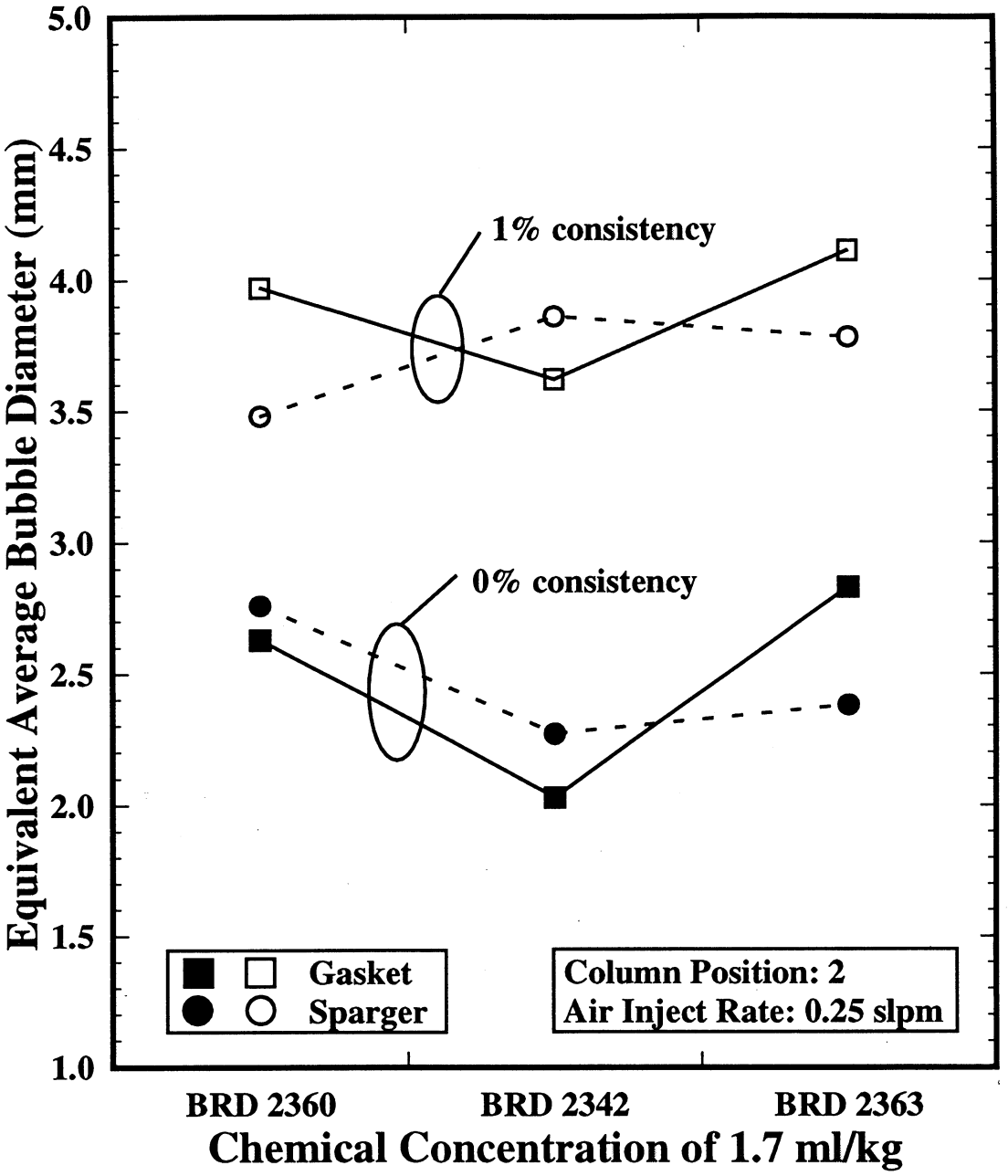

Figure 15: Effect of BRD type (concentration of 1.7 ml/kg) on the average bubble size.

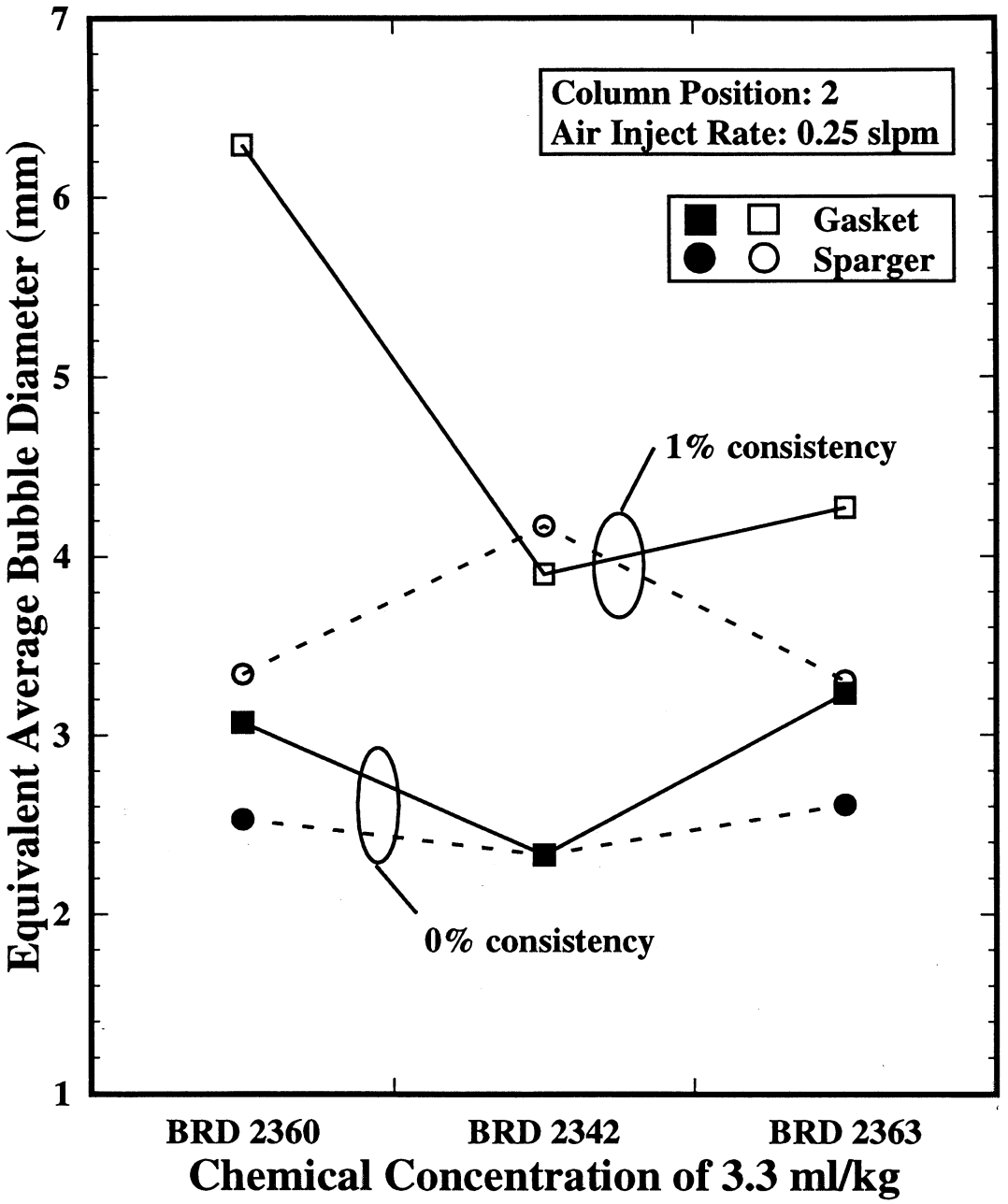

Figure 16: Effect of BRD type (concentration of 3.3 ml/kg) on the average bubble size.

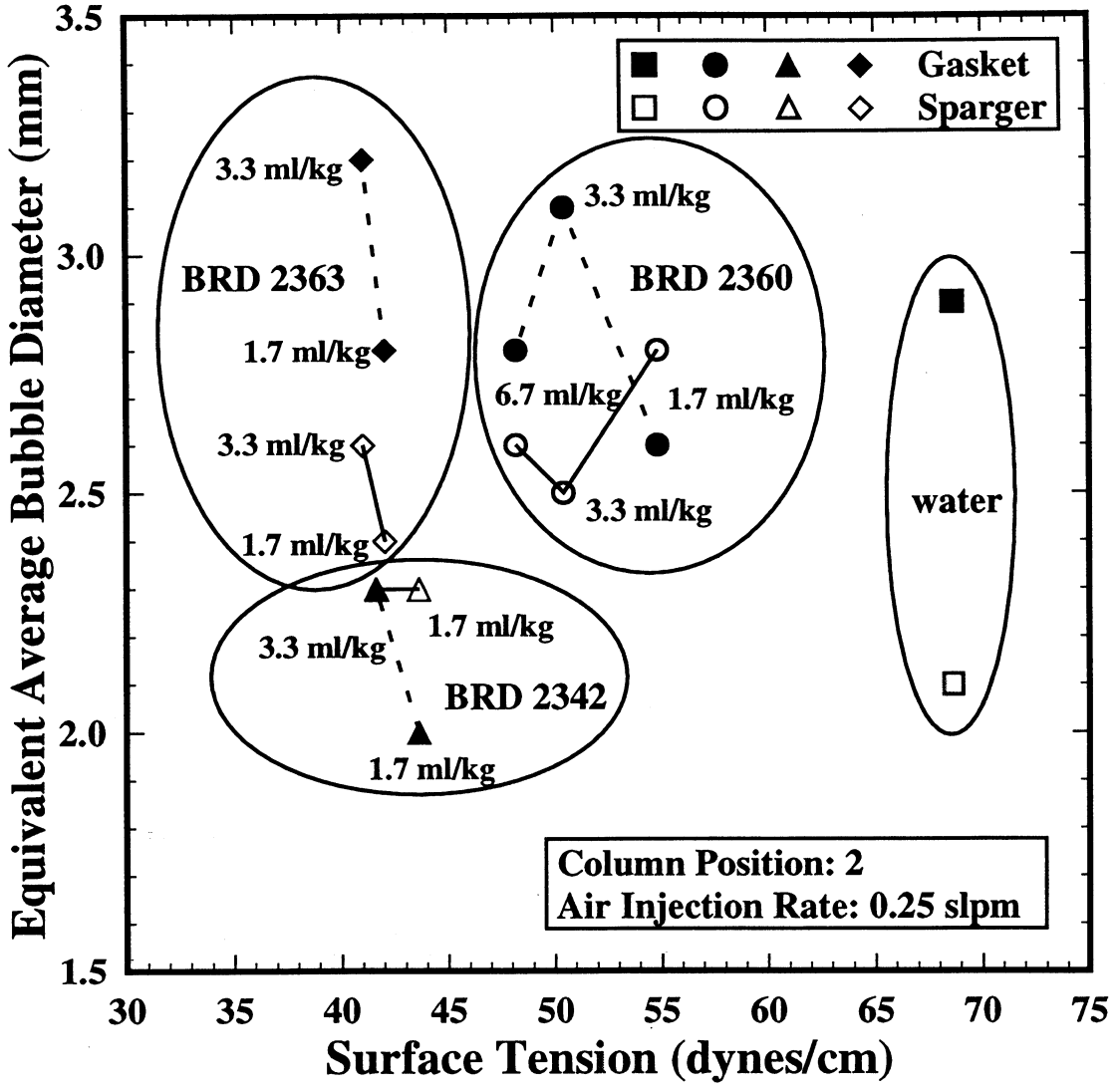

Figure 17: Effect of surface tension on the average bubble size.

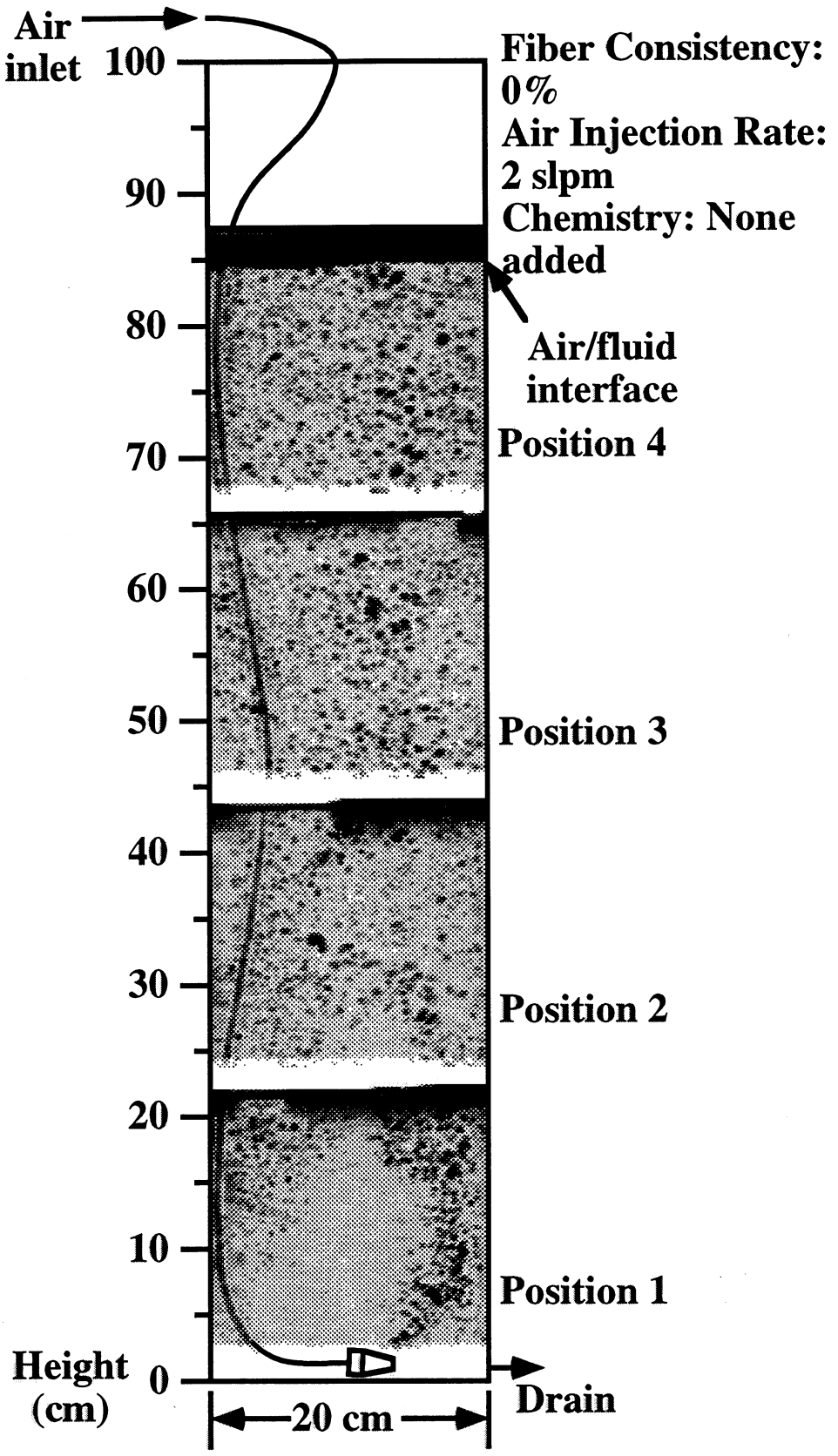

Figure 18: X-ray composite of air bubble flow patterns in an air/water system with air injected at 2 slpm through a sparger with 40 μm openings placed on the column bottom.

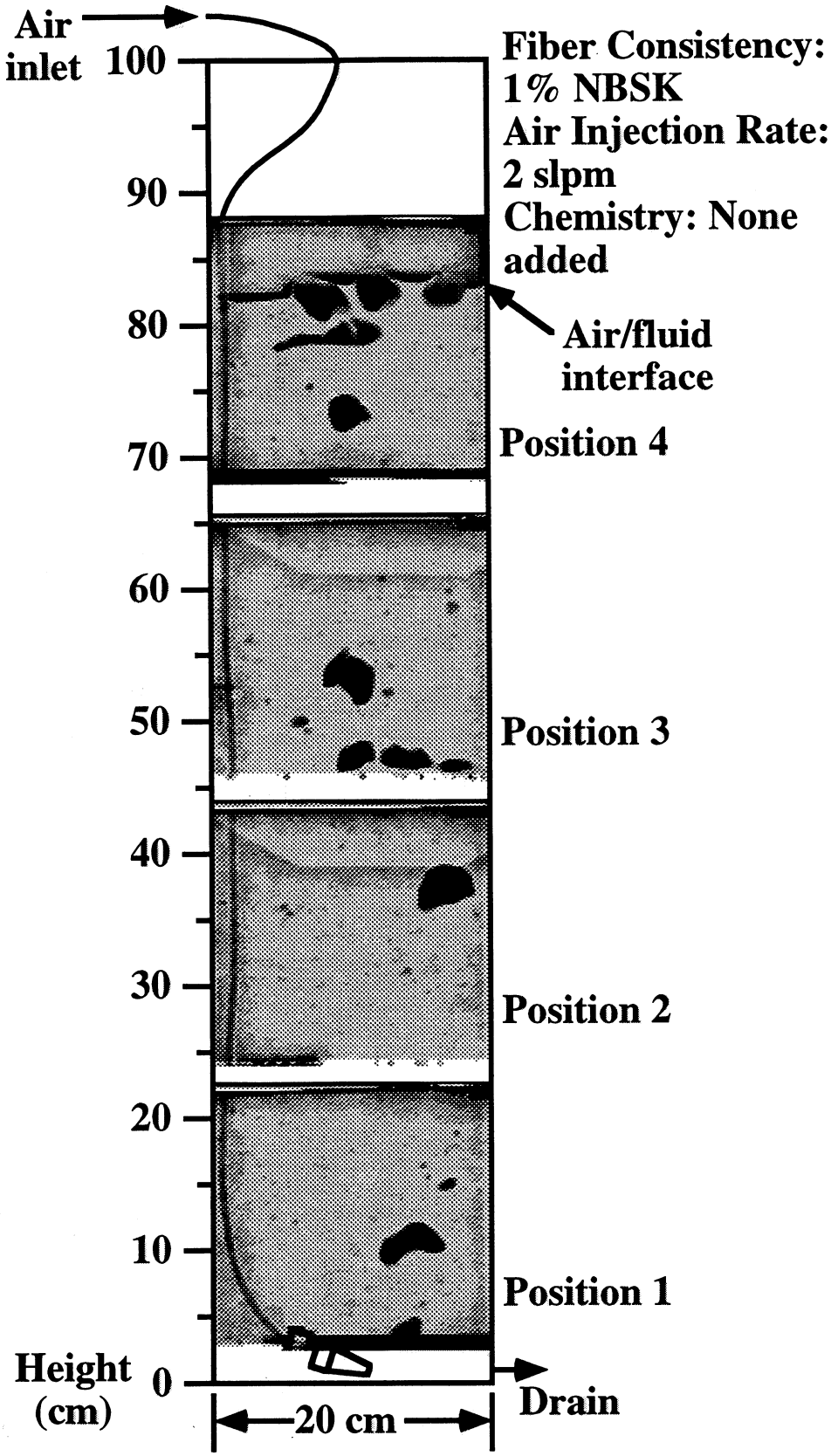

Figure 19: X-ray composite of air bubble flow patterns in an air/water/1% NBSK system with air injected at 2 slpm through a sparger with 40 μm openings placed on the column bottom.

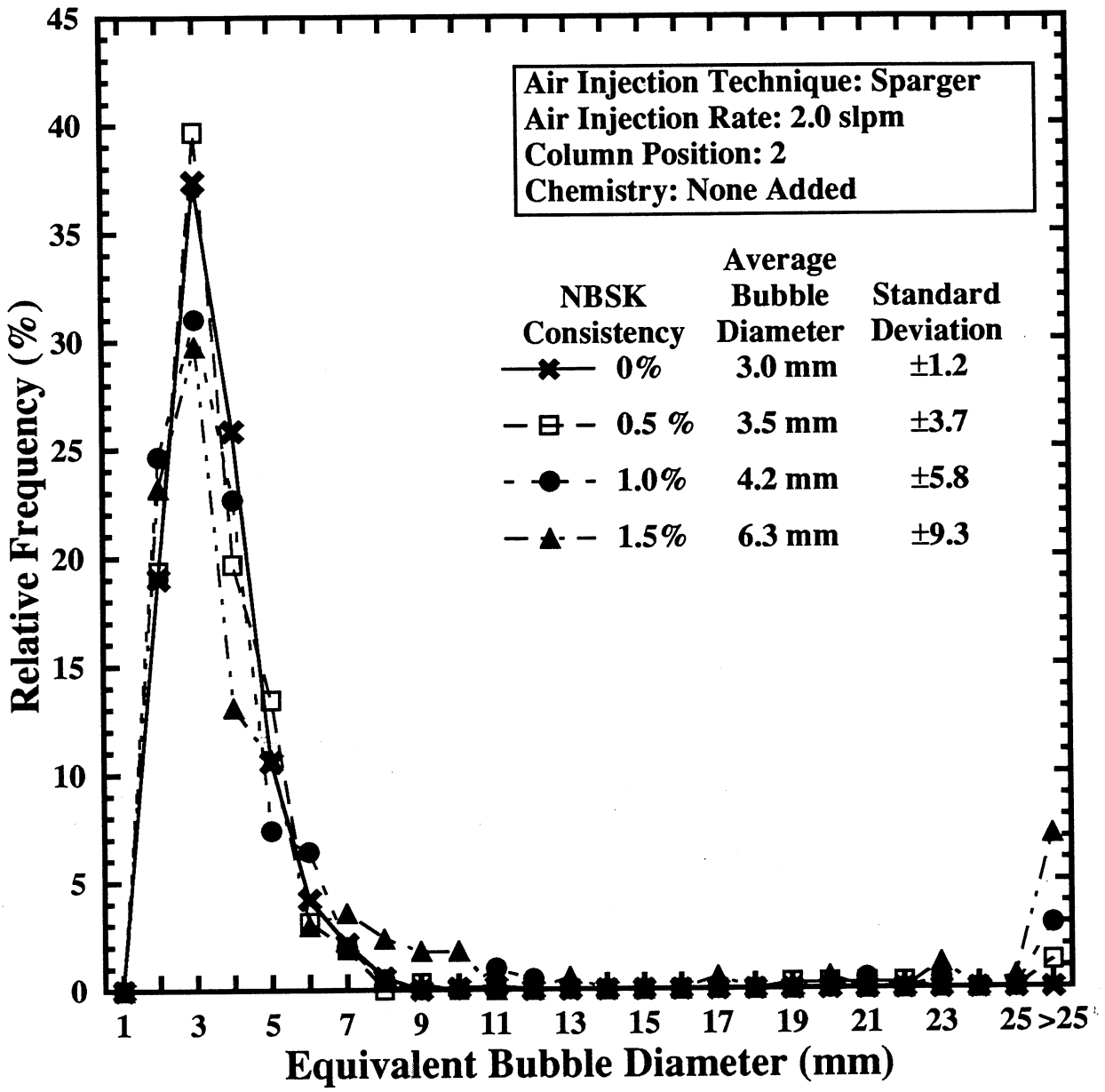

Figure 20: Bubble size distributions obtained with the sparger air injection technique for various NBSK consistencies.

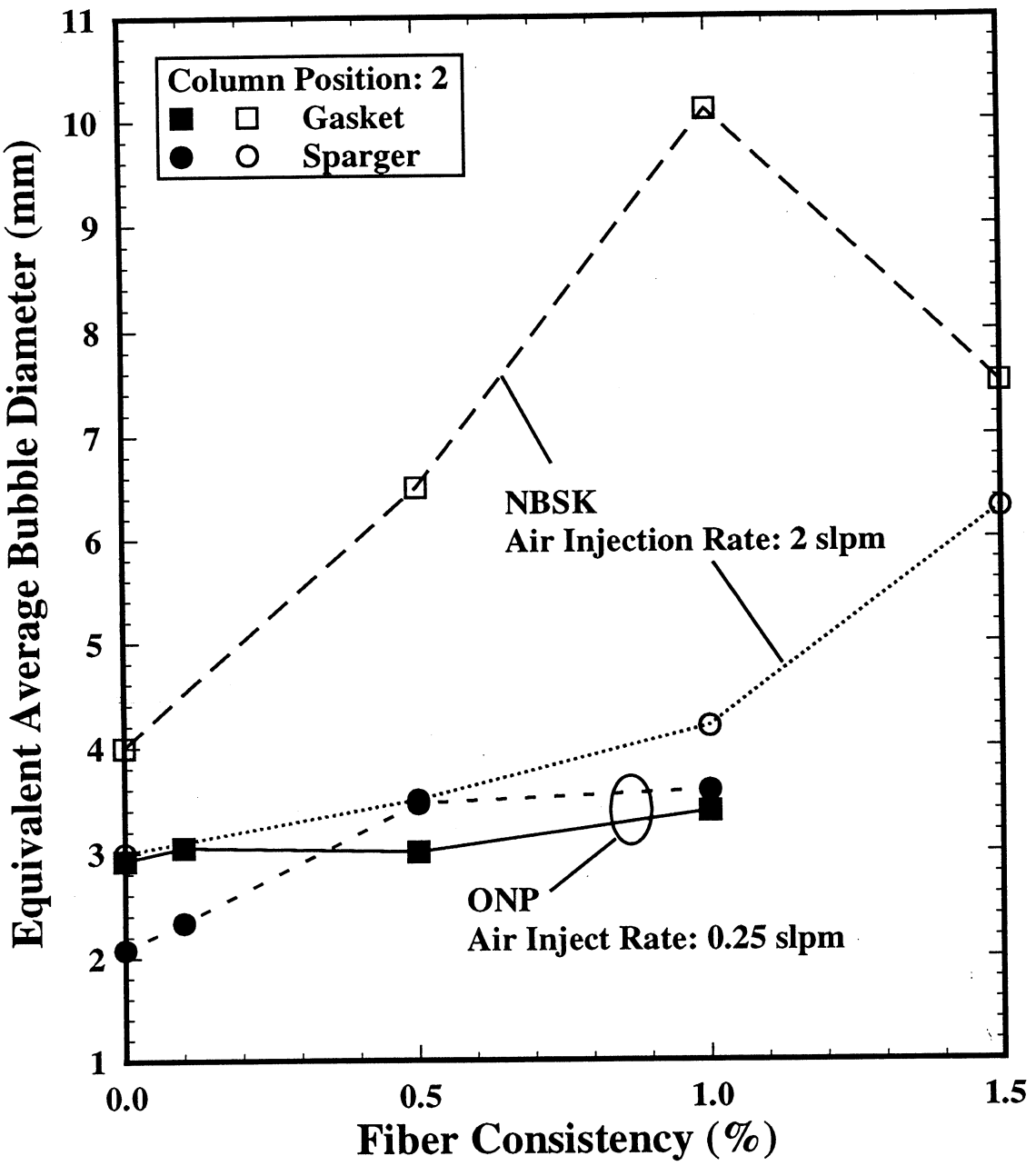

Figure 21: Effect of NBSK consistency on average bubble size.

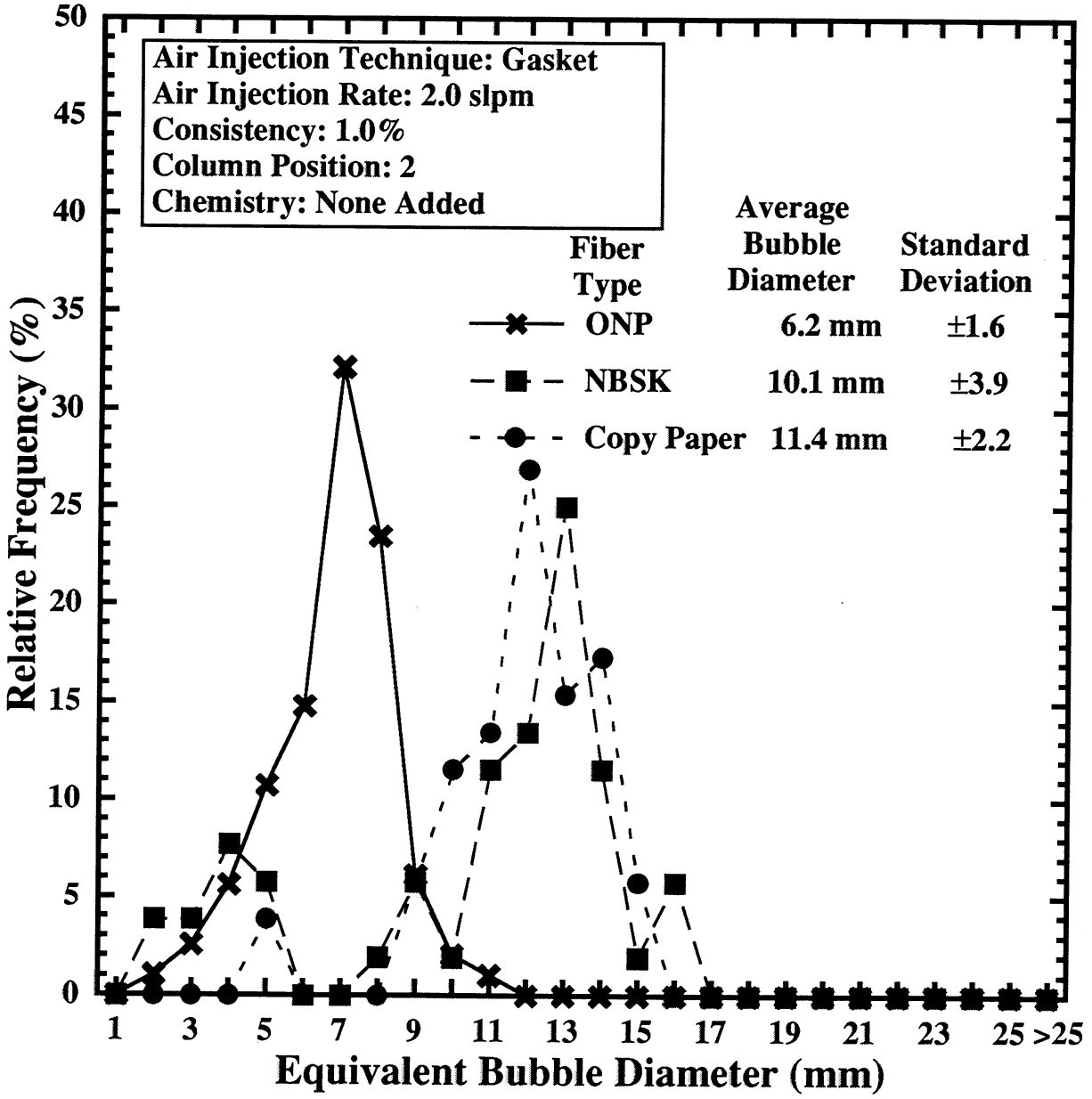

Figure 22: Bubble size distributions for 1% NBSK, copy paper, and ONP systems obtained with the gasket air injection at 2 slpm.

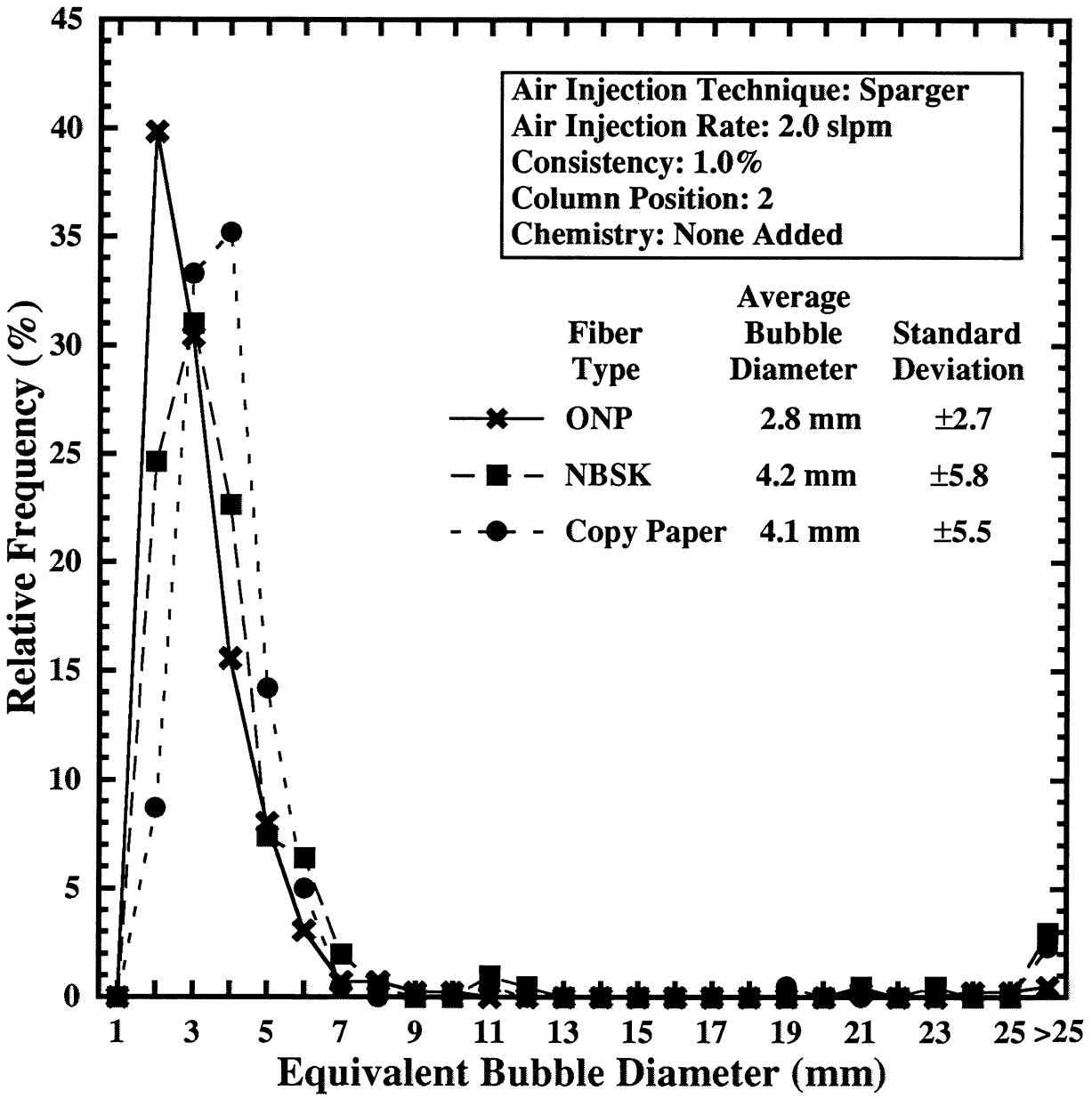

Figure 23: Bubble size distributions for 1% NBSK, copy paper, and ONP systems obtained with the sparger air injection at 2 slpm.

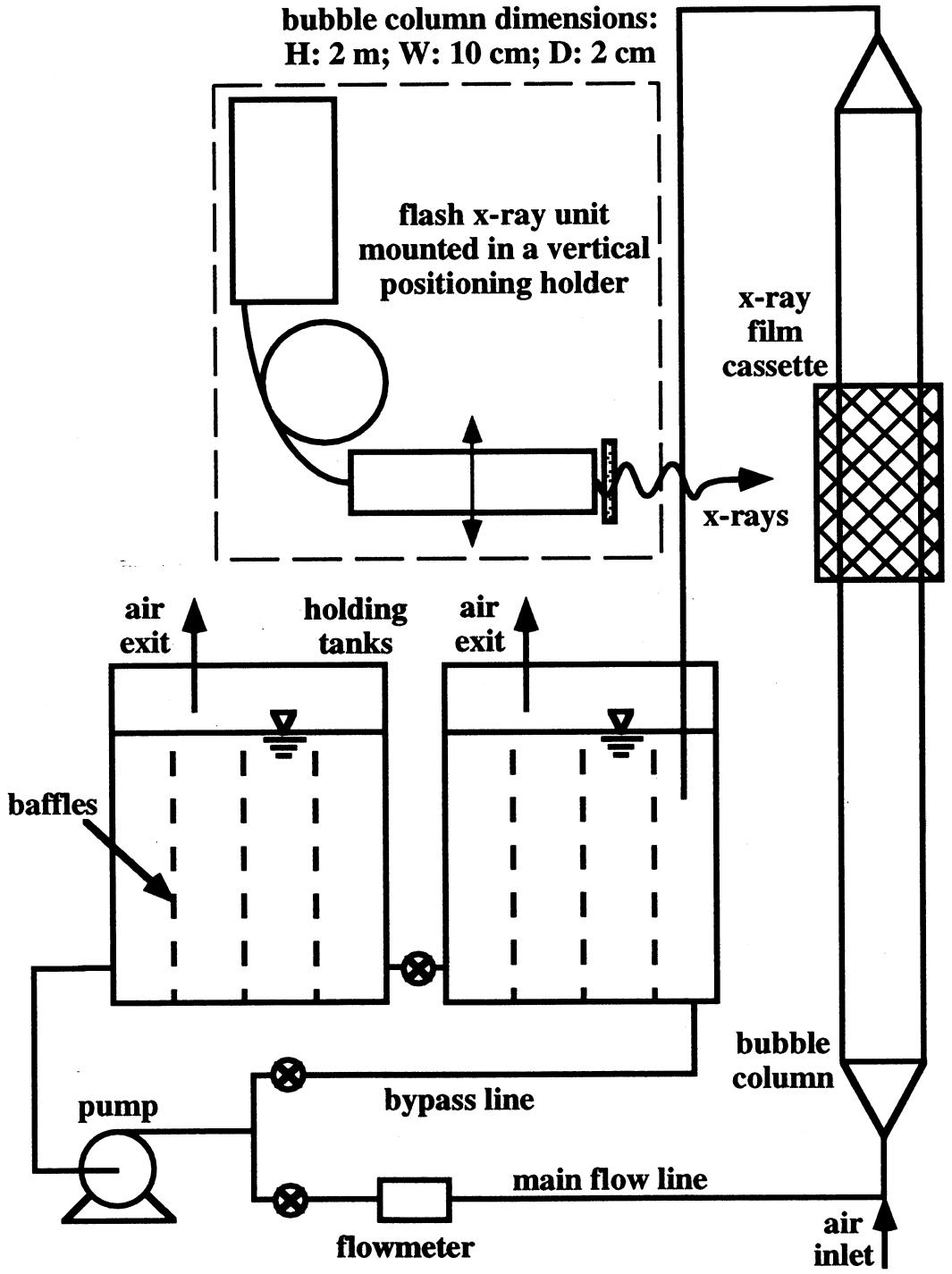

Figure 24: Schematic diagram of the new cocurrent flow loop to be used with the flash x-ray system.

FUNDAMENTALS OF SURFACE CHEMISTRY IN FLOTATION DEINKING

STATUS REPORT

FOR

PROJECT F00904

Yulin Deng

March 23-24, 1998

Institute of Paper Science and Technology
500 10th Street, N.W.
Atlanta, Georgia

GENERAL INFORMATION

PROJECT TITLE: FUNDAMENTALS OF SURFACE CHEMISTRY IN FLOTATION DEINKING

PROJECT NUMBER: F00104

PAC: Recycle/Surface and Colloid Science PAC

DIVISION: Papermaking Engineering

PROJECT CODE: Deinkchem

PROJECT STAFF: Yulin Deng (Assistant Professor)
Marcos Abazeri (Assistant Scientist)

FY 98-99 BUDGET: $84,577

TIME ALLOCATION:

Faculty: Yulin Deng: 20%

Staff: Marcos Abazeri: 85%.

SUPPORTING RESEARCH:

M.S. Students: Kyoung Young Lim

RESEARCH LINE/ROADMAP:

Reduce and/or control contaminants (e.g., stickies, dyes, toners) in recycled-fiber pulp using break-through technologies to allow complete interchange of recycled pulp with virgin pulp of similar fiber makeup at economical cost.

PROJECT OBJECTIVES:

a. Study the surface chemistry of different collectors in toner flotation deinking.
b. Study the effect of fiber types on fiber loss.
c. Study the role of surfactant in the ink-fiber detachment.
d. Study the effect of old magazine (OMG) on the ink removal of old newsprint (ONP).

MAIN RESULTS:

a) Cationic surfactants are the best surfactant systems that have been examined in this study, and these surfactants can be used as both collector and frothing agents for the flotation deinking of xerographic papers.
b) Both fiber adhesion and physical entraimment will contribute to fiber loss, but the entrainment is the dominating factor.
c) The addition of OMG will not enhance the ink removal of ONP in flotation deinking. The improvement of ONP brightness in the presence of OMG is solely caused by introducing more fillers and high-quality fibers.
d) The adsorption of the complex of fatty acid and calcium ions on toner particles will not increase the hydrophobicity of toner particles.
e) Nonionic surfactant, TX-100, will reduce the hydrophobicity of ink, fibers, fines, and fillers.

ABSTRACT

This report is concerned with increasing utilization of recycled fiber and, more specifically, with minimizing fiber loss and maximizing deinking efficiency in flotation deinking. The research program was started in May 1995. The results obtained in Fiscal Years 95-96 and 96-97 have be given in Progress Report I (February 1997). Two papers based on this study, "Contact Angle Measurement of Wood Fibers in Surfactant and Polymer Solutions" and "True Flotation and Physical Entrainment: The Mechanisms of Fiber Loss in Flotation Deinking," have been accepted for publication by Wood and Fiber Science and Nordic Pulp and Paper Research Journal, respectively. The current report will focus only on the results completed in the 97-98 FY.

Although flotation deinking is considered to be one of the most effective deinking methods, many physicochemical properties, such as ink removal efficiency, froth

structure, fiber loss mechanisms, and filler flotation during flotation deinking, remain unclear. To improve deinking efficiency and reduce fiber loss, the surface chemistry of ink, fiber, filler, air bubble, and other colloid materials in flotation deinking has to be studied.

The objectives of the research program conducted in FY 97-98 are to:

a. Study the surface chemistry of different collectors in toner flotation deinking.
b. Study the effect of fiber types on fiber loss.
c. Study the role of surfactant in the ink-fiber detachment.
d. Study the effect of old magazine (OMG) on the ink removal of old newsprint (ONP).

The main results obtained in this research program indicate that

a) Cationic surfactants are the best surfactant systems that have been examined in this study, and these surfactants can be used as both collector and frothing agents for the flotation deinking of xerographic papers.
b) Both fiber adhesion and physical entraimment will contribute to fiber loss, but the entrainment is the dominating factor.
c) The addition of OMG will not enhance the ink removal of ONP in flotation deinking. The improvement of ONP brightness in the presence of OMG is solely caused by introducing more fillers and high-quality fibers.
d) The adsorption of the complex of fatty acid and calcium ions on toner particles will not increase the hydrophobicity of toner particles.
e) Nonionic surfactant, TX-100, will reduce the hydrophobicity of ink, fibers, fines, and fillers.

Because the objectives studied in 97-98 FY are relatively broad and independent of each other, the results accomplished in 97-98 FY will be divided into four sections:

1. Collect chemistry in flotation deinking of xerographic papers;
2. Fiber loss in flotation deinking: effect of fiber types;
3. The role of surfactant in the ink-fiber detachment;
4. Effect of OMG on the flotation deinking of ONP, and fiber loss mechanisms.

1. COLLECT CHEMISTRY IN FLOTATION DEINKING OF XEROGRAPHIC PAPERS

1.1. Background

The recycling of wastepaper is of growing importance due to the shortage of fiber supply and the restricted government regulations on solid wastepaper landfills. Although the paper recycling rate has increased steadily, the quality and cost of recycled fibers are still incompatible with virgin fibers.

Flotation deinking is one of the most important separation techniques widely used in paper recycling industry. Flotation deinking involves three main processes: detachment of the ink particles from wastepaper fibers, effective adhesion of the ink particles onto air bubble surfaces, and the removal of ink particles with the froth from flotation cells **[1-3].** It has been well known that the hydrophobicity and the particle size of ink particles in flotation slurry are two of the most important factors affecting the ink-air bubble interaction. From a surface chemistry point of view, the higher the hydrophobicity of particle surface, the easier it is to remove ink particles from pulp slurry under similar flotation conditions. To improve the hydrophobicity of floated particles, it is very common to apply a collector in the pulp slurry in mineral flotation.

Many collectors have been successfully used in ore flotation, but few of them have been used in flotation deinking. The most common collector used in flotation deinking is fatty acid in the presence of calcium chloride. Many researchers have focused on the understanding of ink removal by adding fatty acid/calcium collector, but the mechanism involved in this system have not been well understood **[1,2].** Although the fatty acid/calcium collector has been traditionally used for flotation deinking of old newsprint and old magazines, Dorris and Page **[4]** recently indicated that fatty acid/calcium collector can also improve the toner removal efficiency during the flotation. They suggested that the increased hydrophobicity of toner particles due to the adsorption of fatty acid/calcium complex onto toner surface is the main reason for toner removal improvement. However, this hypothesis has not been validated by experimental results. Although fatty acid-calcium chloride system is an effective collector for some grades of wastepapers, the deposition of calcium fatty acid particles

on the flotation equipment and paper machine is a serious problem. Therefore, it will be beneficial to the paper industry if more effective collectors that do not have negative effects on the papermaking process can be developed.

It was found that the deinking of mixed office paper by flotation is more difficult than other wastepapers because a) toner is usually fused into the pores of papers and strongly adhered to the fiber surfaces, resulting in a poor toner-fiber separation during repulping **[5,6]**, and b) the broad particle size distribution and the disk-like shape of toner particles result in a poor attachment between toner particles and air bubbles **[7, 8]**. Based on these understandings it is believed that the toner particles must be kept hydrophobic in flotation cell and the optimum particle size must be achieved in order to improve the flotation deinking efficiency of toner printed papers.

This study is to develop a fundamental understanding of collector chemistry in flotation deinking of toner printed papers. The relationship between collector and toner surface hydrophobicity was studied. The agglomeration of toner particles in different collector solutions was examined. Finally, the effects of toner hydrophobicity and toner particle size on the flotation efficiency were investigated.

1.2. Experimental

1.2.1. Chemicals

Triton X-100 (TX-100, a nonionic alkylphenoxy polyethoxy ethanol compound, analyze grade, J. T. Backer Inc.), kerosene (commercial product), sodium oleic acid sodium salt [Aldrich, 98%], dodecyltrimethylammonium bromide [$CH_3(CH_2)_{11}N(CH_3)_3Br$, DTMAB, Aldrich, 99%], cetyltrimethylammonium bromide [$CH_3(CH_2)_{15}N(CH_3)_3Br$, CTMAB, Aldrich, 95%], and calcium chloride [Aldrich, analytical pure] were used as received.

1.2.2. Contact angle measurements

The surface tension of liquid was measured by a dynamic contact angle analyzer (Cahn DCA 312) using a glass plate. Toner samples for contact angle measurement were made by copying 3 layers of Xerox toner on both sides of a

transparency. The coated transparency was cut into 20mm x 30mm pieces before use. The wetting force of coated toner film in different solutions was measured, and the contact angle was calculated using Wilhelmy principle. Both surface tension and contact angle measurements were repeated several times until a stable reading was obtained.

1.2.3. Particle size measurements

The particle size and size distributions of toner suspension in different solutions were measured by a laser diffraction based particle size analyzer (Malvern 2600, Malvern Instruments, MA). The system consists of 2mW He-Ne Laser (633nm wavelength), a Transmitter with 9mm beam expansion, a Receiver with a Fourier transform lens, and a 31 element solid state detector array in concentric semicircular annuli design. The sample used for particle size analysis were made by dispersing Xerox toner in a pulp filtrate in the presence or absence of surfactant.

1.2.4. Flotation deinking

The pulp was made from bond papers printed by Xerox toner with a fixed pattern of X. The papers were pulped at pH of 9.3 and a consistency of 10.5% without adding any chemicals except sodium hydroxide. A laboratory flotation cell was used to conduct the flotation deinking. The deinking cell was made from a polyacrylate pipe with a height of 80cm and a diameter of 10cm. Nitrogen was blown into the pulp suspension at a rate of 14±0.075 SLPM (standard liter per minute) through an air filter (pole size 50 μm) at the bottom of the flotation cell. The air flow rate was measured by an Omega FMA1700/1800 flowmeter. The consistency of the pulp used in flotation was 0.5%. The flotation time was 10 minutes for all experiments.

The handsheets for brightness analysis were made on a 15-cm Büchner funnel according to TAPPI standard method T218 om-91. The brightness of a handsheet was measured by a UV-VIS spectrophotometer (Shimadzu UV-160A) using TAPPI Standard method T452 om-92.

1.3. Results and Discussion

1.3.1. Calcium fatty acid as a collector in toner flotation deinking

In the flotation deinking of mixed office wastepapers, a nonionic surfactant has been commonly used as a dispersant and frothing agent. However, the addition of a nonionic surfactant, such as TX-100, will reduce the hydrophobicity of toner particles, therefore the toner removal efficiency by flotation will be decreased. The reduction of toner particle hydrophobicity due to adsorbed surfactant can be clearly seen from **Fig. 1**, i.e. the advancing contact angle of aqueous solution on a toner film decreases as the concentration of TX-100 increases. When the concentration of TX-100 increases from 0 to 80mg/L (the typical concentration for mixed officewaste deinking in industry practice), the advancing contact angle decreases from 140 to 75 degrees. With a further increase in concentration to 200mg/L, the advancing contact angle decreases to 10 degree or even lower. The significant decrease in the contact angle must result in a reduction in deinking efficiency as will be discussed later.

Because nonionic surfactant usually leads to a reduction in the contact angle of toner particles in pulp suspension, it is interesting if there are some collectors that can restore the contact angle of toner particles. It has been known that calcium fatty acid can be used as a collector for both old newsprint and mixed office waster papers **[4,9,10]**. Therefore, the collector chemistry of calcium fatty acid was first examined in this study.

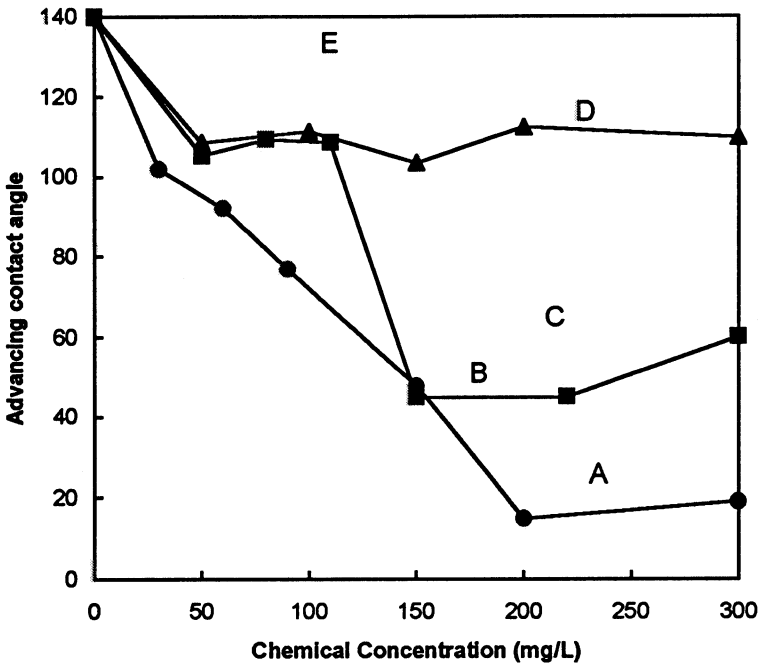

Fig. 1. Advancing contact angle of toner film in aqueous solutions as a function of A: TX-100 concentration without any other chemicals; B: TX-100 concentration in the presence of 50 mg/L sodium oleic acid and 250 mg/L calcium chloride; C: sodium oleic acid concentration in the presence of 500 mg/L calcium chloride.

The contact angle of toner film in water as a function of sodium oleic acid concentration in the presence of 500mg/L calcium chloride is also shown in **Fig. 1**. It can be seen that as the concentration of sodium oleic acid increases, the advancing contact angle decreases rather than increases. . This suggests that although the complex formed by sodium oleic acid and calcium chloride is hydrophobic, the hydrophobicity of toner surface will not be improved by adsorption of this complex because the hydrophobicity of toner itself is higher than that of calcium fatty acid aggregates.

To effectively remove toner particles from pulp slurry, a relatively stable foam is essential. The common method to generate a foam layer is to add frothing agent directly into pulp suspension during stock preparation. Therefore, it is very interesting to know how the interaction between calcium fatty acid and a frothing agent will affect the hydrophobicity of toner particles in a pulp system. **Fig. 1** shows that in the presence of 50 mg/L sodium oleic acid and 250 mg/L calcium chloride, the toner remained at a high contact angle (>105 degrees) until the concentration of TX-100 was increased up to 130 mg/L. Comparing that with the contact angle obtained in the absence of sodium oleic acid/calcium ions (curve A in **Fig. 1**), it can be seen that calcium fatty acid can protect the toner surface from the reduction of the hydrophobicity due to the adsorption of TX-100. This effect is more significant at low TX-100 concentrations (< 130 mg/L). When TX-100 concentration is higher than 130 mg/L, the advancing contact angle of toner film suddenly decreased from 105 to 45 degrees. Although the reason for this sharp decrease is not clear, the solubilization of fatty acid by TX-100 at the concentration close to its critical micellization concentration (185 mg/L) may be one of the possible effects.

Although the hydrophobicity of ink particles is one of the dominating factors in flotation deinking, the particle size is also critical. Obviously, an effective collector should not only remain a high contact angle of ink particles in solution, but also agglomerate the ink particles into an optimum size. **Fig. 2** shows the particle size in aqueous solutions as a function of the concentration of TX-100 or sodium oleic acid. It has been noted from toner particle size measurements that the number distribution of toner particle the presence of TX-100 has normal Gauss distribution, regardless of the concentration of TX-100. It can be seen that, when TX-100 was used alone, the toner particle size slightly decreased as the concentration of TX-100 was increased. This is not surprising because although the toner particles can be dispersed in the pulp filtrate and stabilized by adsorbed anionic trash (they aggregate and floated in pure water), there must be some small toner aggregates because anionic trash in the pulp filtrate is not a very effective stabilizer. When TX-100 was added in the suspension, these small toner aggregates were redispersed by surfactant resulting in a decrease in the average particle size. However, it can also be seen from **Fig. 2** that in the presence of 500 mg/L calcium chloride and 20 mg/L TX-100, the particle size of toner suspension increases

as the concentration of sodium oleic acid increases. This suggests that toner particles were aggregated by calcium sodium oleic acid even in the presence 20 mg/L TX-100. At 90 mg/L of sodium oleic acid solution, the mean toner particle size increased to 27 μm (Sauter Mean Diameter), which was in the optimum size range for flotation reported by Ferguson **[2]**. It was noted that the increase of collector concentration will not only increase the number average particle size, but also the particle size distribution. For example, it is found that the agglomeration of small particles was more significant that of large particles.

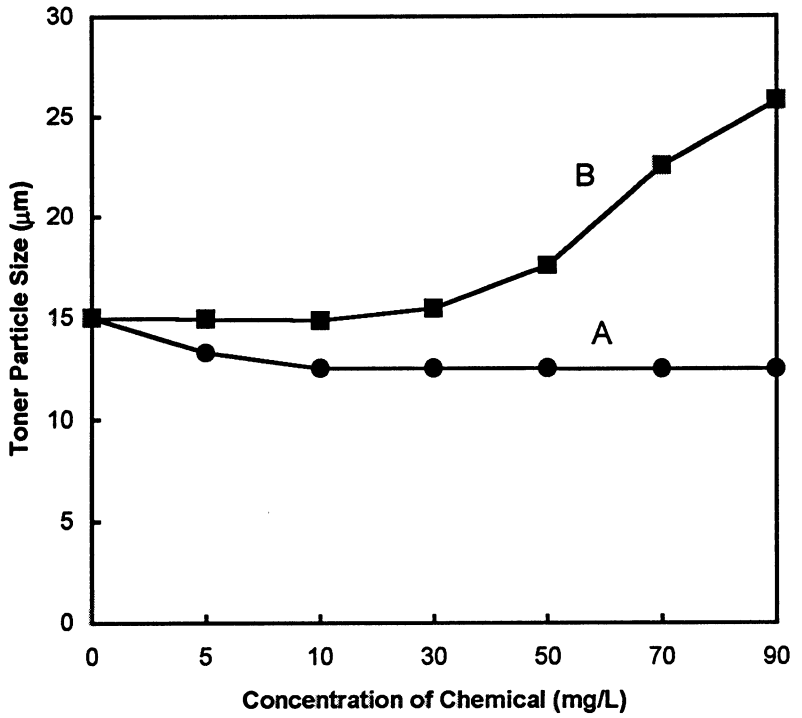

Fig. 2. Toner particle size as a function of A: TX-100 concentration; and B: TX-100 concentration in the presence of 50 mg/L sodium oleic acid and 500 mg/L calcium chloride.

The effect of hydrophobicity and particle size of toner in pulp slurry on the flotation deinking efficiency was investigated by measuring the brightness gain of the handsheets made from deinked xerographic fibers. The brightness gain as a function of TX-100 in either the presence or absence of calcium oleic acid is shown in **Fig. 3**. It can be seen that in the absence of calcium oleic acid, the brightness gain increases as

TX-100 concentration increases up to 120 mg/L, then decreases as TX-100 concentration further increases. The initial increase in the brightness at low TX-100 concentration is due to the increase in the foam stability, and the decrease in the brightness at high concentration is due to the decrease in the hydrophobicity of toner particles by adsorbing TX-100 molecules onto the surface, which is consistent with the contact angle measurement shown in **Fig. 1**. This behavior has also been previously reported **[11]**.

It is reasonable to assume that toner removal can be enhanced by adding a fatty acid and calcium ions because the toners have a high contact angle in the solution, as has been reported previously **[4]**. Surprisingly, our results shown in **Fig. 3** indicate that the presence of 50 mg/L sodium oleic acid and 250 mg/L calcium chloride decreases rather than increases the toner removal in similar pulp systems. Although the mechanism of this reduction in flotation deinking efficiency is not clear, the effect of calcium fatty acid on the foam stability and structure must be accounted. It was observed during the flotation experiments that the foam was much less stable in the presence of calcium fatty acid compared with that using TX-100 alone. Because the bubbles were broken during their rise to the top of the flotation cell, some adhered toner particles returned back to the pulp slurry, which may results in a decrease in the flotation deinking efficiency.

1.3.2. Kerosene as a collector in toner flotation deinking

Hydrocarbon materials that have been widely used in the mineral flotation industry as collectors are getting attention in the paper industry. Snyder and Berg **[7]** described that some hydrocarbon materials can be used as an agglomeration agent for suspended toner particles. Pelton **[12]** also found that ink particles are more easily adhered to hydrocarbon oil coated glass beads. Miller et al. **[13]** found that the toner flotation efficiency can be significantly improved by adding 5% tetrahydrofuran or acetone (based on dry waste) into pulp suspension. In a recent study **[14]**, Oguz indicated that a mixture of kerosene, detergent and borax can significantly improve ink removal. Although these findings are interesting, no fundamental study on the collector chemistry using a mineral oil or hydrocarbon material in flotation deinking has been reported in the literature. In this study, the kerosene was used as a model hydrocarbon collector for toner deinking. The contact angle of toner film in water was measured and

the results are shown in **Fig. 4**. It can be seen that although the advancing contact angle of toner decreases slightly as kerosene concentration is increased, it is still as high as 130 degree at kerosene concentrations of up to 160 mg/L (small kerosene droplets on the surface of solution will be seen with further increases in concentration). However, when TX-100 was added into toner suspension in the presence of 50 mg/L kerosene, the advancing contact angle was decreased. Although this decrease is significant, by comparing with curve C in **Fig. 4**, it can be seen that the addition of kerosene can restore some of the loss in toner hydrophobicity that is caused by the adsorption of TX-100.

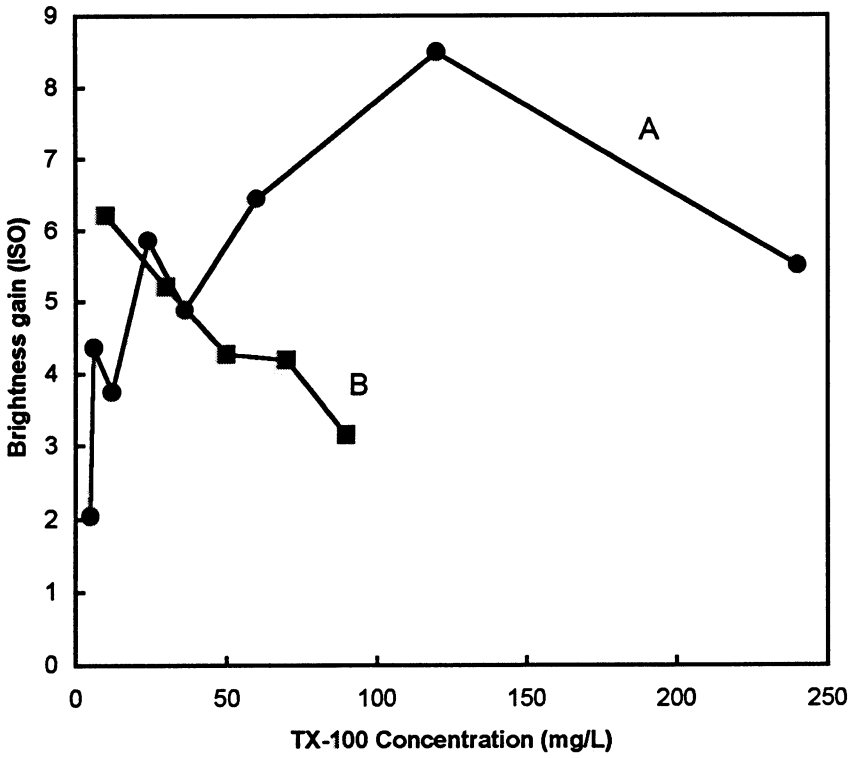

Fig. 3. The brightness gain of handsheed made from deinking fibers as a function of A: TX-100 concentration without other chemicals; B: TX-100 concentration in the presence of 50 mg/L sodium oleic acid and 250 mg/L calcium chloride.

The effect of kerosene on the agglomeration of toner particles in the presence of TX-100 was also examined and the results are shown in **Fig. 5**. It can be seen that the particle size of toner in the presence of 20 mg/L TX-100 increases significantly as the increase in the kerosene concentration, suggesting a significant agglomeration of toner particles in this solution. It is believed that the agglomeration of toner particles was caused by "oil bridging" mechanism as reported by Berg et al. **[7]** using other hydrocarbon solvent.

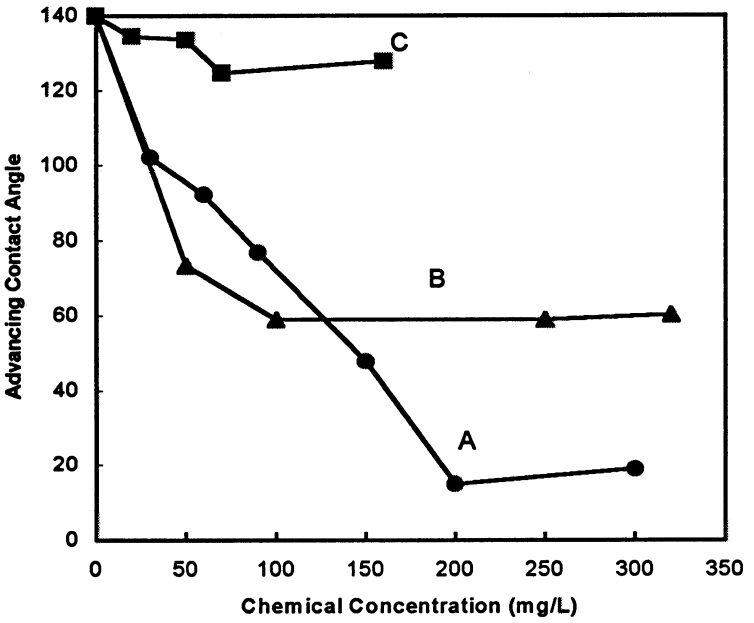

Fig. 4. Advancing contact angle of toner film in aqueous solutions as a function of A: TX-100 concentration without any other chemicals; B: TX-100 concentration in the presence of 50 mg/L kerosene; C: kerosene concentration.

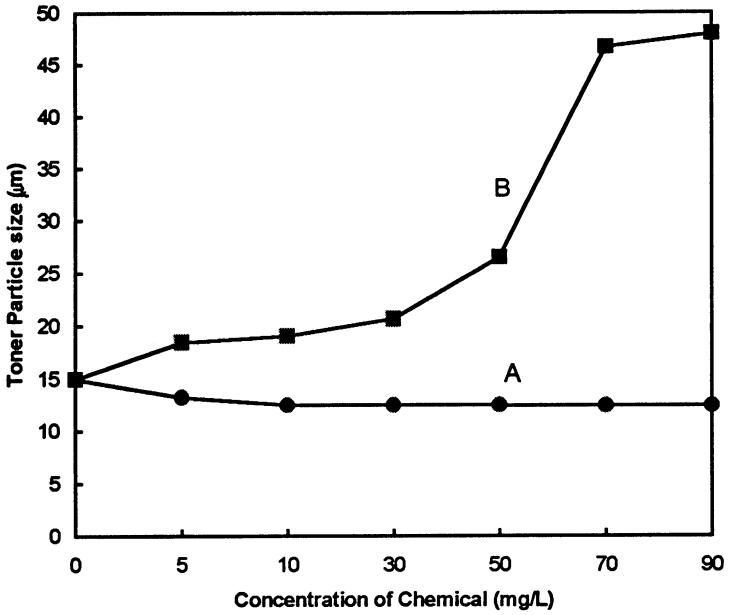

Fig. 5. Toner particle size as a function of A: TX-100 concentration; B: kerosene in the presence of 20 mg/L TX-100.

The effect of kerosene on the flotation deinking efficiency of toner printed papers was studied using TX-100 as a frothing agent. The brightness gain of the handsheets made of recycled fibers is shown in **Fig. 6**. It can be seen that in the presence of 20 mg/L kerosene, the ink removal is higher than that of without kerosene, particularly at low TX-100 concentration. This is consistent with the contact angle and particle size measurement, i.e., a high contact angle and an optimum particle size result in a high deinking efficiency. The results shown in **Fig. 6** indicate that kerosene can be used as a collector for toner flotation deinking when TX-100 is used as a frothing agent.

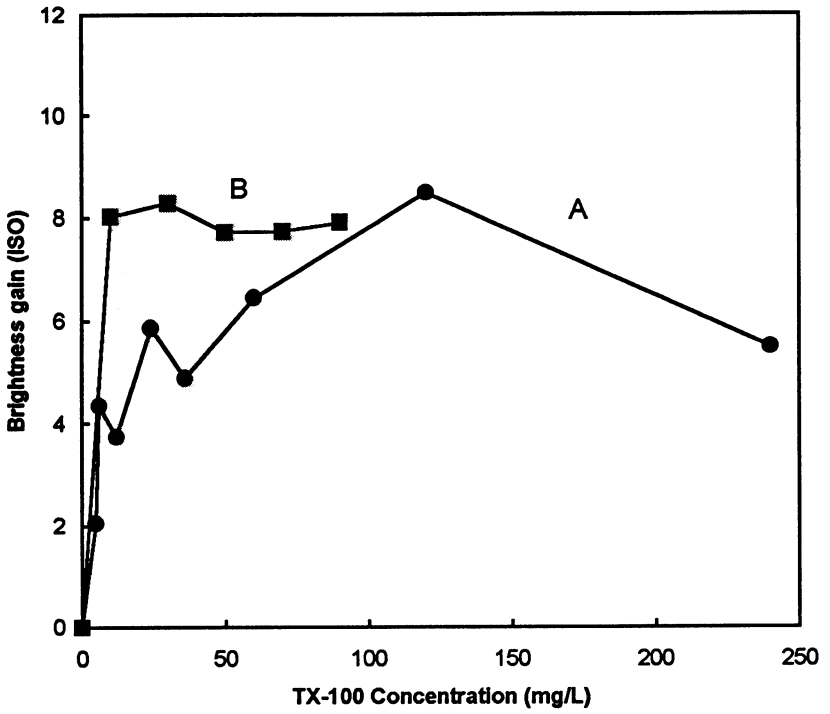

Fig. 6. The brightness gain of handsheed made from deinking fibers as a function of A: TX-100 concentration; B: TX-100 concentration in the presence of 20 mg/L kerosene.

1.3.3. Toner flotation deinking using cationic surfactants

Cationic surfactants have been traditionally used in mineral flotation. One of the advantages of using cationic surfactants is that these chemicals can function as both a collector and a frothing agent for some ores. The effect of cationic surfactant structure on the mineral flotation was studied **[15-17]**. Although cationic surfactants are very effective for flotation of some mineral particles, limited research **[1,2,18,19]** has been done using cationic surfactants for flotation deinking. There is no report in the literature on the application of cationic surfactants to deink toner-printed wastepapers.

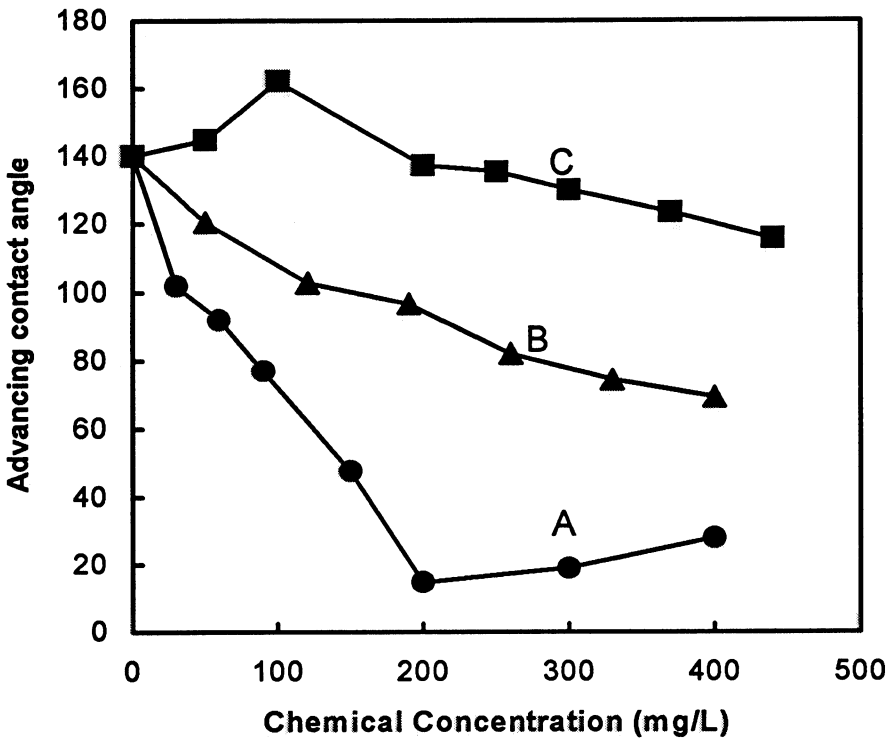

Fig. 7. Advancing contact angle of toner film in aqueous solutions as a function of A: TX-100 concentration; B: DTMAB concentration; C: CTMAB concentration.

Fig. 7 shows the advancing contact angle of toner film in different cationic surfactant solutions. It can been seen that the contact angles of toner film obtained in two different cationic surfactants are much higher than that in the TX-100 solution. More interesting is that the contact angle increases initially as the concentration of CTMAB increases, then decreases as further increase in CTMAB concentration. It is known that the toner particles in wood pulp suspension are negatively charged because of the adsorption of soluble anionic polymers, such as sulphonated lignin and fatty acids from wood fibers, onto the toner surfaces. When cationic surfactant molecules are adsorbed onto these negatively charged toner surfaces, the configuration of adsorbed cationic surfactant should be different from that of anionic and non anionic surfactants. At a low concentration of cationic surfactant, the positively charged surfactant heads anchor to the negatively charged toner surface leaving hydrophobic tail toward the solution. As a result, the contact angle is increased.

However, at a high concentration of cationic surfactant, a double layer adsorption can occur and the hydrophilic heads of cationic surfactant orient to the water phase, which reduced the contact angle. The configurations of cationic surfactant at different concentrations are schematically shown in **Fig. 8**. It should be noted that no contact angle increase was observed for the cationic surfactant of DTMAB, which may be attributed to the fact that the DTMAB has a shorter hydrocarbon chain than the CTMAB, resulting a more hydrophobic adsorption layer on the toner surface.

The effect of cationic surfactants on the agglomeration of toner particles is shown in **Fig. 9**. The particle size of toner particles in pulp filtrate was almost a constant when the concentration of DTMAB was increased, but increased steadily with the increase of CTMAB concentration up to 90 mg/L. The particle size increase is consistent with the hydrophobicity increase of toner particles in cationic surfactant solutions. It is believed that in addition to the hydrophobicity effect, the charge neutralization between cationic surfactant and negatively charge adsorbed materials on the toner surface in a pulp filtrate will also affect the toner particle agglomeration.

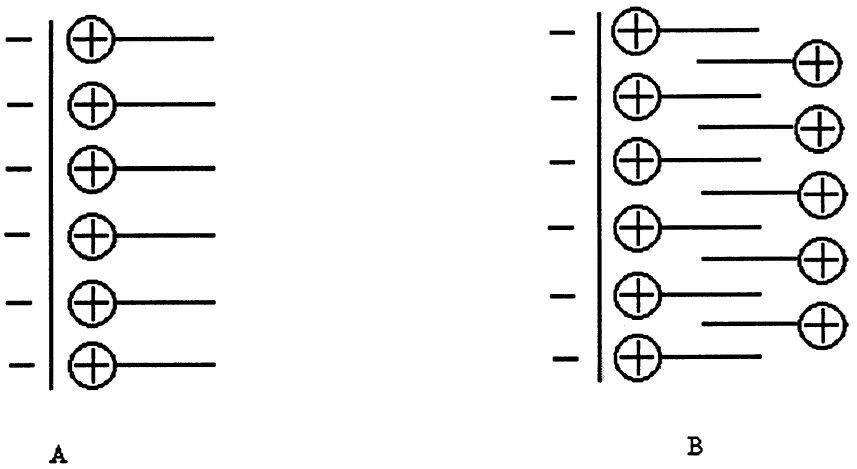

Fig. 8. The orientation of cationic surfactant on a negatively charged toner surface. A: monolayer adsorption at low concentration, and B: double layer adsorption at high concentration.

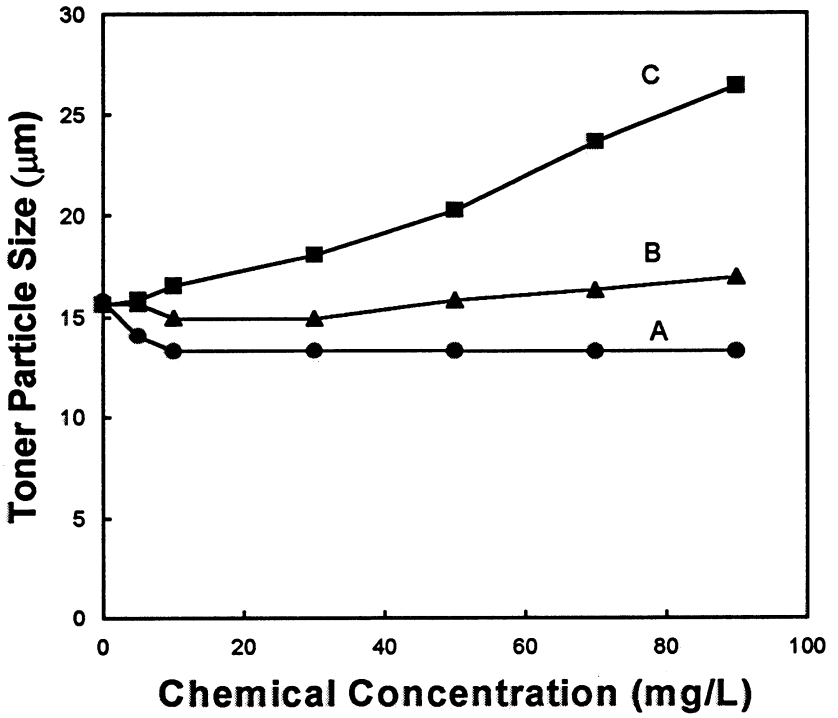

Fig. 9. Toner particle size as a function of A: TX-100 concentration; B: DTMAB concentration; C: CTMAB concentration.

As discussed previously, the toner particle hydrophobicity can remain relatively high and particle size can be increased in CTMAB solutions. It was also found that cationic surfactants are effective frothing agents as well as collectors in pulp suspensions. Therefore, it is not necessary to have a second surface active agent in flotation deinking if a cationic surfactant is used. This advantage may significantly reduce the flotation deinking cost. The brightness gain obtained from handsheets made of deinked fibers as a function of cationic surfactant concentration is shown in **Fig. 10**. It was found that cationic surfactants produced much higher brightness gains than TX-100. The result is consistent with the contact angle and particle size measurements, i.e. CTMAB and DTMAB are very effective collectors and frothing agents for toner flotation deinking.

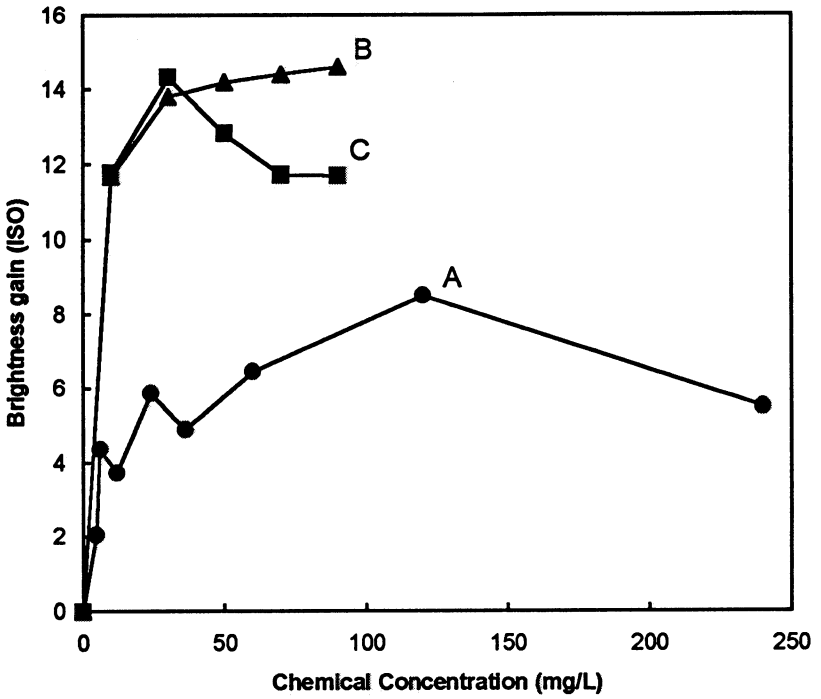

Fig. 10. The brightness gain of handsheed made from deinking fibers as a function of A: TX-100 concentration; B: DTMAB concentration; C: CTMAB concentration.

1.3.4. Concluding remarks

1) The contact angle of toner film in water-surfactant solution decreases with the increase of TX-100 concentration regardless if there is a collector. The balance between froth stability and hydrophobicity leads to an optimized concentration for toner removal if TX-100 is used alone.

2) The addition of fatty acid/calcium ions causes particle agglomeration but does not increase the contact angle of toner particles. The addition of sodium oleic acid/calcium ions in the flotation process does not enhance the toner removal if TX-100 is used as a frothing agent.

3) Kerosene can increase the toner particle size and maintain a relatively high contact angle of toner in TX-100 solution. The flotation deinking efficiency of

toner-printed papers can be improved by adding a small amount of kerosene if TX-100 is used as a frothing agent.

4) Cationic surfactant can be used as both a collector and a frothing agent. For the systems investigated in this study, the cationic surfactants provideed the best ink removal.

2. FIBER LOSS IN FLOTATION DEINKING: EFFECT OF FIBER TYPES

2.1. Background

Although the deinking efficiency is closely related to the brightness and cleanliness of the fibers, brightness figures without any information on the yield of the deinked fibers have only limited value because the achieved brightness strongly depends on the yield. Low yield caused by high fiber loss is one of the biggest problems in flotation deinking. Reported fiber loss is in the range of 4-24 wt% depending on the processes, equipment, and chemicals used in flotation deinking. For highly sized or waxed fibers, such as old corrugating containers, fiber loss is even higher, and the flotation technique cannot be used for these paper products unless a new technique is established.

Most authors **[20-22]** have postulated that the fiber loss in flotation deinking is caused by air bubbles routinely adhering to the fibers during the flotation process. In a series of studies on fiber loss in flotation deinking, Turvey **[20,21]**, and Schwinger and Dobias **[29]** indicated that 1) unprinted fibers do not float; 2) calcium ions can significantly increase fiber loss for printed fibers; 3) nonionic fatty alcohol ethoxylate surfactants cause high fiber loss; and 4) pH plays an insignificant role in fiber loss. From these studies, Turvey **[20,21]** further concluded that fiber loss is due to the fact that part of the fiber becomes hydrophobic and adheres to air bubbles. However, no direct experimental measurement of fiber surface chemistry can support this assumption. Furthermore, some of the conclusions from Turvey **[20]** have been argued by other researchers **[4,5,22-24]** who indicated that unprinted fibers, even very clean bleached fibers, can still float during the flotation deinking process. In contrast to Turvey's study, some recent papers **[4,5,24]** indicated that the fiber loss in flotation

deinking is solely caused by physical entrainment rather than true flotation. The conflicting experimental results obtained by different researchers suggest that the mechanism of fiber loss in flotation deinking has not be well understood.

It was reported that long fibers float easier than wood fines **[22,24]**. To explain this phenomenon, Li and Muvundamina **[22]** assumed that surfactant molecules have different orientations on the fine and fiber surfaces. It is well known that the surface of fines is more hydrophobic than long fibers because of its high lignin content. When surfactants adsorb onto fines, the hydrophobic tails of surfactant molecules anchor onto the hydrophobic sites of fines and leave the charged heads (or hydrophilic parts) toward the water phase. This leads to an increase of hydrophilicity of the surface of wood fines and prevents them from adhering onto air bubble surfaces. For long fibers, on the other hand, the surface is very hydrophilic, and surfactant adsorption is through the interaction between the hydroxyl groups of fiber surfaces and the charged heads of surfactant molecules (or hydrophilic parts of nonionic surfactant), resulting in an increase of hydrophobicity. Li and Muvundamina **[22]** believed that the increase in hydrophobicity of fiber surfaces was the main reason for fiber removal. Once again, this is only an assumption, and there is no direct experimental measurement to support it.

It is clear that there are many arguments on the fiber loss mechanism. In order to study the effect of fiber surface chemistry on the fiber loss, both unsized and AKD-sized fibers from the same bleached softwood kraft pulp were used in this study. The average fiber length was 2.83 mm. Because the sized fibers have the same geometric property as unsized fibers but totally different of surface chemistry, the contribution of fiber surface chemistry and fiber length to the total fiber loss can be separately studied.

The flotation cell used in this study includes a polyacrylate column (12 cm in diameter; variable in height) and a gas inlet filter. Nitrogen was injected from the bottom of the flotation cell through a air inlet filter. Two types of inlet filters with pore sizes of 10 or 2μm were used. Both the fibers that were removed from the cell (fiber loss) and those that remained in the cell were filtered, oven dried, and weighed. The detail description of flotation facility and experiments have been given in our lass year's progress report **[25]**. In our study, the water loss was controlled by varying the froth

height (adding extra columns to the top of the flotation cell) at a fixed nitrogen flow rate and flotation time. This method is totally different from previously reported studies **[3,4,24]** in which the water loss was controlled by varying the flotation time at fixed froth height. We believe that our method is more scientific for fiber loss mechanism study than the method used in previous studies. The detail discussion can be found in our recently published paper **[24]**.

In the Progress Report of FY96-97 **[25]** we studied the mechanisms of fiber loss using a AKD-sized and a clean BSK (bleached softwood kraft) pulps. In this progress report, the effects of fiber and surfactant types on the total yield are discussed.

2.2. Experimental

The pulp properties used in this study are given in **Table I**. *Atlanta Journal-Constitution* and New York Times were used as old newsprint (ONP). The average aging time of ONP used in this study is about 1.5 months. Pump Magazine and Paper Maker Magazine were used as old magazine (OMG). Old magazines were collected different times.

Table I. Fiber properties.

Fiber*	Ash Content (%)	advancing contact angle in water (degree)	Advancing contact angle in 100 g/L TX-100 (degree)	Fiber length (mm)
ONP (*Atlanta Journal-Constitution*)	0.93%	52	26	1.60
Bond paper	16.24%	28	-	1.79
OMG		-	-	
BSK	0	32	4	2.83
0.2% AKD emulsion sized BSK	0	76	28	2.83
0.6% AKD emulsion sized BSK	0	106	34	2.83

*: ONP: Old newsprint; OMG: Old magazine; BSK: Bleached softwood kraft fiber.

The fiber lengths were determined by image analysis. The width and lumen diameter of fibers were measured using 400× magnification with the aid of OPTIMAS image analysis software. The fiber perimeter was calculated from number average fiber width and lumen diameter. The ash content was obtained at 550 °C according to the TAPPI standard method (T211 om-93).

The PCC content was analyzed by potential titration using EDTA salt as titrate. The pulp slurry was firstly adjusted to pH <3 by adding HCl and stood up for ~0.5 hr. After calcium carbonate dissolved and CO_2 evaporated, ~1 ml NH_3H_2O was added in the solution to bring pH up to ~9.2. The Ca^{2+} concentration was determined by titration using a 0.002M EDTA (ethylenediamine tetraacetic acid disodium, Aldrich, 99+%) solution. A calcium selective electrode (Fisher product) and a glass pH reference electrode (Fisher product) were used as the detector. A detail description about the titration technique can be found from Fisher's product menu.

The sized fibers were made by the reaction of fibers with varying amounts of a cationic AKD (alkyl ketene dimmer) sizing emulsion (Hercon 70, Hercules Inc.) in ~3% fiber consistency for 5 min. The furnishes were filtered and air dried about 2 hr. The air-dried fibers were heated to 100°C in a vacuum oven for ~30 min.

The handsheets for brightness analysis were made on a 15-cm Büchner funnel using TAPPI standard method (T452 om-92). The brightness of the handsheets was measured using a Shimadzu UV-VIS Spectrophotometer (UV-160A).

2.3. Effect of Fiber Hydrophobicity on the Fiber Loss

The flotation of solid materials can be divided into "true flotation" and "entrainment." True flotation occurs when solids attach to air bubbles and are floated with them. A basic requirement for true flotation is that the solid particles must be hydrophobic enough so that they can strongly adhere onto the bubble surface. Entrainment occurs when particles enter the froth with the water and occupy the spaces between the bubbles. When froth raises up, part of the water and particles entrained in the froth will drain back to the pulp suspension, but the remainders are carried upwards and scraped off. As a result, fiber removal by physical entrainment should be a function of water removal, and at ideal conditions, a linear relationship between fiber removal and water removal is expected. The contributions of true flotation and entrainment in mineral flotation have been discussed, and the following equation has been suggested **[26]**:

$$R = A + CV_{water} \quad (1)$$

where R is the total recovery of the given solid suspension at experimental conditions; A is the recovery of the solid by true flotation; C is the concentration of entrained solids in removed water; and V_{water} is the volume of removed water. At ideal conditions, the true flotation A and the concentration C of entrained solids in removed water can be obtained from the intercept and the slope of removed solids versus removed water, respectively.

In order to separately study the true flotation and entrainment of fibers in flotation deinking, a bleached softwood kraft pulp was first used in this study. Direct measurement of wettability using a separated fiber group technique indicated that the receding and advancing contact angles of the bleached softwood fiber in a 100-mg/L TX-100 solution are zero and <5 degrees, respectively. This suggests that the bleached softwood kraft fibers are very hydrophilic and they cannot adhere to air bubbles by hydrophobic force in the flotation process. In other words, the loss of these hydrophilic fibers in the flotation cell should be caused solely by the physical entrainment.

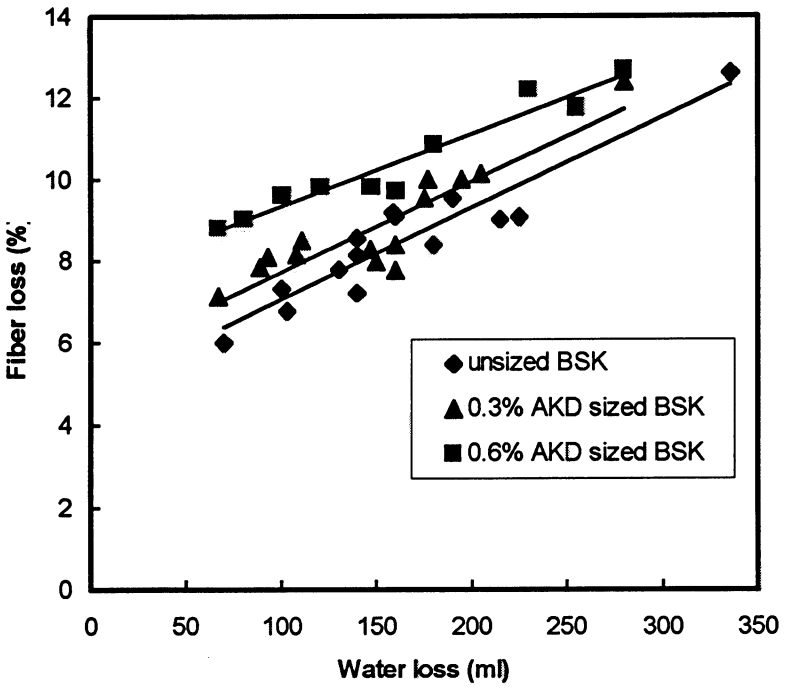

Fig. 11. Fiber loss as a function of water loss for unsized and AKD-sized bleached softwood fibers. The water and fiber losses were measured at different froth heights. Pore size of air inlet filter: 10 μm; fiber consistency: 0.52%; concentration of TX-100: 100 mg/L; nitrogen flow rate: 1800 cm^3/min; flotation time: 2 minutes.

Fig. 11 shows fiber loss as a function of water loss for different fibers after a 2-minute flotation. According to **Equation (1)**, a zero intercept of fiber loss against water loss should be expected for these hydrophilic unsized fibers because these fibers have a zero receding contact angle and very low advancing contact angle (<5 degrees). In other words, all floated fibers in this system should be solely caused by physical entrainment. However, the results of **Fig. 11** clearly show that both the slope and intercept for bleached softwood kraft fibers (unsized) are not zero. This strongly indicates that although **Equation (1)** has been used for the mineral flotation system, it cannot be directly used to describe the fiber loss in flotation deinking. It should be noted that **Equation (1)** is based on the assumption that the concentration of entrained (excluding adhered) solids in the froth phase is a constant during the water drainage, and all entrained solid particles will be washed back to the pulp phase if the water is

fully drained from the froth. This may be true if the size of entrained particles is small and the density of the particles is high, such as mineral particles, but it is not the case for wood fibers because some entrained fibers cannot pass through the microchannels between bubbles during the drainage of water in the froth phase due to their large size and small density. As a result, a nonzero intercept of fiber loss plotting water loss must be obtained even though the flotation of wood fibers is solely caused by entrainment. Because some of entrained fibers cannot be washed away during water drainage, a correction for these "unwashable" entrapped fibers must be made in order to use **Equation (1)** for wood fibers. It should be noted that unwashable entrapped fibers are different from true flotation fibers, although both of them cannot be washed away during water drainage. Obviously, the consistency of these "unwashable" entrapped fibers in the froth should be a function of foam structure, fluid dynamics of water in the froth microchannels, the fiber length, and orientation, etc. If all experimental conditions remain constant during the foam raising up in the flotation cell, it can be approximately assumed that the weight of unwashable entrained fibers is constant in the froth. Therefore, **Equation (1)** should be modified to

$$R = A + B + CV_{water} \quad (2)$$

where B is the weight of unwashable entrained fibers.

Equation (2) indicates that the intercept of the plot of total fiber loss R versus water removal should equal the sum of the fiber loss caused by true flotation A and unwashable entrapped fiber B rather than true flotation A alone, and this intercept is independent of total removed water V_{water} at a fixed flotation time. **Equation (2)** also indicates that although the true flotation A is zero for hydrophilic wood fibers, the intercept of the plot of total fiber loss versus water loss should equal B rather than zero. By plotting total fiber loss against water removal for unsized fibers shown in **Fig. 11**, the weight of "unwashable" entrapped fiber B and the consistency of "washable" entrained fiber C were 0.29 g and 0.8 g/L, respectively.

Fig. 11 also gives the comparison of fiber losses for unsized and AKD-sized fibers. It has been known from our previous study **[25]** that the advancing contact angles for 0.2 and 0.6% AKD-sized fibers in a 100mg/L TX-100 surfactant solution are

28 and 39 degrees, respectively, which are much higher than that of unsized fibers (<5 degrees) in the same solution. From **Fig. 11** it can be seen that the fiber losses of sized fibers are consistently higher than unsized fibers. This result indicates that the fiber surface chemistry will also contribute to the fiber loss. Because both the sized and unsized fibers used in this study have the same length, it is reasonable to assume that the entrainment factors *B* and *C* in **Equation (2)** are the same for all of the sized and unsized fibers. Therefore, the difference in the fiber loss between unsized and sized fibers is attributed solely to the true flotation *A*. Although this assumption may be too simple, the experimental results of **Fig. 11** indicate that the slope *C* is almost constant for all three fibers.

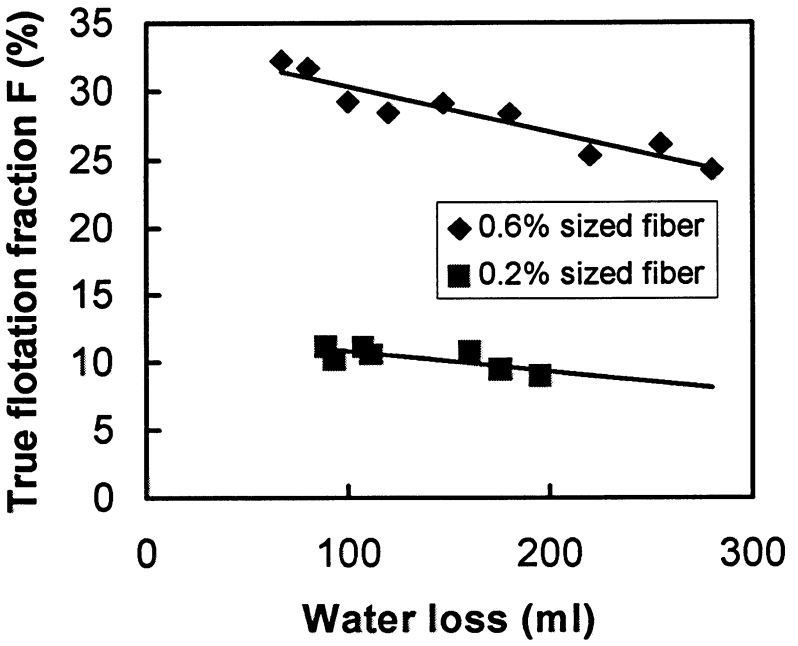

Fig. 12. True flotation fraction F as a function of water loss. The true flotation fraction for unsized bleached softwood fiber is assumed as zero. Pore size of air inlet filter: 10 μm; fiber consistency: 0.52%; concentration of TX-100: 100 mg/L; nitrogen flow rate: 1800 cm^3/min; flotation time: 2 minutes.

In terms of the above assumption, by applying B = 0.29 g and C = 0.8 g/L to **Equation (2)**, the weights of true flotation A for 0.2 and 0.6% AKD-sized fibers were obtained and they were 0.025 and 0.15 g, respectively. Comparing the value of true flotation A with total entrained fibers $B + CV_{water}$, it can be found that true flotation A is smaller than total entrained fibers even for highly sized fibers.

The true flotation fraction F is defined as

$$F = A/R \quad (3)$$

The plots of F as a function of water loss fiber loss are shown in **Fig. 12**.It can be seen from **Fig. 12** that the true flotation fraction F for 0.2 and 0.6% AKD-sized fibers is in the range of 8-12 and 25-33%, respectively, depending on the froth heights. The results suggest that although true flotation is one of the mechanisms of fiber loss, most lost fibers (>88% for 0.2% AKD-sized and >33% for 0.6% AKD-sized fibers) in flotation deinking are mainly attributed to physical entrainment for these systems. **Fig. 12** also shows that the true flotation factor F increases as the froth height is increased. This is because the total fiber loss R is decreased, but the true flotation contribution A remains constant when froth height is increased.

Although water loss in flotation deinking has not been considered as a problem in the paper mill, the energy saved by reducing water loss can also benefit the paper industry. Even for a fully closed flotation deinking mill, water loss by froth removal can still be as high as 10% of the total water in the flotation cell, which corresponds to a water loss of ~10 tons/(ton pulp). Because the discharged water contains many deinking chemicals, such as the surfactant and basic materials, reducing water removal is also important for a deinking mill. The results of a study conducted at IPST indicates that properly controlling the froth height and froth stability is a cost-effective method to reduce both water consumption and fiber loss.

2.4. Effect of Fiber Types on Fiber Loss

Fig. 13 shows fiber loss as a function of water loss obtained from different froth heights. The experimental conditions for all of the experiments are the same except different fibers were used.

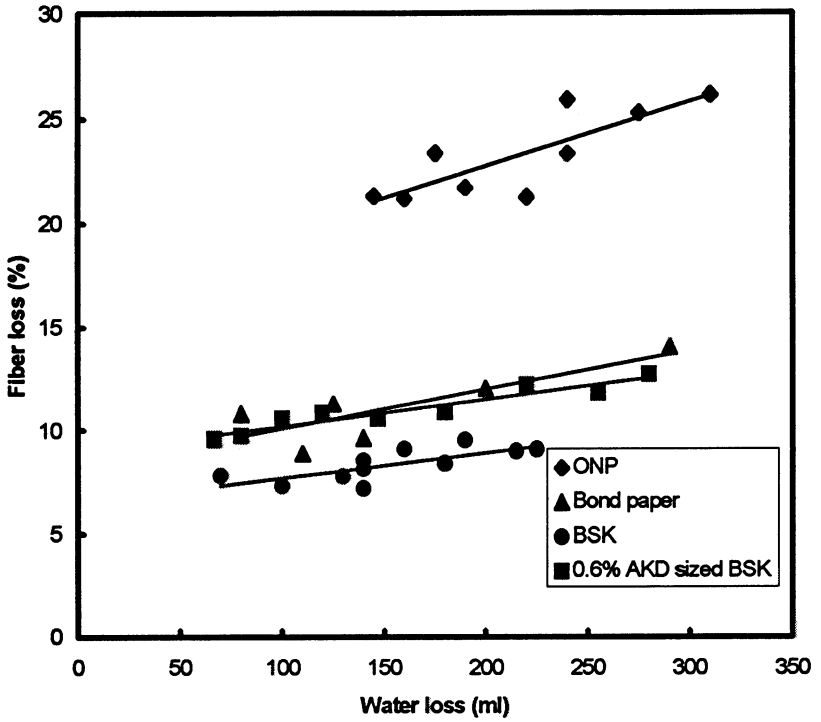

Fig. 13. Fiber loss as a function of water loss for different fibers. Fiber consistency: 0.52%; Surfactant: 100 mg/L TX-100; Nitrogen flow rate: 1800 cm^3/min; flotation time: 2 minutes.

It can be seen that, at the same water loss volume (same froth height), the ONP gave the highest fiber loss. The single fiber wettability measurement indicates (see Table I) that the advancing contact angle of ONP in water is 52.2°, that is much higher than bond paper (28.3°) and unsized BSK (32.0°) fibers. Even in 100 mg/L TX-100 solution (the same concentration as used in flotation deinking), the advancing contact angle of ONP fibers is still higher than others. Because of this high contact angle, it is expected that ONP should give a higher fiber loss than bond paper and BSK fibers, which was confirmed by the experimental results shown in **Fig. 13.** However, it is surprising that ONP gave a higher fiber loss than AKD-sized BSK fibers because 0.6% AKD-sized fiber has a much higher advancing contact angle than ONP in both pure water and 100 mg/L TX-100 solution (see Table 1). This suggests that the higher fiber loss of ONP than other fibers cannot be simply explained by hydrophobicity alone. As discussed in last year's report **[25]** and our recent publication **[23]**, the physical

entrainment rather than true flotation is the major contributor to fiber loss. Because the physical entrainment strongly depends on the geometry of the fibers and froth structure, the difference in fiber length among these fibers has to been considered. It can be seen from **Table I** that the fiber length of ONP is much shorter than that of BSK. The higher fiber loss of ONP than AKD-sized fibers may suggest that ONP can be entrapped in the foam network much easier than long BSK fibers. However, more work is needed for a full understanding of the relationship among fiber geometry, foam structure, and fiber loss. It is expected that there may be an optimized fiber length that will causes the highest fiber loss under a fixed foam structure.

2.5. Effect of Different Surfactants On Fiber Loss

Because many different surfactants, including anionic, cationic, and nonionic, have been used in flotation deinking, it is necessary to know if the above conclusion obtained from TX-100 can be applied to other surfactant systems. For this purpose, fiber loss in an anionic surfactant (SDS) and a cationic surfactant (CTMAB) solution was studied. However, it was found that the maximum froth height generated by SDS was only about 20 cm, which did not allow us to study the effect of froth height on fiber loss. Therefore, only cationic surfactant CTMAB was studied in detail. **Fig. 14** shows fiber loss as a function of water loss in a CTMAB solution. Although the foam stability and microstructure could be significantly different when different surfactants were used, a similar trend of fiber loss against water loss was observed for the systems of TX-100 and CTMAB, i.e., sized fibers resulted in a higher fiber loss, and the intercept of fiber loss as a function of water loss was not zero. This may suggest that although the true flotation and the physical entrainment will contribute to total fiber loss, the ratio between these two may be different when different surfactants are used.

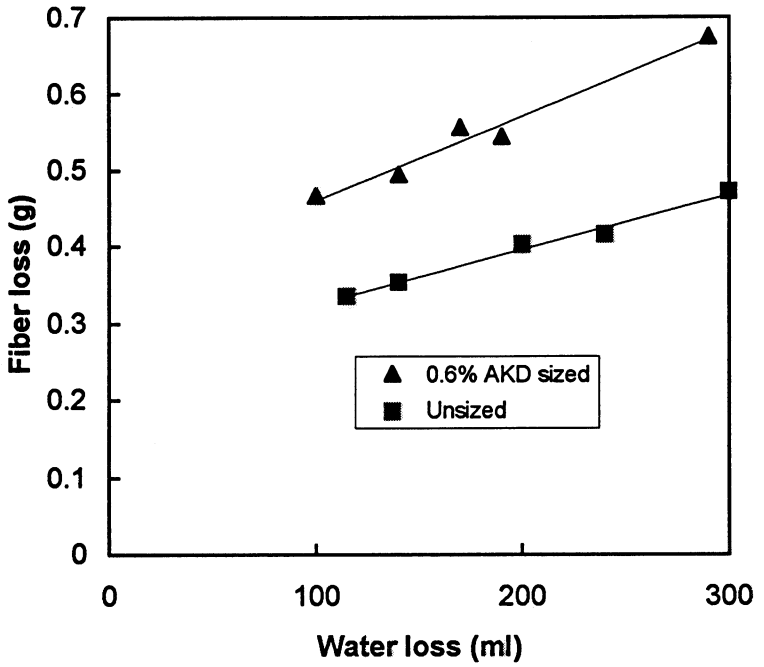

Fig. 14. Fiber loss as a function of water loss for unsized and AKD-sized bleached softwood fibers using cationic surfactant. The water and fiber losses were measured at different froth heights. Pore size of air inlet filter: 10 μm; fiber consistency: 0.52%; concentration of CTMAB: 100 mg/L; nitrogen flow rate: 1800 cm^3/min; flotation time: 2 minutes.

2.6. Concluding Remarks

1) Both physical entrainment and true flotation will contribute to total fiber loss in flotation deinking, but the physical entrainment is the dominant factor.

2) Old newsprint gives a higher fiber loss compared with other fibers when TX-100 was used as a surfactant. Possible reasons for this higher fiber loss may be due to the short fiber length and high hydrophobicity of ONP.

3. THE ROLE OF SURFACTANT IN THE INK-FIBER DETACHMENT

3.1. Backgroud

It is quite common in the deinking operation to add a surfactant in pulps before or during the pulping because most people believe that surfactant can stabilize the ink particles and improve the ink-fiber detachment. However, it is well-known that the adsorption of dispersant has many negative effects, such as rendering the ink particles from hydrophilic to hydrophobic, reducing the agglomeration of ink particles, and increasing the stearic or electrical repulsion force between ink particles and air bubbles. To overcome some of the problems given above, chemicals called displectors have been developed **[27,28]**. However, the mechanism of dispersant-collector has not been fully understood, and the effectiveness of this chemical has not been widely tested.

The process surfactant used in deinking has many negative effects. One of the problems is that the process surfactant will cause foaming problem in pulpers, which will reduce the capacity of the equipment. Foaming can also cause overflow of the process unit. Although the foaming problem can be partially solved by adding a deformer agent, it is always cheaper to use less surfactant than to add defoamer. The remaining surfactant in recycled pulp will also cause foaming problems on a paper machine. Another problem related to the remaining deinking surfactants is that they will contaminate recycled fibers, therefore, the fiber-fiber bonding and paper quality will be reduced. The pollution of processing surfactant will also be a serious problem for paper mills. As discussed above, the reduction of the surfactant consumption in the deinking process will improve the paper quality and papermaking process, and reduce the cost of water clarification.

In order to reduce the surfactant consumption, it is important to first understand the real role of surfactant in different deinking steps, including pulping, washing, screening, and flotation. It is interesting to know a) how the surfactant will affect the ink detachment? b) what type of wastepaper needs a dispersant during pulping? c) what type of dispersant is the most effective for certain paper grades? and d) what addition point is most effective and gives the least negative effects? This study will focus on the

role of surfactant in the repulping process, i.e., how the surfactant will affect the ink-fiber detachment.

Calcium soaps of fatty acids are the classic collector used in flotation deinking. Borchardt indicated that calcium ions should be added to the pulp simultaneously or before the fatty acid [29]. The reason for that is because the fatty acid will server as a dispersant to reduce the particle surface hydrophobicity and particle size. However, it should be argued that if the fatty acids have formed complexes with calcium ions before or during the pulping, the ink detachment will also be reduced. In other words, it may be more effective if this surfactant is added during flotation rather than repulping. Even for nonionic surfactants that are traditionally added into the pulper, any differences between adding surfactant before and after pulping are not very clear. Therefore, it is interesting to know where is the best addition point for flotation deinking surfactant.

3.2. Experimental

The effect of surfactant on the ink-fiber detachment was studied by comparison of handsheet brightness. The recycled fibers from either washing or flotation were used to make a handsheet. Two types of wastepapers were repulped at neutral pH in the presence or absence of surface activities. For the washing experiment, repulped pulps were washed by tap water (~4 times of the volume of pulp slurry) using a dynamic drainage jar equipped with a 125-mesh screen. It is assumed that all of the detached ink in the pulp slurry can be washed away, but the bound ink will still remain in the fiber suspension after washing. By comparing the brightness of the washed fibers that were repulped in the presence of different amounts of surfactant, the role of surfactant in the ink-fiber detachment will be evaluated.

A column flotation cell was used in flotation deinking. The initial distance from pulp suspension to the top of the flotation cell was 5 cm. The wastepaper used for this study included *Atlanta Journal-Constitution* and bond papers. Nonionic surfactant (TX-100) and anionic surfactant (sodium oleic acid) were used.

It was found that the ink particles printed on the ONP are very small, and they can pass through the fiber web and screen easily during the handsheet preparation,

resulting in an increase in the brightness and causing two-sideness problems on the handsheet. To solve these problems, several retention aids were used during the handsheet preparation. It was found that polyethylene oxide (PEO)/phenol formaldehyde resin (PFR) is the best retention system for ink retention during handsheet preparation. The brightness showed in this study was obtained in the presence of 4 ppm PEO (M_w = 8 million, Aldrich) and 8 ppm water-soluble PFR (Cascophen C27, Borden Chemical, Canada) except additional description being given.

3.3. Results and Discussions

3.3.1. The effect of sodium oleic acid on the ink-fiber detachment and ink removal

The brightness of flotation recycled ONP as a function of sodium oleic acid concentration in the presence of 500 ppm $CaCl_2$ is shown in **Fig. 15**. The two curves showed in **Fig. 15** were obtained in similar flotation conditions but different addition sequences of fatty acid, i.e., in one case, the sodium was added before pulping, and in another case, the sodium surfactant was directly added into the flotation cell. It can be seen that the two processes resulted in only a small difference in handsheet brightness. This suggests that although adding fatty acid before pulping (without Ca^{2+}) may enhance the ink detachment of offset ink from ONP fibers, this enhancement is not significant. This conclusion was further confirmed by washing experiments. In these experiments, the ONP was repulped in the presence of different concentrations of sodium oleic acid. After repulping, the fibers were extensively washed by tap water using a dynamic drainage jar. The brightness of washed fibers as a function of sodium oleic acid concentration is shown in **Fig. 16**. Two conclusions can be drawn from **Fig. 16,** 1) the brightness of the handsheet increases as sodium oleic acid concentration is increased regardless of whether the sodium oleic acid was added before or after pulping. This is not surprising because sodium oleic acid will act as a stabilizer for small offset ink particles, which makes ink particles easier to separate from the fiber surface; 2) the addition order of fatty acid will slightly improve the brightness. This is consistent with the flotation deinking results showed in **Fig. 15**, i.e., adding fatty acid into the pulper will slightly improve the ink detachment from the ONP fiber surface.

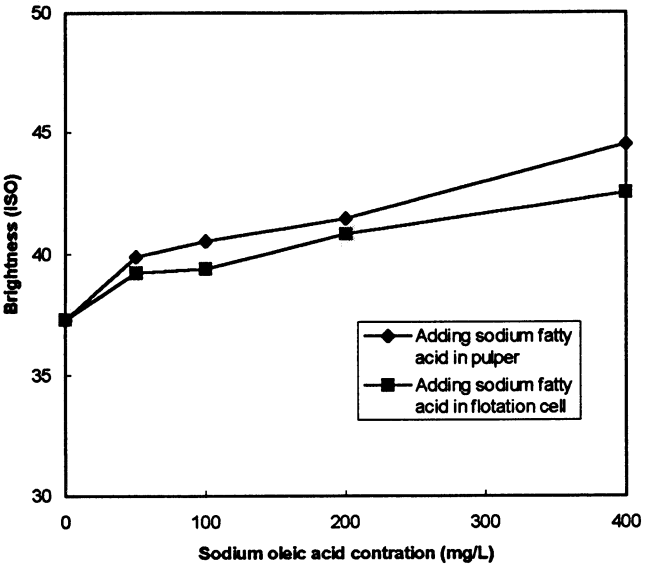

Fig. 15: Brightness of handsheet prepared from flotation deinked ONP. Pulp consistency: 0.52%; Nitrogen flow rate: 1800 cm^3/min; Calcium chloride concentration: 500 mg/L (added to the pulp after pulping); Flotation time: 2 minutes.

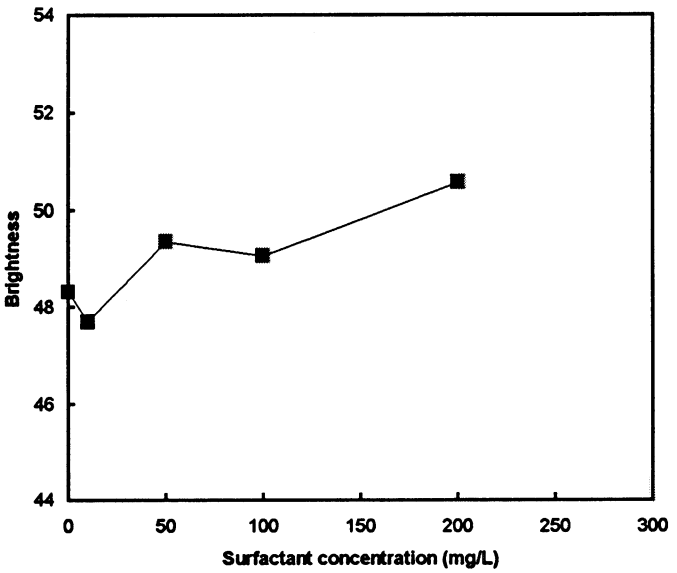

Fig. 16. Brightness of handsheet made from washed ONP. The wastepaper was pulped at a consistency of 1.31% for 30 minutes.

3.3.2. The effect of TX-100 on the ink-fiber detachment and ink removal

The effect of the addition point of nonionic surfactant, TX-100, on the ink removal was studied only by flotation deinking, and the results are shown in **Fig. 17**. It can be seen from **Fig. 17** that TX-100 did not improve ink removal when it was added before pulping, but it did enhance ink removal if it was added after pulping. This is surprising because it is well-known that TX-100 is an effective surfactant for stabilizing many solid suspensions in water. In other words, it is expected that the addition of a stabilizer will enhance the detachment of ink particles from the fiber surface, therefore, improving flotation deinking efficiency. One possible reason for the decrease in the ink removal efficiency may be due to the fact that TX-100 will reduce the agglomeration of ink particles if TX-100 is added before pulping. If this is true, the decrease in the agglomeration of ink particles will result in a decrease particle size; therefore, the ink removal efficiency in the flotation process will be decreased. In contrast to the flotation results, the brightness of handsheets made from washed ONP was increased with the increase of TX-100 concentration when TX-100 was added into the pulp before pulping. This can be seen from **Fig. 18**. The results obtained from washed ONP suggest that TX-100 will enhance the ink-fiber detachment. It is clear from the above discussion that more work is needed in order to obtain a full understanding of the role of TX-100 in the pulping process.

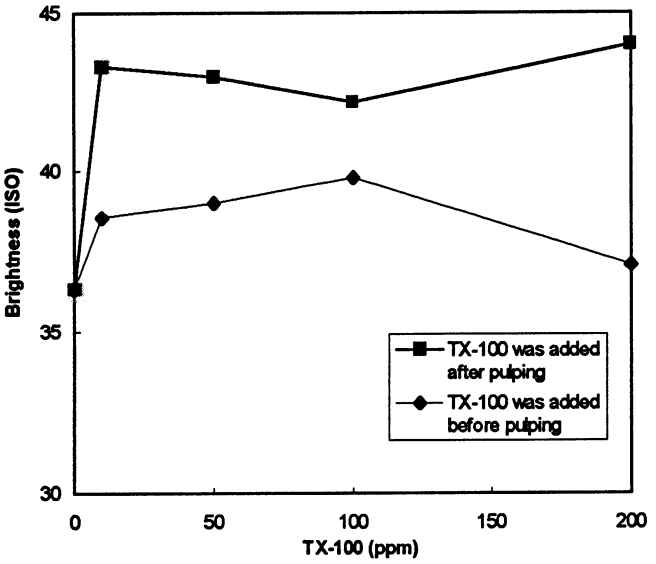

Fig. 17. Brightness of handsheet made by flotation deinked ONP (*Atlanta Journal-Constitution*) as a function of TX-100 concentration. ONP consistence during pulping: 1.31%; Pulp consistency in flotation cell: 0.5%; pH: 6.5; Nitrogen flow rate: 2000 cm^3/min; flotation cell: column flotation cell with a 10 μm-air inlet filter.

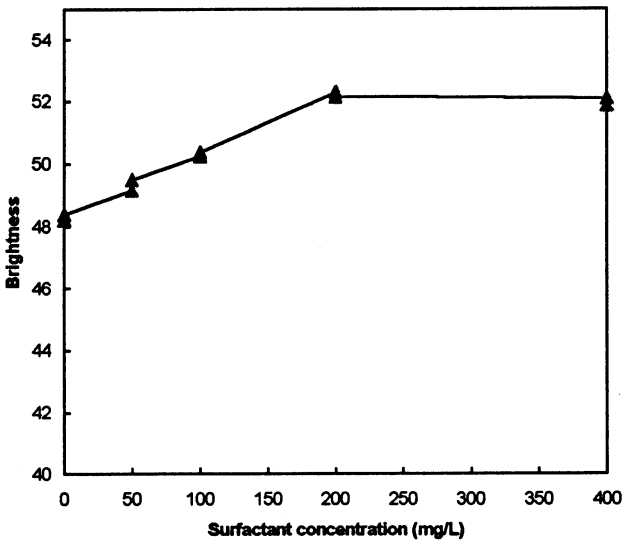

Fig. 18. Brightness of handsheet made from washed ONP. Surfactant was added in pulper. ONP consistency during pulping: 1.31%.

4. EFFECT OF OMG ON THE FLOTATION DEINKING OF ONP

4.1 Backround

The deinking mills usually add certain amounts of OMG (10-30 %) to ONP in flotation deinking because the brightness of final products made from recycled fibers will increase in the presence of OMG. Because of the increase in OMG pricing, the paper recycling industry would like to reduce its consumption of OMG. Therefore, it is important to know what is the role of OMG in the flotation deinking of ONP.

Some authors **[30-34]** postulated that OMG can enhance ink removal from ONP pulp by some unknown reasons, but others **[35-36]** indicated that the addition of OMG will give no positive effect on ink removal during flotation.

Two reasons may be possible for the increase in the brightness of recycled ONP by adding OMG in flotation deinking:

a) Addition of OMG will introduce fillers and high quality fibers into ONP resulting in an increase in the brighness, but will not enhance ink removal;

b) There are some interactions among OMG, ONP, and process chemicals resulting an increase in ink removal effecience.

In order to understand which mechanism is the dominating factor for the brightness increase in recycled ONP pulp after flotation, ONP handsheets were made by adding different ratios of OMG into ONP either before or after flotation deinking, and the brightness of these handsheets was examined in this study.

4.2. Experimental

ONP and OMG were separately pulped in the absence of surfactant. After pulping, the ONP and OMG were mixed under different ratios. After adding the required surfactant, the mixed pulps were subjected to flotation deinking using a

column flotation deinking cell. The brightness of the handsheet was measured using the method described in **Section 3.2.**

4.3. Results and Discussions

Fig. 19 shows the brightness of flotation deinked ONP handsheets as a function of calcium ion concentration after flotation in the presence of 100 ppm sodium oleic acid. It can be seen that, for 100% ONP, the brightness slightly increased with the increase in calcium concentration. This is consistent with previous reported results, i.e., water hardness will improve ink removal if fatty acid is used as a deinking chemical. However, there is almost no effect of calcium concentration on the handsheet brightness of OMG. This is not surprising because the calcium concentration in OMG pulps is already high enough due to dissolved calcium-containing fillers.

It also can be seen from **Fig. 19** that the brightness of handsheets made of 70% ONP/30% OMG is a little higher than that of 100% ONP, but is consistently lower than that of 100 OMG. In order to know if this small brightness gain is due to the improvement of ONP deinking by adding OMG, two different experiments were conducted. In the first experiment, the ONP and OMG were separately pulped. After pulping, the 70% ONP was mixed with 30% OMG. The mixed pulp was deinked using the flotation technique. In the second experiment, the ONP and OMG were separately pulped and separately flotation deinked. After flotation deinking, these separately deinked pulps were mixed. The brightness of these two types of handsheets as a function of concentration of calcium ions is shown in **Fig. 20.** The assumption is that if OMG can really enhance the ink removal of ONP, the brightness of the handsheet should be higher when ONP and OMG are mixed before flotation. It can be clearly seen from **Fig. 20** that the brightness of handsheets is lower if the OMG and ONP are mixed before flotation (<1 ISO). This result strongly suggests that the increase in brightness is solely due to the increase of the content of filler and high-quality pulp rather than the improvement of flotation deinking when OMG is mixed with ONP.

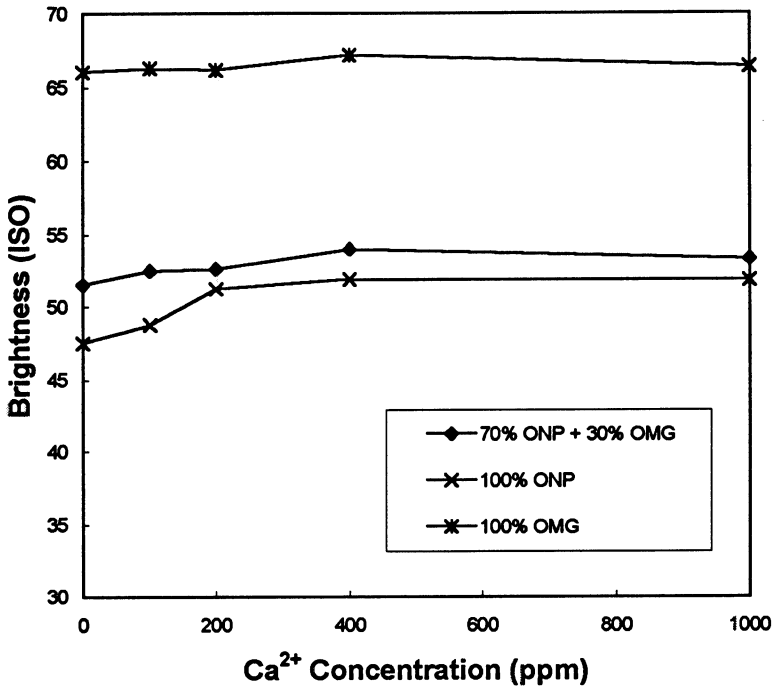

Fig. 19. The handsheet brightness of 100% ONP, 100% OMG, and the mixture of 70% ONP + 30% OMG as a function of Ca^{2+} concentration after flotation (ONP and OMG were mixed before flotation). Sodium oleic acid concentration: 100 mg/L; Fiber consistency: 0.5%; pH: neutral; Nitrogen flow rate: 18 cm^3/min. The brightness was measured from the top side of the handsheet. No retention aid was used for handsheet making.

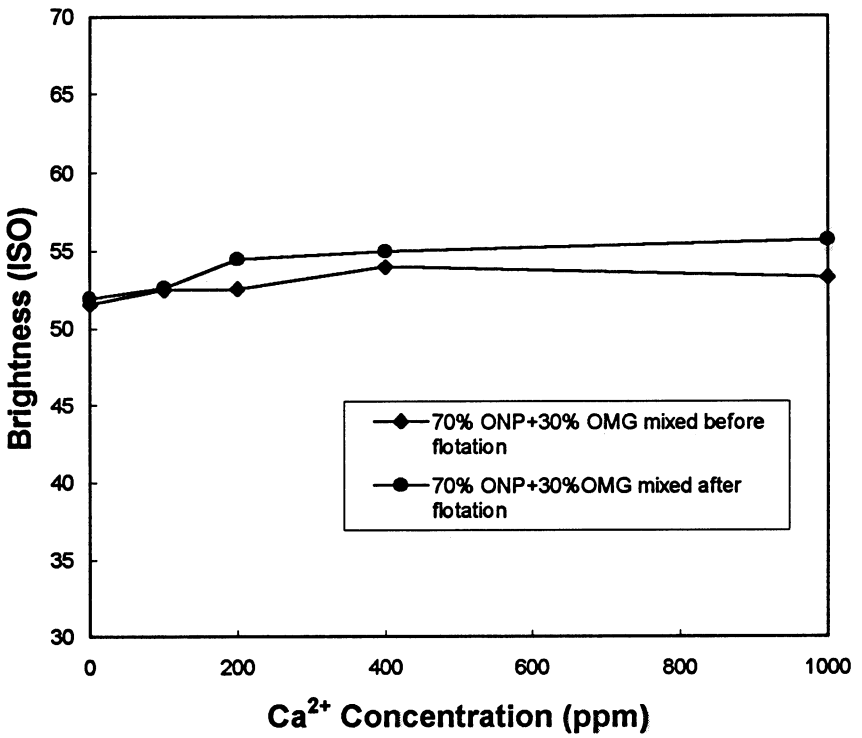

Fig. 20: The brightness of handseets made of 70% ONP plus 30% OMG as a function of calcium ion concentration. Sodium oleic acid concentration: 100 mg/L; Fiber consistency: 0.5%; pH: neutral; Nitrogen flow rate: 18 cm^3/min. The brightness was measured from the top side of the handsheet. No retention aid was used for handsheet making.

The effect of OMG on ONP deinking was further studied by the flotation deinking of ONP in the presence of OMG filtrate or OMG fines. The OMG filtrate was obtained by filtering a 1.0% pulp slurry using a filter paper, and the OMG fines were obtained from the same pulp using a dynamic drainage jar (125 mesh). OMG fines of 453ml were mixed with the required ONP pulp (1.0%) to give 0.5% of total solid content. The mixed pulp slurry was subjected to flotation deinking in the presence of sodium oleic acid and calcium chloride. It is believed that if the brightness of ONP is improved by adding OMG filtrate after flotation deinking, the soluble polymers in the OMG filtrate will contribute to the ink removal of ONP. On the other hand, if the brightness of ONP will be improved by adding OMG fines after flotation deinking, the fines (mainly the fillers) in the OMG filtrate will be the major contributor to the ink removal. The results shown in

Fig. 21 are surprising because both the filtrate and the fines consistently reduced rather from increased the brightness of ONP. This observation supports the results obtained in **Fig. 20**, i.e., the addition of OMG in ONP will not give any positive effect on ink removal during flotation when sodium oleic acid/calcium chloride are used as deinking chemicals.

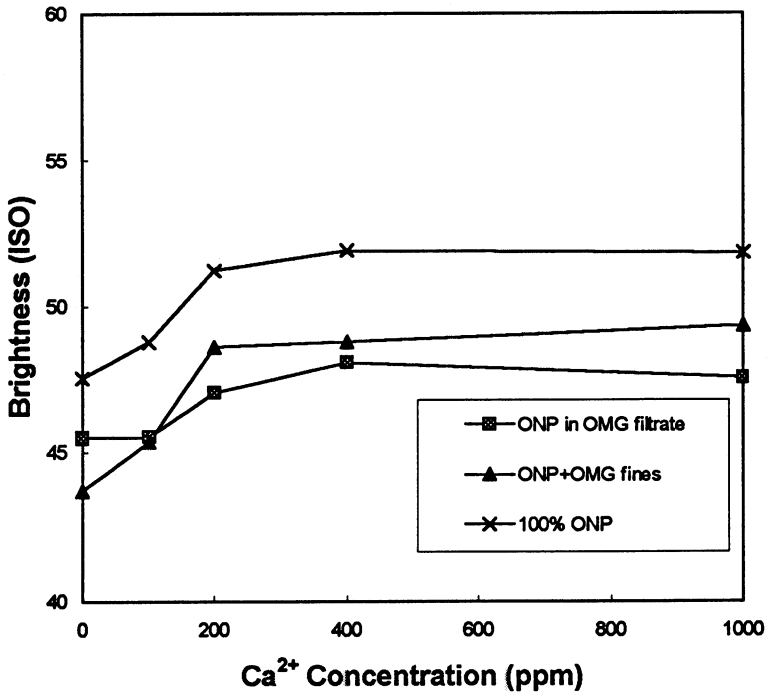

Fig. 20: The brightness of handseets made of ONP in the presence of OMG filtrate and OMG fines as a function of calcium ion concentration. Sodium oleic acid concentration: 100 mg/L; Fiber consistency: 0.5%; pH: neutral; Nitrogen flow rate: 2000 cm^3/min. The brightness was measured from the top side of the handsheet. No retention aid was used for handsheet making.

4.4. Concluding Remarks

1. The increase of ONP brightness by adding OMG is not caused by improvement of ONP deinking efficiency, but is solely due to the increase of filler and high-quality fiber in recycled ONP.

2. Neither the soluble chemicals nor the fillers in OMG will improve the flotation deinking efficiency of ONP.

OBJECTIVES OF FY 98-99

1. Examine the filler chemistry (PCC and clay) in surfactant solutions (TX-100, oleic acid-calcium chloride, and cationic surfactants).
2. Study the filler flotation (PCC and clay) during flotation deinking.
3. Study the flotation deinking of ONP using cationic surfactants.
4. Investigate the effect of the remaining surfactant on the fiber surface chemistry and paper properties.

GOALS FOR FY 98-99

1. Fundamental understanding of filler flotation in deinking process.
2. Fundamental understanding of the effect of remaining surfactant on the fiber properties.
3. Evaluation of the advantages and disadvantages of using cationic surfactant in the flotation deinking.

DELIVERABLES

Four papers, "Contact angle measurement of wood fibers in surfactant and polymer solutions", "Effect of fiber surface chemistry on the fiber loss in flotation deinking", "Flotation deinking chemistry: the current research program at IPST", and "Collector chemistry in flotation deinking of xerographic papers" will be submitted to the scientific journals for the consideration of publication in FY99.

SCHEDULE IN MONTH

Tasks	1	2	3	4	5	6	7	8	9	10	11	12
1. Examine the filler chemistry (PCC and clay) in surfactant solutions (TX-100, oleic acid-calcium chloride, and cationic surfactants)	X	X	X									
2. Study the filler flotation (PCC and clay) in during flotation deinking			X	X	X	X						
3. Study the flotation deinking of ONP using cationic surfactants					X	X	X	X				
4. Investigate the effect of the remaining surfactant on the fiber surface chemistry and paper properties									X	X	X	X

REFERENCES

1. Ferguson, L. D. Deinking Chemistry: Part 1, Tappi J. **75 (7)**, 75 (1992).
2. Ferguson, L. D. Deinking Chemistry: Part 2, Tappi J. **75 (8)**, 49 (1992).
3. Amand, F. J. S. Hydrodynamics of Flotation: Experimental Studies and Theoretical Analysis. TAPPI Recycling Symp., TAPPI Press, Atlanta, GA, 219 (1997).
4. Dorris, G. M.; Page, M. Deinking of Toner-Printed Papers. Part 1: Flotation Kinetics, Froth Stability and Fiber Entrainment. J. Pulp Paper Sci., **23 (5)**, 206 (1997).
5. Dorris, G. M.; Sayegh, N. N. The Role of Print Layer Thickness and Cohesiveness on Deinking of Toner-printed Papers. Tappi J. **80 (4)**, 80 (1997).
6. Johnson, D. A.; Thompson, E. V. Fiber/toner Detachment Studies: Repulping and Flotation of Laser Printed Paper. Part I., Proc. TAPPI Pulping Conf., TAPPI Press, Atlanta, GA, 1291 (1995).
7. Snyder, B. A.; Berg, J. C. Liquid Bridge Agglomeration: A Fundamental Approach to Toner Deinking. TAPPI Recycling Symp., TAPPI Press, Atlanta, GA, 277 (1994).
8. Paulsen, F. G.; Berg, S. R.; Vidotti, R. M.; Johnson, D. A.; Thompson, E. V. Measurement of Long-Range Hydrophobic Attraction Forces and Their Relationship to Deinking Flotation. Part 2. TAPPI Recycling Symp., TAPPI Press, Atlanta, GA, 41 (1997).
9. Mak, N.; Stevens, J. Characteristics of Fatty Acid as an Effective Flotation Deinking Collector. 2nd Research Forum on Recycling (1993).
10. Johanson, B.; Wickman, M.; Strom, G. Mechanism of Offset Ink Particles Agglomeration in a Calcium-fatty Acid Collector System, J. Pulp Paper Sci., **22 (10)**, 381 (1996).
11. Epple, M.; Schmidt, D. C.; Berg, J. C. The Effect of Froth Stability and Wettability on the Flotation of a Xerographic Toner. Colloid & Polymer Sci., **272**, 1264 (1994).
12. Wasmund, B.; Pelton, R. Model Deinking Studies: Carbon Black Removal by Oil-Coated Beads. Pulp Conference Proc., TAPPI Press, Atlanta, GA, 1005 (1994).
13. Miller, J. D.; Azevedo, M. A. D.; Xie, X.; Drelich J. Recycling Office Waste - Recovered Paper Deinking Research at the University of Utah, In Paper

Recycling Challenge Vol. 2 - Deinking & Bleaching, Doshi, M. R. and Dyer, J. M. Eds., Doshi & Associates Inc., Appleton, WI, 167, (1997).

14. Oguz, M.; Enuysal, M. Recovery of Deinked Paper Stock from Waste Newspapers. International J. Environmental Studies A & B, 263 (1994).
15. Shergold, H. L. Cationic Surfactants in Mineral Processing. Industrial Application of Surfactants, the Proceedings of a Symposium Organized by the North West Region of the Industrial Division of Royal Society of Chemistry, University of Salford, 269 (1986).
16. James, A. D.; Ogden, P. H.; Wates, J. M. Cationic Surfactants. Industrial Application of Surfactants, the Proceedings of a Symposium Organized by the North West Region of the Industrial Division of Royal Society of Chemistry, University of Salford, 251 (1986).
17. Kenny, F. J. Use of Surfactant in Mineral Flotation. Industrial Application of Surfactants II, The Proceedings of a Symposium Organized by the North West Region of the Industrial Division of Royal Society of Chemistry, 367, University of Salford, (1989).
18. Borchardt, J. K. An Introduction to Deinking Chemistry. In Paper Recycling Challenge Vol. 2: Deinking & Bleaching, Doshi, M. R. and Dyer, J. M. Eds., Doshi & Associates Inc., WI, Appleton, (1997).
19. Putz, H. J.; Schaffrath, H. J.; Gottsching, L. Deinking of Oil- and Water-Borne Printing Inks: A New Flotation Deinking Model, Pulp and Paper Canada, **94 (7)** 193, (1993).
20. Turvey, R. W. Why Do Fibers Float, J. Pulp Paper Sci., **19**, 52 (1993).
21. Turvey, R. W. Stock Loss as a Function of Water Hardness in Flotation Deinking, Paper Techn. Ind., 366 (1987).
22. Li, M.; Muvundamina, M. Fractionation of Fiber Slurries via Froth Flotation and Sedimentation, Prog. Pap. Recycling, **4 (3)**, 32 (1995).
23. Deng, Y.; Abazeri, M. True Flotation and Physical Entrainment: The Mechanisms of Fiber Loss in Flotation Deinking, Nordic Pulp Paper Res. J., in press.
24. Ajersch, M.; Pelton, R. Mechanisms of Pulp Loss in Flotation Deinking, J. Pulp Paper Sci., **22 (9)**, 338 (1996).
25. Deng, Y. Fundamentals of Surface Chemistry in Flotation Deinking, IPST Annual Report, (1997).

26. Warren, L. Determination of the Contributions of True Flotation and Entrainment in Batch Flotation Tests, Int. J. Min. Proc. **14**, 34 (1985).

27. Ishibashi, Y.; Myauchi, Y.; Inoe, M. Japanese Patent 06 49 790, February 24 (1994).

28. Masamizu, K.; Tai, Y.; Hagiwara, M.; Ukigai, T. Development of Deinking Agents for Flotation Systems, Proc. TAPPI Pulping Conf., 39, TAPPI Press, Atlanta, GA, (1994).

29. Borchardt, J. An introduction to Deinking Chemistry, in Paper Recycling Challenge Vol. 2: Deinking & Bleaching, Eds. Doshi, M. R. and Dyer, J. M., Doshi & Associates Inc., Appleton WI, 18, (1997).

30. Morel, P. Secondary Fiber for Newsprint. TAPPI Pulping Conf., TAPPI Press, Atlanta, GA, 367 (1989).

31. Fulton, T. Improved Deinked Pulp for Newsprint, Pulping Conf., TAPPI Press, Atlanta, GA, 535 (1997).

32. Rao, R.; Kuys, K.; Abbot, J. The Role of Coated Paper and Fillers in Flotation Deinking of Newsprint, Progress in Paper Recycling, **5 (2),** 103, (1996).

33. Schriver, K.; Bingham, S.; Fraizer, M. The Function of Clay in Flotation Deinking, Pulping Conference, 133 (1990).

34. Schriver, K. Mill Chemistry Must Be Considered Before Making Deink Line Decision, Pulp & Paper, **64 (3),** 76 (1990).

35. Mahagaonkar, M; Stack, K.; Banham, P. The Effects of Coated Magazines on Deinking of Newsprint After Pulping and Flotation, Recycling Symposium, TAPPI Press, Atlanta, GA, 193 (1997).

36. Letscher, M.; Sutman, F. The Effect of Magazine and Filler on the Flotation Deinking of Newsprint, J. Pulp and Paper Sci., **28 (6)**, 225 (1992).

APPLICATION OF SURFACTANT SPRAY IN FLOTATION DEINKING

STATUS REPORT

FOR

PROJECT E010

Junyong Zhu
and
Yulin Deng

March 23-24, 1998

Institute of Paper Science and Technology
500 10th Street, N.W.
Atlanta, Georgia

GENERAL INFORMATION

PROJECT TITLE: FUNDAMENTALS OF SURFACE CHEMISTRY IN FLOTATION DEINKING

PROJECT NUMBER: E010

PAC: Recycle/Surface and Colloid Science PAC

PROJECT CODE: Deinkchem

DIVISION: Chemical Recovery and Corrosion Division (J.Y. Zhu)

Papermaking Engineering (Yulin Deng)

PROJECT STAFF: Junyong Zhu (Assistant Professor)

Yulin Deng (Assistant Professor)

Guohua Wu (Postdoctoral Fellow)

FY 98-99 BUDGET: $85,000

TIME ALLOCATION:

Faculty: Junyong Zhu: 5%

Yulin Deng: 5%

Staff: Guohua Wu: 85%.

SUPPORTING RESEARCH: NONE

RESEARCH LINE/ROADMAP: Reduce and/or control contaminants (e.g., stickies, dyes, toners) in recycled-fiber pulp using break-through technologies to allow complete interchange of recycled pulp with virgin pulp of similar fiber makeup at economical cost.

PROJECT OBJECTIVES:

The overall objective of the proposed research is to conduct a feasibility study of spray wash to control fiber loss, reduce consumption of surfactant, and maintain ink particle hydrophobicity in a laboratory flotation cell. The research includes the following tasks:

(1) Design a laboratory batch type spray wash flotation deinking cell.

(2) Study the effect of spray characteristics, droplet size distribution, momentum, and spray pattern on the ink particle removal efficiency.

(3) Study the effect of spray wash on the selectivity of wash away fibers over ink particles.

MAIN RESULTS:

The research program was started in October 1997 with a fund of $85,000. During the last 4 months, the proposed research program was tested using a laboratory flotation cell. The primary results indicated that the surfactant spray approach can reduce fiber loss by 50%, water loss by 75%, and surfactant consumption by 95% without sacrificing deinking efficiency. The proposed approach can also prevent fiber from contaminating of process surfactant. More importantly, this study developed a simple method to mechanically control froth stability when the physicochemical properties of the pulp source vary.

ABSTRACT

This report is concerned with increasing utilization of recycled fiber and, more specifically, with improving the ink removal efficiency; reducing the fiber loss, the water loss, the chemical consumption, and the contamination of fibers by processing chemicals. The research program was started in September 1997. One paper based on the results obtained in the last 4 months has prepared, and a patent has been filed.

In this report, the fundamental understanding of the flotation deinking process is first discussed, then experimentally study using innovative approach to control several key process variables that affect ink removal, froth stability, fluidynamics in froth, fiber contamination, fiber and water losses, and surfactant consumption are discribed. Instead of adding surfactant into the pulp slurry directly before flotation in the conventional process, a pressure atomizer was used to spray the surfactant solution from the top of the flotation column during flotation. Results indicated that the surfactant spray approach can reduce fiber loss by 50%, water loss by 75%, and surfactant consumption by 95% without sacrificing deinking efficiency. The proposed approach can also prevent fiber from contaminating of process surfactant. More importantly, this study developed a simple method to mechanically control froth stability when the physicochemical properties of the pulp source vary.

INTRODUCTION

Flotation deinking is a common practice for removing ink from wastepaper, and it is becoming a key process in many recycling paper mills. The application of flotation was successfully introduced to the paper recycling industry in the 1980s, and its applications in wax removal, sticky control, and fiber fractionation have attracted great research interest. The chemistry of the flotation process has been reviewed [1-3]. The deinking chemistry and the physicochemical interactions among air bubbles, fibers, and ink particles are very complex. Existing technologies and process designs of flotation deinking are based on experiences obtained from mineral flotation processes. Limited process control mechanisms are available. Many problems remain unsolved such as high fiber and water losses [4-9], fiber contamination by deinking chemicals, adverse chemistry modification due to surfactant [1,2,10,11], low efficiency in removal of small ink particles [12-14], etc. Therefore, innovative technologies based on the mechanistic understanding of flotation processes are greatly needed to solve or alleviate the above problems. Because of the significant variability in the supply of secondary fibers in recycling practices, process control in flotation deinking is very important to improve recycling operations.

UNDERSTANDING THE FLOTATION DEINKING PROCESS

Flotation deinking processes involve interactions among air bubbles, ink particles, and fibers. A successful flotation process typically has three major efficient subprocesses: detachment of the ink particles from waste fibers, effective adhesion of the ink particles onto air bubble surfaces, and removal of froth and ink particles from flotation cells.

The Roles of Surfactants

The roles of surfactants have been discussed in detail by Ferguson [1,2]. In general, surfactants play three roles in flotation deinking: as a dispersant to separate the ink particles from the fiber surface and prevent the redeposition of separated particles on fibers, as a collector to agglomerate small particles to large ones and change the surface of particles from hydrophilic to hydrophobic, and as a frother to

generate a foam layer at the top of the flotation cell for ink removal. Although surfactants play important roles, they will also cause some adverse effects on ink removal, fiber quality, and water reuse. For example, both hydrophobicity and ink removal efficiency will decrease by the adsorption of dispersant and frother [10,11]. The remaining surfactant in recycled fibers is another problem that may cause a decrease in fiber-fiber bonding, an increase in foams during the papermaking process, an adverse effect on printing, etc. Because surfactants have both positive and negative effects, it is of interest whether dispersant, collector, and frother can be separately controlled.

The surfactants used in mineral flotation may not be necessary in flotation deinking. For instance, some ink particles, such as xerox toner, are hydrophobic in nature and no collector is necessary. The dispersant may also be unnecessary if the ink particles can be removed from fibers by other chemicals, such as sodium silicate, sodium hydroxide and enzyme, or by mechanical actions, such as magnetic and electrical fields, and ultrasonic irradiation. Although dispersant and collector may not be necessary for some pulps, a frother has to be used in order to obtain a stable foam layer for removing ink particles. Traditionally, the frother and other surfactants are added in to the pulp suspension during pulping. However, the surfactant presented in pulp slurry will not only contribute to the foam stabilization, but also adsorb onto ink particle surfaces and cause a decrease in the hydrophobicity of ink particles. Furthermore, the mechanical control of froth stability is very difficult if the surfactant is directly added into the pulp slurry because the properties of wastepaper may vary significantly.

Because the foams are stabilized by surfactant only on the top of the flotation cell, it is interest to develop a feasible method to directly add the frother to the top of the flotation cell rather than in the pulp suspension. As a result, a separate control of the addition of various surfactants to improve the performance of deinking processes can be achieved.

The Mechanism of Ink Removal

Ink removal efficiency depends on several factors such as the ability to separate the ink particles from the fibers, the collision probability between ink particles and air bubbles, the interfacial energy between ink particles and the air bubble surface, the specific contact surface area between ink particles and air bubbles, the stability of the froth for final ink removal, etc. It is well-known that surface chemistry plays a key role in flotation deinking. It has also been identified that the froth stability is critical for ink removal. Ink removal efficiency increases with an increase in froth stability, so that there is an increase in surfactant concentration in conventional flotation systems. Unfortunately, the increase in surfactant concentration in the pulp suspension will increase the adsorption of surfactant onto ink particles, resulting in a reduction of the surface hydrophobicity of ink particles and ink removal [10]. Therefore, there must be an optimum surfactant concentration and ink removal efficiency. Practically, it is difficult to optimize the surfactant concentration in a paper recycle mill because of the variability in the secondary fiber sources. This indicates that a good control of surfactant concentration and its distribution within a flotation column can significantly improve the flotation deinking operation.

The Mechanisms of Fiber and Water Losses

The understanding of fiber loss in flotation is very limited. Turvey [5,6] indicated that calcium ions can significantly increase fiber loss when a fatty acid soap was used. Turvey also indicated that nonionic fatty alcohol ethoxylate surfactants cause higher fiber loss compared to fatty acid soap. It was postulated by Turvey [5,6] and later by Li and Muvundamina [15,16] that fiber loss was due to fiber adhesion to air bubbles and then was removed with the froth. This postulation was challenged by Ajersch and Pelton [7-9] and most recently by Dorris and Page [17]. They found that the hydrophobicity of a fiber surface does not contribute to fiber loss, and fiber loss is due to the mechanical entrapment of fibers in the froth. In our recent study [18], it was found that both physical entrapment of fibers in an air bubble network and adhesion of hydrophobic parts of fiber surfaces on air bubble surfaces will contribute to the total fiber loss. However, the physical entrapment is the major contributor. It was also found

that the fiber and water losses are directly related to the froth stability and froth structure. The fiber entrapment is dictated by the gravitational, buoyant, fluidynamic drag, and surface forces. In general, a froth with a structure consisting of small bubbles causes high fiber and water losses due mainly to the high void space between air bubbles for fiber and water carrying over.

Because mechanical entrapment of fiber and water in the froth is the major reason for fiber and water losses, an effective method to mechanically control the stability, structure, and fluidynamics of froth is critical for reducing fiber and water losses. It is also clear that, if other parameters remain constant, an effective mechanical control of the froth properties can be achieved by controlling surfactant concentration and distribution in the froth.

THE MECHANICAL CONTROL CONCEPT

Based on the above fundamental understandings of flotation deinking, it is clear that effective controls of key process variables can increase ink removal and reduce fiber and water losses. In this study, we propose an innovative approach to use one simple mechanical device, i.e. surfactant spray at the top of the flotation column as shown in Fig. 1, to control several key process variables, i.e., surfactant consumption, concentration and its distribution, froth structure and stability, and fluidynamics in the froth. Therefore, surfactant (frother) is not directly added into the pulp suspension during stock preparation, rather it is delivered through a spray during the flotation process. The surfactant spray concept is conceived based on the following arguments:

1. The froth that is necessary for ink removal can be established and stabilized by a surfactant spray rather than conventionally adding surfactant directly into the pulp suspension. The surfactant addition through the spray from the top of the flotation column will give a degree of freedom to control surfactant addition in flotation deinking. With this degree of freedom, we can control the froth stability through the change of surfactant concentration of the spray solution or flow rate of the spray during flotation because the froth structure and stability are related to these parameters. When a change of the fiber source is observed, the surfactant application can be easily adjusted. Because the

surfactant is only applied to the froth layer to stabilize the foam, the amount of surfactant required will be much less compared with that for conventional flotation through directly adding it into the pulp suspension.

2. The spray will have a wash effect on the froth, i.e., the momentum of the spray droplets penetrated into the froth will modify the fluidynamics within the microchannels of the froth to help the fibers or fiber flocks to overcome the lifting and the fluidynamic drag forces to flow down under the gravity. The water wash technique has been applied to mineral flotation processes [19-21] to increase mineral flotation selectivity. The effect of water drainage in the froth phase on the fiber loss was also studied [18]. Because the hydrophobic ink particles have stronger affinity to the air bubbles than fibers, the liquid drainage in the froth microchannels may move hydrophilic fibers more effectively than hydrophobic ink particles. Therefore, it can reduce fiber and water losses but does not significantly affect the ink removal efficiency.

3. For flotation processes that do not require collectors or dispersants, surfactant spray can control the distribution of surfactant in a flotation column so that surfactant will be concentrated in the top layer of the froth and will not be present in the pulp suspension. There is a strong surfactant concentration gradient in the region of the froth and pulp suspension interface, and the concentration gradient is supported by the froth liquid holdup capacity and the bulk convective flow of the pulp suspension driven by motions of the air bubbles. Therefore, the hydrophobicity of ink particles will not be affected, and the ink removal efficiency can be increased, or more specifically, the surfactant consumption will be significantly reduced under the same ink removal efficiency. Moreover, the contamination of fibers by surfactant can perhaps also be completely avoided using the surfactant spray approach. Furthermore, the so-called optimum ink removal surfactant concentration observed by Epple et al., [10] and the present study in conventional flotation deinking systems does not exist, easing process control for ink removal.

4. There are significant engineering and economical advantage of using a surfactant spray to control flotation deinking: the spray is a very simple

mechanical device; it is very easy to implement a feedback control mechanism using a surfactant spray for industrial applications without significant modifications to existing conventional flotation equipment; and it can control most of the key process variables in flotation deinking.

EXPERIMENTAL

A laboratory batch-type deinking column is used to conduct the feasibility of the proposed mechanical control concept using surfactant spray. As shown in Fig. 1., the deinking column has an inner diameter of 10.16 cm. The height of the flotation cell is 86 cm, and the volume of the pulp slurry for each batch run is 6 liters. A pressure spray nozzle is mounted at the top of the deinking column approximately 2 cm above the pulp suspension surface to the spray surfactant. The nozzle orifice diameter is about 0.46 mm. The nozzle is operated at a gauge pressure of 0.5 atm with a flow rate of 1.42 g/s. The mean spray droplet size Sauter mean diameter (SMD) is about 50 mm measured by a laser diffraction instrument (Malvern 2600). The flotation air flow rate is 11-15 SLPM.

The pulp was made from xerox copied bond papers printed with a fixed pattern. The papers were pulped at a pH of 10 at a consistency of 8% without adding any chemicals except sodium hydroxide. The water and fiber losses were obtained by a gravimetric method. The ash contents in the original pulp and removed solid were 16 and 8.2%, respectively. The pulp consistency used in the flotation process was 0.5%. Triton-100 (analyze grade, J.T. Backer Inc.) was used as surfactant. The required amount of Triton-100 was added directly into the pulp in "conventional flotation", but was sprayed through a nozzle from the top of the pulp in "surfactant spray flotation". The equilibrium time for surfactant adsorption in "conventional flotation" was ~5 minutes. The handsheets for brightness analysis were made on a 15-cm Büchner funnel according to TAPPI standard method. The brightness of the handsheets was measured using a Shimadzu UV-VIS spectrophotometer (UV-160A).

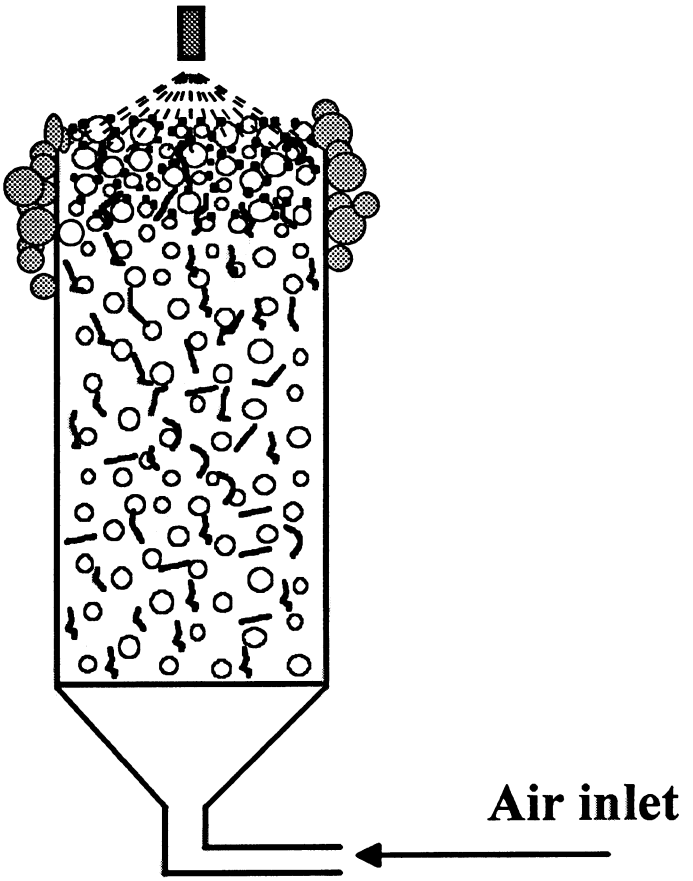

Fig. 1. Schematic diagram of a batch-type flotation deinking cell with mechanically controlled surfactant addition through a pressure atomizer.

The surfactant diffusion in the flotation column was analyzed by the concentration change as a function of time and depth along the flotation cell. The surfactant diffusion in the flotation cell was only conducted in the absence of fibers. The concentration of the surfactant (TX-100) was measured using a Shinazu UV160U spectrophotometer at a wavelength of 223 nm. Deionized water was used as a reference.

RESULTS AND DISCUSSION

Froth Establishment by Surfactant Sprays

The froth formation under the application of surfactant spray from the top of a flotation column was first examined in the absence of fibers. No foam layer was established when air bubbles were injected from the bottom of the flotation column that contains only pure water. However, when a small amount of Triton-100 solution was sprayed from the top of the flotation cell, a stable foam layer was established on the surface of the pure water phase in less than 0.5 minutes. The rate of foam formation on the top of pure water depends on the spray rate and surfactant concentration of the spray solution, and usually a few seconds are needed to generate a constant froth height.

Surfactant Distribution between Froth and Pulp Suspension

Direct sampling measurements of the surfactant concentration distribution within the flotation column as a function of spray time and depth from froth/suspension interface were conducted. It was found that surfactant is mainly concentrated in the froth rather than in the pulp suspension, and there is a strong surfactant concentration gradient in the region of the froth and pulp suspension interface. The first set of experiments was conducted by taking samples from 20 and 50 cm down from the froth and pulp suspension interface at various times up to 13 minutes during flotation with surfactant spray. UV analysis of all the samples found no absorbance at 223 nm, indicating the surfactant concentration was essentially zero at these two locations. The similar results were obtained from analysis of the samples taken from different depth (1 cm to 50 cm down from the froth/pulp suspension interface) at the end of flotation (10 minute flotation time), i.e., no detectable surfactant was found in the flotation cell.

These results strongly suggest that fiber contamination and surfactant adsorption onto the ink particle surface can be completely eliminated using the proposed surfactant spray approach in flotation deinking.

Comparisons of Ink Removal

Fig. 2 shows the comparison of the brightness gain of handsheets made from deinked fibers using surfactant spray flotation and conventional flotation under the same operation conditions, respectively. The results clearly show that the surfactant consumption used in the surfactant spray flotation is only about 2-3% of that required for the conventional flotation process in order to achieve the same brightness gain. This is not surprising because the surfactant is applied directly to the froth phase to stabilize the foam in the surfactant spray flotation, but most surfactants dissolved in pulp in the conventional flotation process will not contribute to froth stabilization. Theoretically, the surfactant consumption used in the spray flotation process can be further decreased if the ratio of the height of the flotation column to the surface area is increased because the surfactant consumption in spraying flotation is independent of the total volume, but is only dependent on the total surface area of the pulp suspension.

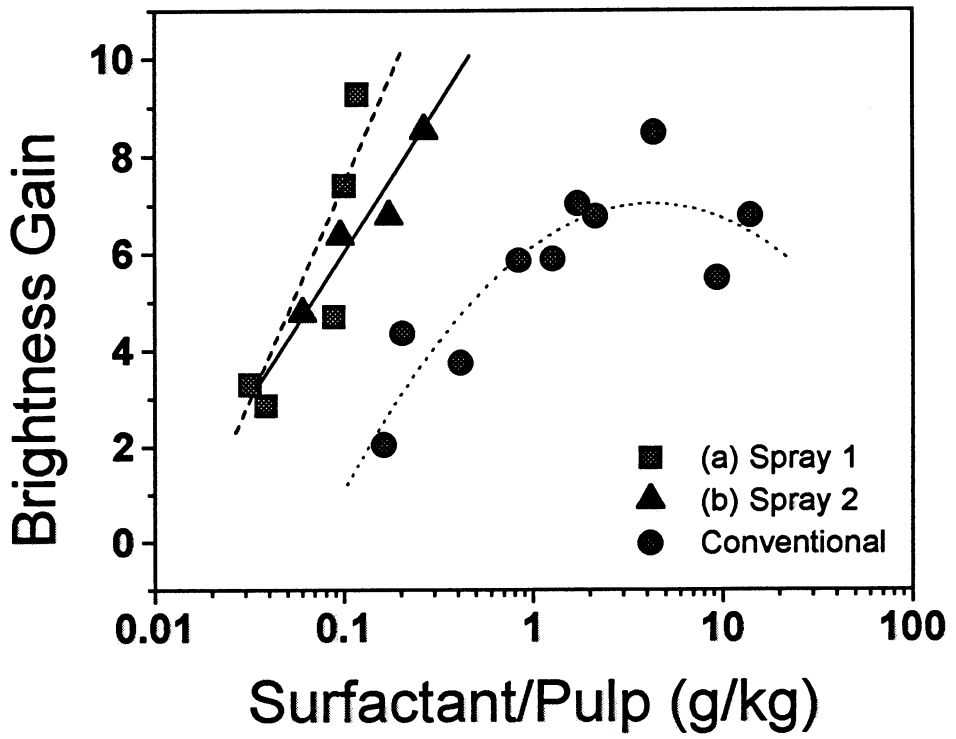

Fig. 2. Froth height vs. time with surfactant spray at different surfactant solutions in the spray solution. The surfactant concentrations in the spray solutions were 16 and 40 mg/L for Spray 1 and Spray 2, respectively. Flotation time was 10 minutes.

It can be seen from Fig. 2 that, for conventional flotation, the deinking efficiency increases with surfactant concentrations up to 5 g/kg dry pulp, then decreases suddenly as the surfactant concentration is further increased. An optimum surfactant concentration in flotation deinking was also observed in previous studies [10,11,18]. Combining present results with that of previous studies, it is believed that the increase in deinking efficiency at low surfactant concentration is because of the increase in the froth stability, and the decrease in deinking efficiency at high surfactant concentration is because of the decrease in the hydrophobicity of ink particle surfaces. Because there is an optimum surfactant concentration in conventional flotation deinking, it is often difficult to control surfactant concentration in industrial applications as it often changes with fiber sources. In contrast to the conventional flotation method, it is not necessary to find an optimum surfactant concentration if the surfactant is added from the top of the flotation cell as indicated by the data shown in Fig. 2.

Comparisons of Fiber and Water Losses

Fig. 3 plots the correlation of fiber loss as a function of brightness gain. The results show that fiber loss was reduced by 50% when surfactant is sprayed from the top of the flotation column compared to that obtained using conventional technology at the maximum ink removal condition. This indicated the success of the proposed technology in reducing fiber loss without reducing the deinking efficiency. The reduction in fiber loss, perhaps, can be attributed to the froth structure that affects the fiber drainage and spray washing that modifies the fluidynamics within the microchannels of the froth. The results

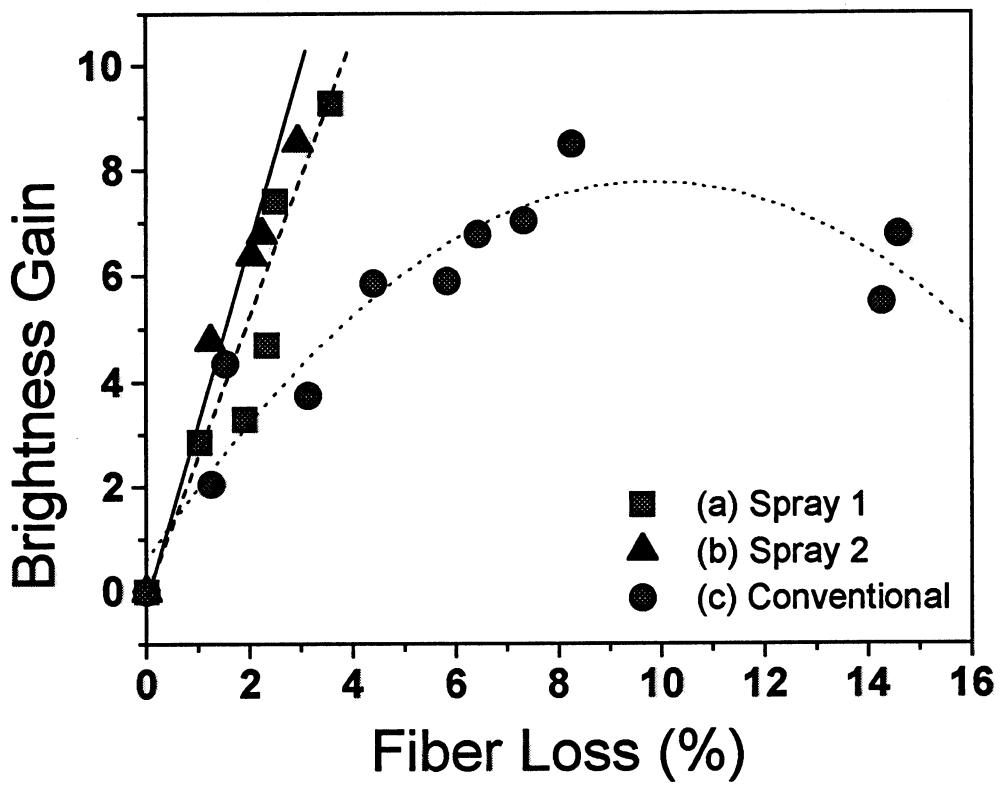

Fig. 3. The comparison of the correlation of fiber loss and deinking efficiency between the surfactant spray flotation and the conventional technology. The surfactant concentrations in the spray solutions were 16 and 40 mg/L for Spray 1 and Spray 2, respectively. Fiber loss was measured at different surfactant additions. Flotation time was 10 minutes.

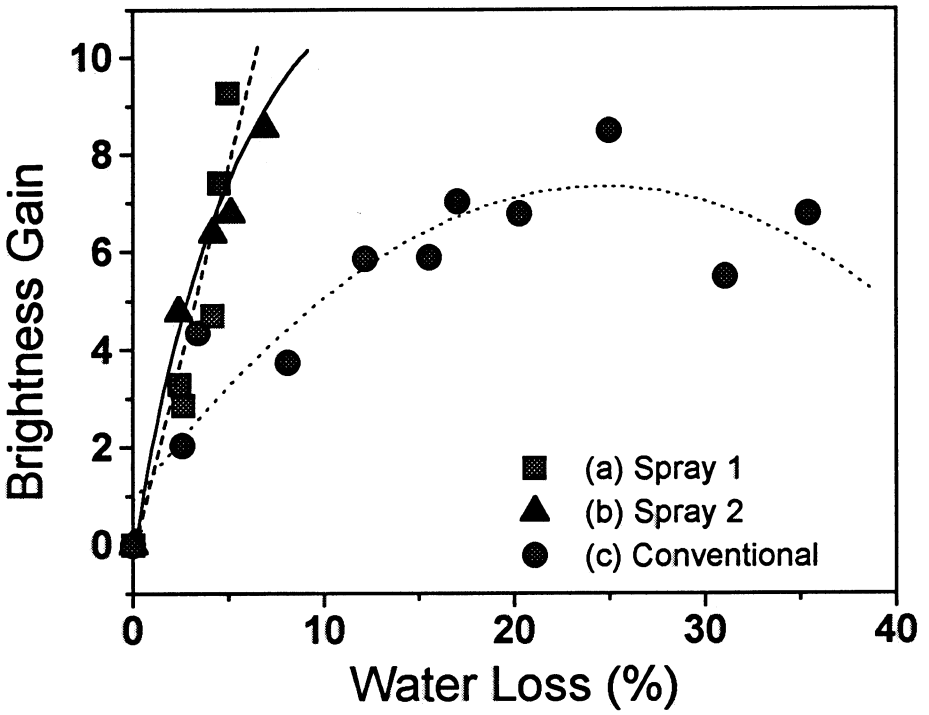

Fig. 4. The comparison of the correlation of water loss and deinking efficiency between the surfactant spray floatation and the conventional technology. The surfactant concentrations in spray solutions were 16 and 40 mg/L for Spray 1 and Spray 2, respectively. Water loss was measured at different surfactant additions. Flotation time was 10 minutes.

obtained in mineral flotation [19-23] support this explanation. However, a quantitative study of the relationship between fiber loss and froth structure is required.

Fig. 4 plots the correlation of water loss with brightness gain. The results show that the water loss was reduced by 75% when surfactant was sprayed using the proposed approach compared to that with the conventional flotation process at the maximum ink removal conditions. This indicated the success of the proposed technology in reducing water loss without reducing deinking efficiency. The reduction of water loss can be explained as that for fiber loss. According to our recent survey, water loss caused by froth entrainment in flotation deinking is about 10 tons/ton dry paper. Although the water loss caused by froth entrainment in the flotation deinking process has not been considered a serious problem, it is believed that this issue will attract more and more attention as environmental consideration increases.

Comparison of Ink Removal Rates

Fig. 5 shows the time-dependent characteristics of ink removal in the surfactant spray flotation and the conventional flotation processes. Ink removal increases as an initial increase in flotation time for all of the four experiments conducted. However, for the conventional flotation conducted at a surfactant concentration of 2 mg/L, ink removal efficiency reached a constant value after 80 seconds. A constant ink removal is solely because there was not enough surfactant in the system after 80 seconds so that the foam was not stable. The results in Fig. 5 also indicate that the ink removal rate using the proposed innovative technology is compatible with that of the conventional technology even though the surfactant consumption was reduced more than 95%.

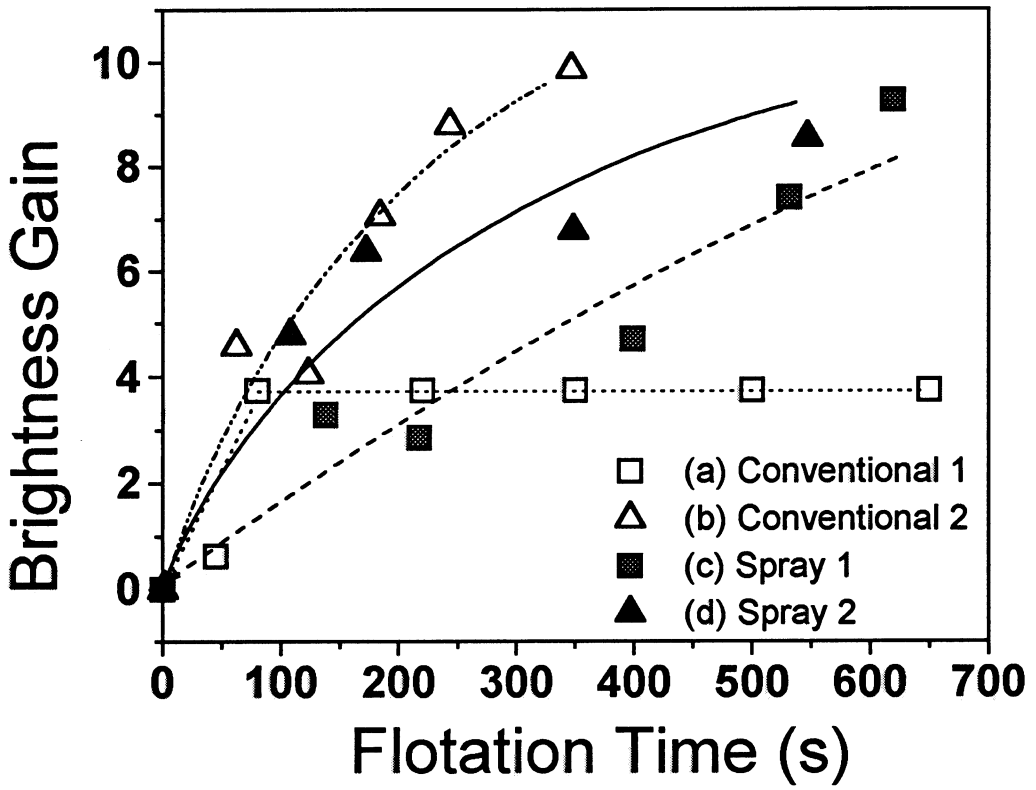

Fig. 5. Comparison of the time-dependent deinking characteristics between the surfactant spray flotation and the conventional technology. The surfactant concentrations in the spray solutions were 16 and 40 mg/L for Spray 1 and Spray 2, respectively. The surfactant concentrations in Conventional 1 and Conventional 2 were 2 and 20 mg/L, respectively.

CONCLUSIONS

In summary, the proposed approach of applying process control in flotation deinking using surfactant spray demonstrates several advantages compared with the conventional flotation deinking process:

1. Spray surfactant at the top of the flotation column can effectively establish a stable froth for good ink removal.

2. Surfactant application through a spray at the top of the column can effectively prevent the fiber from surfactant contamination, and reduce the modification of deinking chemistry through surfactant adsorption, resulting in higher ink removal, lower surfactant consumption, and lower fiber and water losses.

3. Control of surfactant delivery through mechanical devices, such as a spray, is an excellent approach to control froth stability and to improve the performance of the flotation deinking process significantly.

4. Control of surfactant delivery is a potential effective method to improve the roles of dispersant, collector, and frother in flotation deinking.

5. Control of surfactant delivery has potential advantages in whole process control in flotation deinking, and particularly can be used for stabilizing flotation operations when pulp sources are changed.

6. Laboratory studies demonstrate that without sacrificing deinking efficiency, the proposed approach can reduce fiber loss by 50%, water loss by 75%, and surfactant consumption by 95%.

OBJECTIVES FOR THE NEXT SIX MONTHS

Because the funding is available for only one year (9/97 - 8/98), the objectives given here are based on the study that will conducted in the next six months.

1. Demonstrate the proposed technology in a pilot scale flotation facility using office wastepaper.

2. Perform a feasibility study for ONP papers using the novel surfactant spray technique.

DELIVERABLES

1. Final report will be sent to the member companies in September 1998.

2. If promise results are obtained from a continue flow flotation cell, we will contact recycling mills and equipment manufacture to transfer our results.

SCHEDULE IN MONTH

Tasks	1	2	3	4	5	6
1. Install a continue flotation cell	X	X	X			
2. Demonstrate the proposed technology in a pilot scale flotation facility using office wastepaper.				X	X	X
3. Perform a feasibility study for ONP papers using the novel surfactant spray technique.				X	X	X

REFERENCES

1. Ferguson, L.D., "Deinking Chemistry: Part 1", *Tappi J.*, **75(7):** J75-83 (1992).

2. Ferguson, L.D., "Deinking Chemistry: Part 2", *Tappi J.*, **75(8):** J49-58 (1992).

3. Schulze, H.J., "Physico-chemical Elementary Processes in Flotation", Elsevier, Amsterdam (1984).

4. Larson, A., Stenius, P., and Oderg, L., "Surface Chemistry in Flotation Deinking", Part II, *Svensk PAPPER* 87: J165-169 (1985).

5. Turvey, R.W., "Why Do Fibers Float", *J. Pulp and Paper Sci.*, **19:** J52-57 (1993).

6. Turvey, R.W., "Stock Loss as a Function of Water Hardness in Flotation Deinking", *Paper Technology and Industry*, J366-368, February (1987).

7. Ajersch, M. and Pelton, R., "Mechanisms of Pulp Loss in Flotation Deinking", *J. Pulp and Paper Sci.*, 22, 9:J338-345 (1996).

8. Ajersch, M. and Pelton, R., "The Growth of Bubbles on Pulp Fibers and on Carbon Black Dispersed in Supersaturated Carbon Dioxide Solution", *2nd Research Forum on Recycling*, Montreal, Canada, 129-134, (1993)

9. Ajersch, M., Pelton, R., Loewen, S., and Chan, A., "Measurement of Dispersed Air in Newsprint Pulp Suspensions", *Tappi J.* **75** (2): J125-129 (1992).

10. Epple, M., Schmidt, D.C., and Berg, J.C., "The Effect of Froth Stability and Wettability on the Flotation of a Xerographic Toner", *Colloid & Polymer Sci.,* **272:**J1264-1272 (1994).

11. Panek, J. and Pfromm, P., "Interfacial Properties of Toner in Flotation Deinking", *Progress in Paper Recycling*, 5 (2): J49-57 (1996).

12. Putz, H.J., Torok, I., and Schaffrath, H.J., "Deinking of Flexographic Newsprint", *World Pulp and Paper Technology*, J85-90 (1992).

13. Dorris, G.M. and Nguyen, N., "Flotation of Model Inks, Part II, Flexo Ink Dispersions without Fiber", *2nd Research Forum on Recycling*, 13-22, (1993).

14. Larson, E.H., "Effects of Polymeric Additives in Flotation of Water Based Pigments During Recycling of Newsprints", *1997 Recycling Symposium*, Atlanta, TAPPI Press, 167-173, (1997).

15. Li, M. and Muvundamina, M., "Fractionation of Recycled Pulps Obtained from Mixed Paper", *1994 TAPPI Recycling Symp.,* Atlanta, TAPPI Press, 303-308,(1994).

16. Li, M. and Muvundamina, M., "Fractionation of Fiber Slurries Via Froth Flotation and Sedimentation", *Progress in Paper Recycling*, 4 (3): J32-38 (1995).

17. Dorris, G. and Page, M., "Deinking of Toner-Printed Papers. Part I: Flotation Kinetics, Froth Stability and Fibre Entrainment", *J. Pulp Paper Sci.,* 23 (5): J206-215 (1997),

18. Deng, Y., "Fundamentals of Fiber Loss in Flotation Deinking", *Progress Report of Institute of Paper Science and Technology,* 43-111, (1997).

19. Moys, M.H. and Finch, J.A., "Column Flotation", U.S. Patent 480460 (1989).

20. Yang, D.C., "Column Froth Flotation", US Patent 4592834 (1986).

21. Yianatos, J.B., Finch, J.A., and Laplante, A.R., "Selectivity in Column Flotation Froths", *Int. J. Mineral Proceedings,* **23:** J279-292 (1988).

22. Subrahmanyam, T.V. and Forssberg, E., "Froth Stability, Particle Entrainment and Drainage in Flotation - A Review", *Int. J. Mineral Proceedings,* **23:** J33-50 (1988).

23. Weaire, D., Pittet, N., and Hutzler, S., "Steady-State Drainage of An Aqueous Foam", *Phy. Rev. Lett.,* **71**(16): J2670-2673 (1993).

WET END CHEMISTRY CONTROL ADVISOR

STATUS REPORT

FOR

PROJECT WECCA

Collaboration Established Between
the
Institute of Paper Science and Technology
and the
Miami University Paper Science and Engineering Department

March 23-24, 1998

Institute of Paper Science and Technology
500 10th Street, N.W.
Atlanta, Georgia

Wet End Chemistry Control Advisor (WECCA)

Introduction

This is the first project proposed for the wet end chemistry research and education collaboration established between The Institute of Paper Science and Technology (IPST) and the Miami University Paper Science and Engineering Department. The objective of the collaboration is to:

> *Improve the efficiency and productivity of US mills through the advancement of papermaking chemistry knowledge and technology and the application of this knowledge and technical in mill operations.*

The following two research areas identified by the collaboration are addressed in this proposal.

1. Invention and application of new papermaking chemistry on-line sensors
2. Development of new papermaking chemistry process control strategies

Since wet end chemistry process control has long been an area of individual interest to both Miami and IPST, the WECCA project is a logical point from which to launch the collaboration.

Background

While wet end chemistry has always been important to papermakers, present-day trends place even more emphasis on this subject. Examples include

- increased use of recycled fibers
- increased filler levels
- closed white water systems,
- decreased basis weights,
- increased machine speeds
- acid-to-alkaline conversions.

All of these developments produce more difficult papermaking conditions at a time when customers demand ever higher quality, and economic conditions require improved productivity.

On-line wet end process monitoring has not been as rapidly adopted by process engineers and paper production managers as was dry-end on-line monitoring. There are many reasons for this, such as the fact that there are few manpower replacement costs to be recovered by installing on-line wet end testing equipment. Another impediment is the fact that output from wet end chemistry sensors is not always straightforward, and it is often necessary to have a wet end chemistry expert on hand to interpret the data. For these two reasons, and others, it can be concluded that there is great potential for the development and implementation of monitoring and control systems that help papermakers and chemical suppliers deal with variations in pulps, fillers, and chemicals, and maximize paper quality and machine productivity.

Papermakers and suppliers understand that wet end chemistry be brought under control to get the best paper quality and the best paper machine performance. Thus, the papermaker needs real-time knowledge about what is happening in the mill areas leading up to, and including, the wet end of the paper machine in order to make rapid control decisions that affect product quality and paper machine productivity. Currently, this goal is achieved in piecemeal fashion in most mills and not even approached in others. This proposal suggests a solution to this problem.

WECCA program goals and objectives

The overall goal of the *WECCA* project can be stated as:

> *Maximizing paper quality and paper machine productivity through comprehensive wet end chemistry control.*

The primary objective of this project is to develop an advanced process control system that combines wet end chemistry knowledge with paper mill measurements and predictive control models to achieve effective wet end chemistry process control.

WECCA functions

The following functions are envisaged for the WECCA system.

Table I

WECCA Functions

Provide information and advice:

- related to potential paper machine productivity problems
- related to potential paper quality problems
- needed to maintain uniform operation of wet end chemistry processes
- needed to facilitate wet end chemistry control during grade changes
- related to the future development of closed loop control systems
- related to the economics of machine operation

WECCA users

The WECCA system is intended for use in the paper mill by stock preparation operators, machine tenders, production managers, process engineers, and researchers. In addition, it will also provide support for chemical supplier technical sales and service personnel.

Development of the overall WECCA strategy

Deficiencies in current wet end chemistry process control practice that will be addressed in this research program

The deficiencies in current wet end chemistry control can be boiled down to the following three major areas.

1. Long lag time between input variable changes and measurement of paper properties or measurement of the paper machine "reaction" -- The solution to this problem requires either the installation of appropriate sensors earlier in the process or, where that is impossible, application of mathematical models that provide accurate prediction of a property or machine parameter. In a sense, such mathematical models can be considered to be "software sensors" in that they provide the same types of information as hardware sensors.
2. Historical absence of "key" on-line sensors to provide real-time data upon which to base control models and control decisions -- In the most recent issue of the Pulp and Paper Manufacture Textbook Series, Volume 10 ("Mill-Wide Process Control and Information Systems", page 192), Brewster states that:

   The effects of additive rates on the chemical environment and in turn on retention, formation, etc. depend on the specific physical environment (hydrodynamics, etc.). For this reason, these relationships must be determined (or confirmed) on-line, which points to the availability of adequate sensors as being the restraint to development.

   This issue has been aggressively addressed by instrument suppliers and on-line wet end chemistry measurements are now available to support an advanced control strategy. However, the industry has not yet adopted them widely. This may be the result of not knowing how to apply the instruments in a way that provides a clear return on investment. This project directly addresses this issue.
3. Mathematical control models that relate multiple, interacting wet end chemistry variables to paper properties and paper machine productivity measures are unavailable. -- In the same reference cited above, Brewster has the following to say about control models:

   The prerequisite to design of robust wet-end control for any particular system is an approximate, quantitative understanding of the relationships among chemical addition, chemical environment variables, retention, formation, sizing, etc. These are non-linear and interacting relationships. Then, the design and implementation of robust multi-variable control functions, including optimization to take care of the various trade-offs, will be required.

It is widely accepted that the development of first principles wet end chemistry control models is impossible and that other modeling approaches must be adopted. Fortunately, the advancement of computing capabilities and modeling methods, coupled with the massive amounts of archived process data available strongly suggests that the development of empirical control models should be possible.

General description of overall WECCA concept

In the jargon of process control engineers, the proposed WECCA strategy employs *model predictive control, coupled with artificial intelligence (i.e. expert systems*). Figure 1 illustrates this schematically. In the figure it can be seen that process data is passed to a mathematical control model whose function is to compute predicted paper properties or machine runnability parameters, such as first pass retention or tray consistency.

The computed outputs from the control model are passed to two expert systems and, possibly, to additive flow controllers. In one sense, the model serves as a "sensor" and provides values that can be used in wet end chemistry control decision making. Since most of the model input data comes from the stock preparation area, the predicted quantities are available for use in control decisions much sooner than if reel measurements were involved. This greatly reduces the lag times between input variable measurements and response variable measurements.

The first expert system checks the continuing validity of the model by comparing its computed paper property or machine parameter output to actual measured values taken from the produced paper or operating machine and decides whether or not the model needs to be updated.

The second expert system advises the operator about control actions when the wet end chemistry gets out of control, as indicated by a difference between a computed paper property or computed machine parameter and the specification for that property or parameter. This expert system also has the same process input data passed to it as the control model and it uses this data to make control decisions for the operator, and to do other computations and decision making needed by the mill.

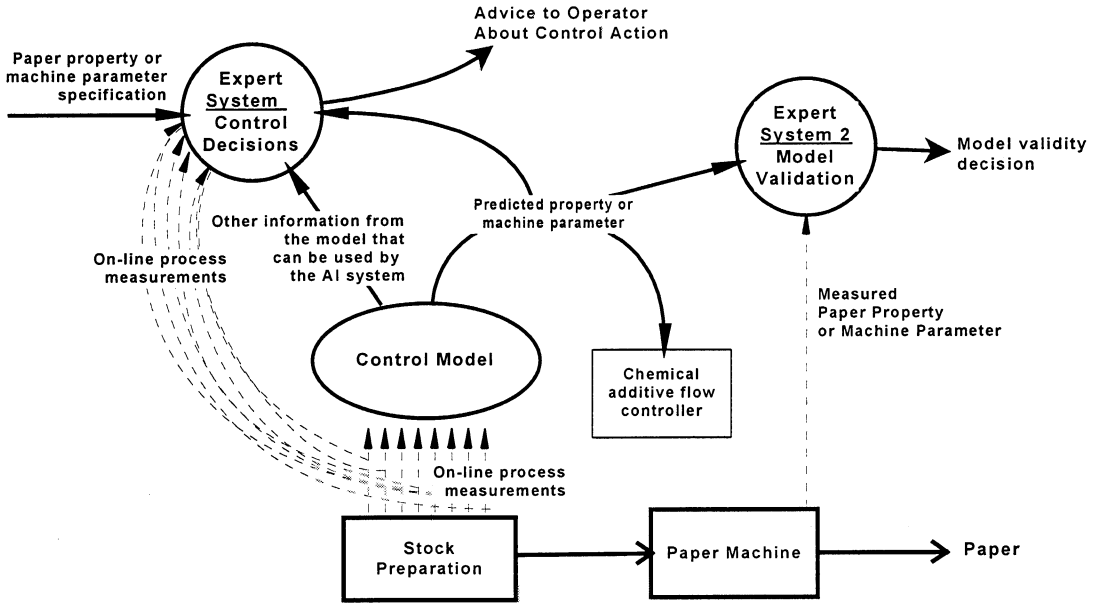

Figure 1. Schematic of general WECCA control strategy

Previously published studies

A literature search using the IPST literature database *PaperChem* covering the period 1990-1997 discovered a number of references pertaining to the application of expert systems and neural networks in the paper industry. Table II summarizes the studies contained in the *PaperChem* database related to expert systems and Table III does the same for neural network models.

The objective of the literature search was to determine the level of recent industry activity in the areas of neural network modeling and expert systems. It is evident from Tables II and III that the industry has been active in these arenas and that most of the major processes are represented. Wet end chemistry is an exception. Only two references – one about sizing and one about pitch –refer to this area. This shortcoming is addressed by this proposal.

Description of specific WECCA modules

Preliminary control modules have been developed for optical properties, strength properties, and first-pass retention based on the general control concept outlined above. Specific descriptions of these three modules follow.

Paper Optical Property Process Control Strategy

Introduction

Opacity, brightness, and color are all paper properties that depend upon interacting papermaking process and furnish variables. Current process control practice is reactive

Table II

***PaperChem* references pertaining to expert systems in the paper industry**

Category	Reference
Papermachine troubleshooting	1,10
Paper machine optimization and monitoring	2,8
Environmental monitoring of landfills	3
General papers	4,5,6,7,14,20,21,23,25,26,27,28,29,30,35,46
Process control of coating operation	9
Process control of fiber recycling operation	11
Control and optimization of activated sludge operation	12,17,40
Assist recovery operation	13,18,32,36,37,38,41,42
Lime Kiln automation	15
Troubleshooting and optimizing dryer steam and condensate systems	16,22
Kraft pitch problem troubleshooting expert system	19,31
Recovery unit of recausticizing chemicals – control	24
Multiple effect evaporator models and control	33
CD diagnosis in weight control	34
Batch digester control	39
CMP and mechanical pulp advanced control, tmp refiner control	43
WEDGE system for wet end chemistry control and diagnosis	40,44
Identification of visual defects, diagnose their origins, and find solutions	45

Table III

***PaperChem* references pertaining to the applications of neural network modeling in the paper industry**

General applications of neural network models in the paper industry	47, 57, 58, 59, 60, 61, 63
Feedforward control of an activated sludge process	46
Control of CD basis weight by slice bolt position control	48
Kappa number estimation in continuous Kraft pulp digesters through online measurements of alkali, solids content, and dissolved lignin	49, 64
Predictive emissions monitoring systems (PEMS): a computer modeling approach to air monitoring	50, 51
Predict effect of process variables on deinked pulp brightness and chemical usage; model and test process changes off-line	52
Model of the relationship between rosin and alum and paper sizing	53, 54
Diagnosis of paper web breaks on a commercial newsprint machine	55
Mathematical simulation of the paper forming process	56
Closed loop control of specific energy in the refining process.	62

and the operator only makes process changes when a problem is reported by the dry end testing lab or when an on-line sensor located at the reel indicates that paper has gone out of specification.

A few machines have placed opacity, brightness, or color on automatic control. In these instances, feedback loops are employed and control actions are limited to changing one or a few input variables. No account is taken of changes in other input variables nor are feedforward strategies employed. A new strategy is proposed here that addresses these issues.

Figure 2 depicts the more important papermaking process and furnish parameters that affect optical properties.

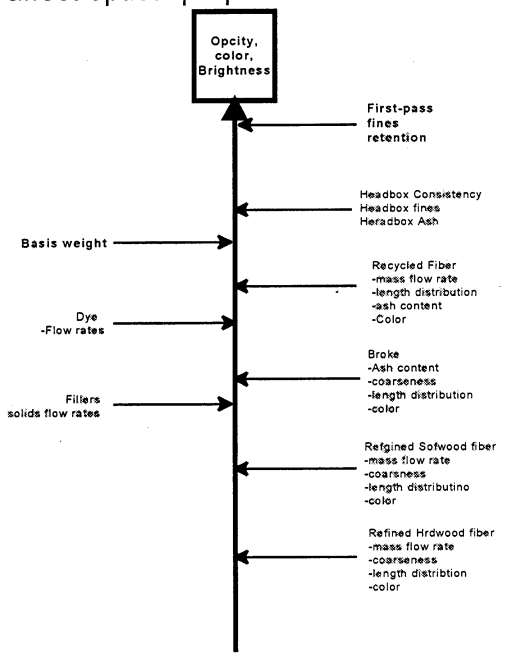

Figure 2. Parameters that affect paper optical properties

Proposed control strategy

A two component control strategy is proposed. (Table IV) The two components are a mathematical model that will compute paper optical properties from the values of papermaking process and furnish input variables plus an expert system that compares the computed optical properties with the desired values and decides whether or a control action is needed. If so, then the expert system advises the operator of this fact and provides guidance about what to do.

Table IV
Functions of control components

Component	Functions
Opticals control model	• Receives input data from the stock preparation and paper machine areas and computes predicted paper optical properties • Passes predicted paper optical properties and ranked input parameter variabilities to expert system.
Opticals control expert system	• Compares predicted paper optical properties with desired opticals (opticals specifications) and makes decision whether or not a control action is required. —If a control action is required, considers parameter variability input and makes recommendations to operator regarding preferred control actions • Compares predicted paper optical properties with measured paper optical properties and makes decision whether or not the model is sufficiently accurate –If model is inaccurate, makes recommendation to appropriate person that the model needs to be revised.

The expert system also compares the predicted optical properties with the actual property values measured at the reel and decides whether the control model needs to be updated. If so, then the expert system notifies the appropriate person of this fact. Note that even though only a single expert system is shown in Figure 3, it has both principal functions assigned to the expert systems in Figure 1 above. It is also assumed that process input data is passed to the expert system, even though it is not indicated in Figure 3.

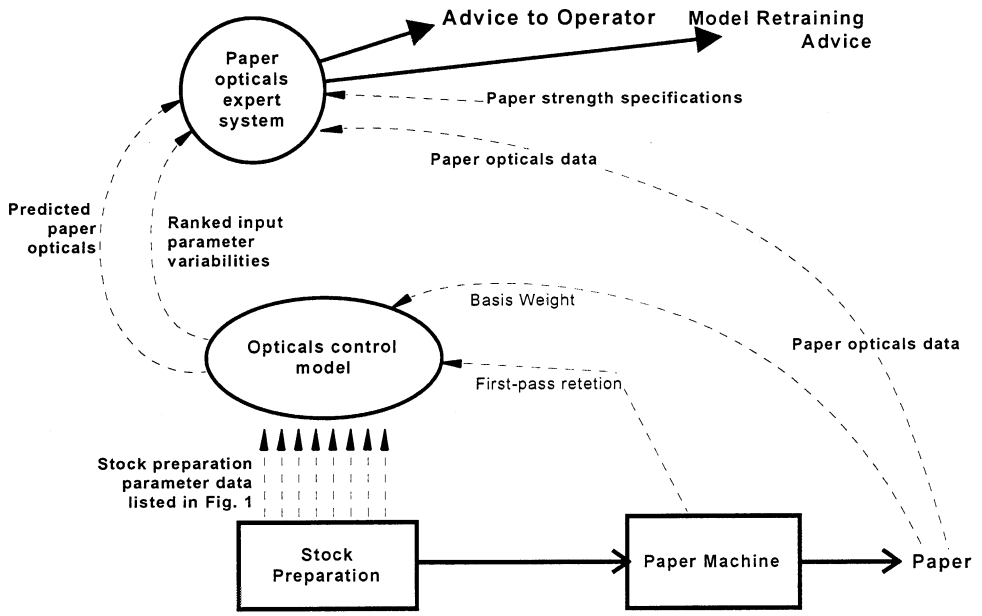

Figure 3. Optical property control strategy

Strength Properties

Introduction

A large number of interacting stock preparation, paper machine, and furnish variables contribute to the final strength of produced paper. Some of the most important ones are displayed in Figure 4.

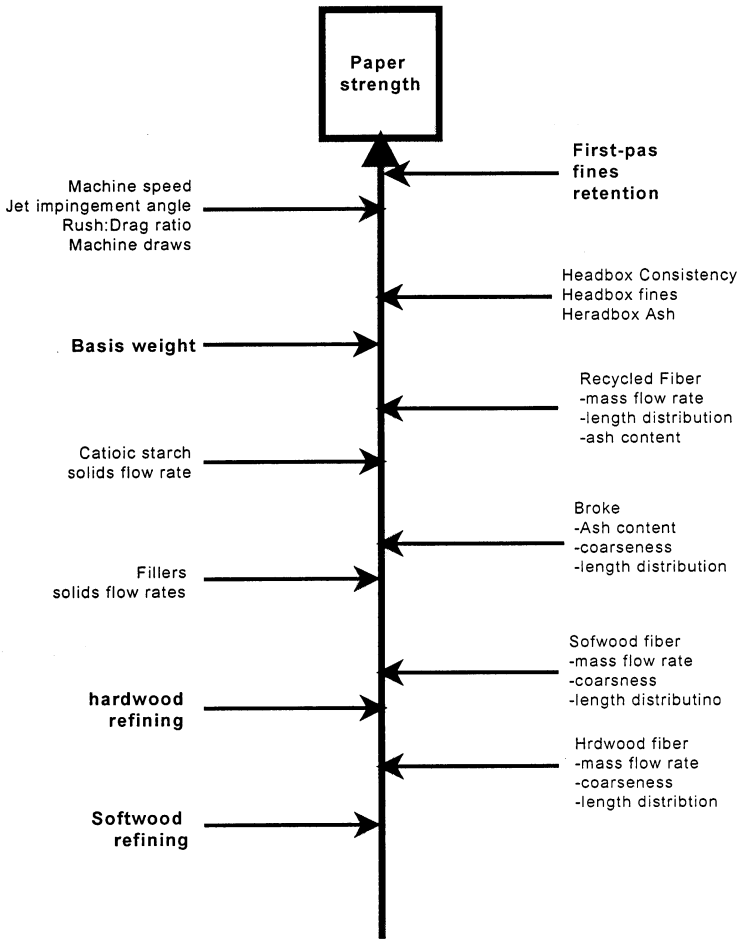

Figure 4. Papermaking parameters that affect paper strength

A Proposed Process Control Strategy for Controlling Paper Strength

The papermaker has a number of alternative options for controlling paper strength. In matters of control, operators typically adopt a strategy of reacting to strength problems as they are reported by dry end test results. As a result, considerable quantities of off-specification paper can be produced before a problem is identified. A more pro-active, strength process control strategy is proposed here.

The proposed strategy is based on a mathematical model that predicts paper strength from the values of process and furnish input variables coupled with an expert system that assists the operator in making control decisions. Automatic control loops are envisaged at the lowest control levels. All higher level control is accomplished through the operator via supervisory control. Figure 5 depicts the proposed interactions among the control model, expert system, and operator and Table V lists the major functions of each component in the scheme.

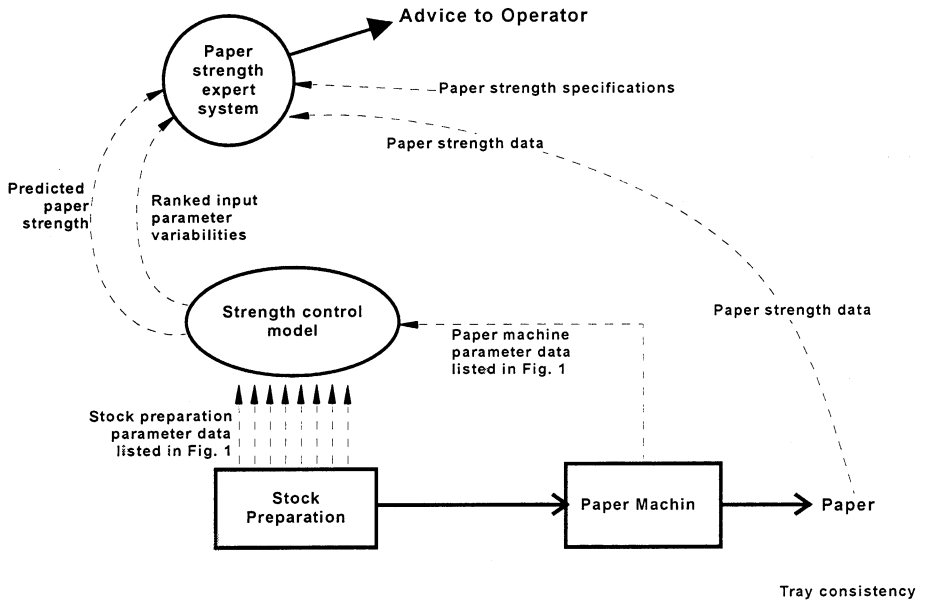

Figure 5. Proposed supervisory control strategy for paper strength

Table V
Functions of control components

Component	Functions
Strength control model	• Receives input data from the stock preparation and paper machine areas and computes a predicted paper strength • Passes predicted paper strength and ranked input parameter variabilities to expert system.
Strength control expert system	• Compares predicted paper strength with the strength specification value and makes decision whether or not a control action is required. —If a control action is required, considers parameter variability input and makes recommendations to operator regarding preferred control actions (Note that even though it is not shown in the Figure, the expert system has the same process input data passed to it as does the control model.) • Compares predicted paper strength with measured paper strength and makes decision whether or not the model is sufficiently accurate –If model is inaccurate, makes recommendation to appropriate person that the model needs to be revised.

First pass retention

Introduction

First pass retention of fines and fibers is known to be affected by a large number of variables, examples of which are depicted in Figure 6. The best current retention control practice in the industry involves real-time measurement of tray consistency, followed by adjustment of retention aid or some other retention control additive. This approach is effective as long as the stock preparation system remains stable so that only relatively small changes in tray consistency occur and these can be controlled by small changes in a single retention control additive.

While a positive development, the above approach suffers from the fact that most large, high speed paper machines undergo relatively large and frequent excursions in retention due to changes in incoming raw materials and these deviations are too large to be dealt with by retention aid alone. The proposed research program will result in a broader retention control strategy that will overcome this deficiency.

Figure 6. Process variables that affect first pass furnish and first pass fines and ash retention and the feedback measurements suggested for the proposed retention control scheme.

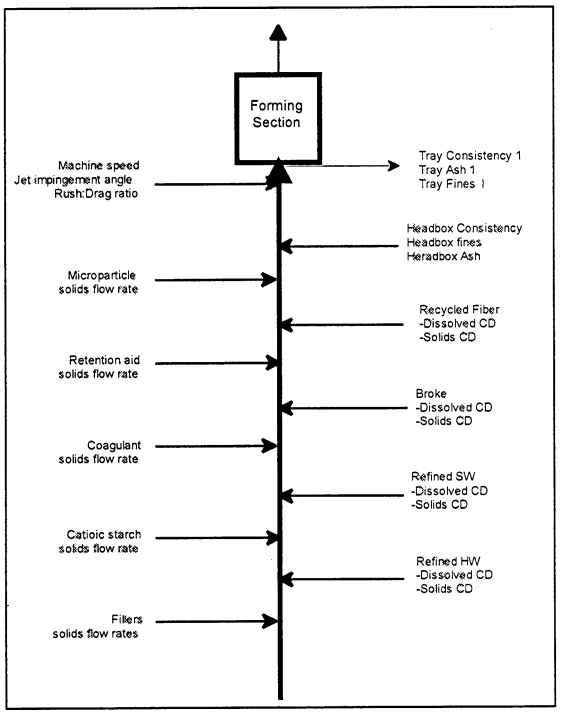

Proposed Retention Control Strategy

The envisaged retention control strategy employs a mathematical model that computes the retention additive flow rate setpoint required to achieve a desired tray consistency, given the "state" of the system; and an expert system that advises the operator about what to do when the tray consistency exceeds specific upper and lower control limits. Table VI summarizes how these elements are integrated into the control system. Figure 7 schematically illustrates how the various components could be integrated into a comprehensive retention control strategy.

Table VI
Two control levels and their respective elements

Level	Trigger	Control Agent	Control Mode	Comment
1	$C_{t,\,min1} < C_t \leq C_{t,\,min2}$ or, $C_{t,\,max1} < C_t \leq C_{t,\,max2}$	Retention control additive	Automatic	This level is transparent to the operator
2	$C_t > C_{t,\,max2}$ or $C_t < C_{t,\,min2}$	Coagulant, dispersant, or other appropriate treatment carried out in the stock prep area by an operator	Supervisory	The operator carries out one or more actions based on advice from the expert system combined with his/her experience.

The C_t, $C_{t,\,max2}$, and other related parameters in the table, column two, refer to inner and outer control limits developed for tray consistency in the mill. When the tray consistency lies between the two control limits, then level 1 control is in effect. When the tray consistency lies outside of the outer control limits, then level 2 control is activated.

What needs to be done to bring this about?

Available on-line measurements -- The technologies for measuring consistencies, flow rates, and pH values are well-established. Fiber fines and fiber length distribution can be measured with instruments that are relatively new to the market. There are also at least two instruments available for measuring dissolved cationic demand. One can also do temperature, conductivity, and specific ions on-line in most streams. The principal problem is collection of a filtrate sample for these measurements. Thin stock ash content is possible, as is thick stock ash (in principle).

Development of a mathematical model that will compute the retention aid flow required to achieve a given tray consistency -- Others have found that neural network modeling is a good way to approach problems involving many variables and numerous dynamic, nonlinear interactions, such as the problem posed here. Several examples of the successful use of this technique have been published in the recent literature.

Development of an expert system that will assist an operator in counteracting retention excursions beyond the capability of the primary retention control additive -- Expert

systems have found widespread use in industry and there are many software packages available for their development.

Integrating data systems – It is envisaged that this entire project will be carried out at a mill site. The biggest challenge will be to find a mill that is instrumented and networked adequately enough to provide the data needed to develop a neural network model. The same mill will be used as the basis for an expert system and for prototyping the control system. IPST member companies will be surveyed for candidate mills. It will also be preferable if the selected mill has a single, full-service chemical additive vendor who is dedicated to working with the project.

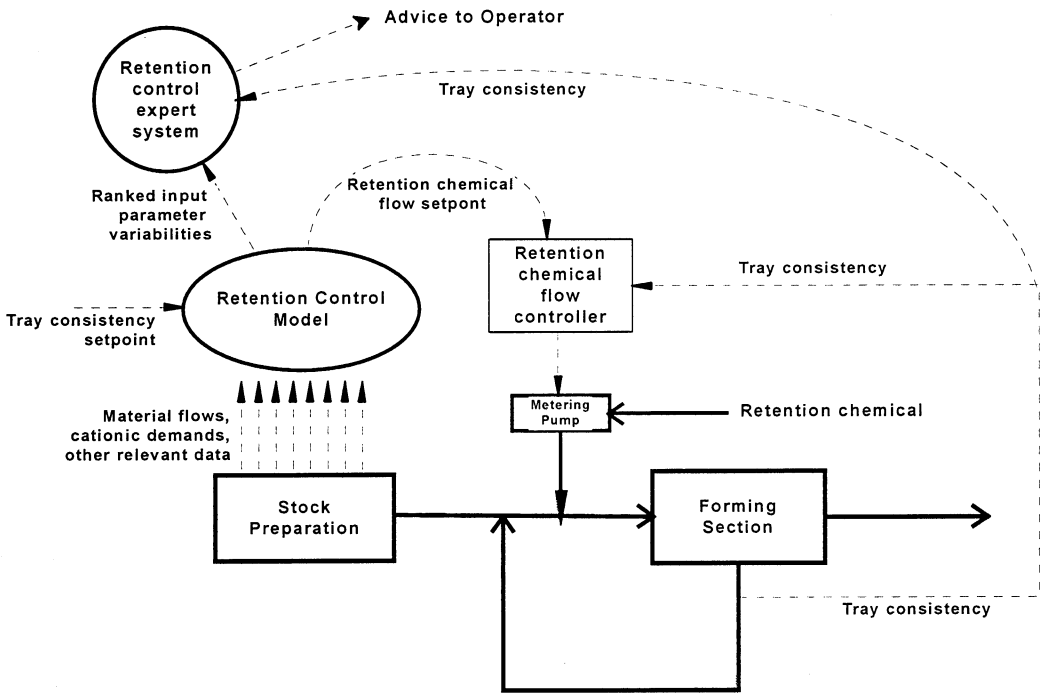

Figure 7. Schematic of proposed retention control strategy

Development and implementation phases and activities for the WECCA project

The following table lists the activities required to develop a neural network model that will provide the predictive component of the WECCA system. It is expected that this work will occupy the first year of the project.

Table VII
List of project activities: Year One

Phases	Activities
1. Test mill site selection	• Define desirable test mill criteria a. Cooperative mill management and technical group b. Installed and operating PI system c. On-line property or retention measurements d. Willingness to turn PI compression off e. Good sensor calibration program f. Knowledge of time lags or ability to measure them • Advertise needs among IPST member companies • Evaluate "volunteer" mill against site criteria • Select test mill site
2. Data set definition	• Define input variables to collect • Define output variables to collect • Define manual and on-line inputs • Determine data sampling frequency • Determine time period or time periods to collect data • Calibrate sensors • Turn off PI data compression on monitored variables
3. Time lag determination	• Determine time lag relationships among input variables and output variables.
4. Data collection	• Collect data
5. Data reduction	• Remove outliers • Do 'bump' tests to fill in data gaps • Recollect points, if necessary • Adjust for time lags
6. Modeling strategy determination	• Decide whether to purchase a program and do in-house modeling or to collaborate with a vendor, such as Pavilion.
7. Model creation and refinement	• Train neural network with modeling data set • Validate initial model with additional data • Refine model

Year One Timetable

Table VIII contains a proposed timetable for the activities listed in Table IVI.

Table VIII
Preliminary Gantt Chart for the WECCA project

Month →	1	2	3	4	5	6	7	8	9	10	11	12
Phase ↓												
Test mill selection	X											
Data set definition		X	X									
Time lag determinations				X	X	X						
Data Collection			X	X	X	X	X	X				
Data reduction									X			
Modeling strategy determination						X	X	X				
Model creation and refinement										X	X	X

The specific activities to be undertaken in years two and beyond will depend, in part, on the achievements of year one. If one assumes that the modeling work in year one is successful, then year two will focus on testing the model in a mill environment and developing and expert system development. Table IX lists some expected activities.

Table IX

Preliminary list of project activities: Years two and on

Test neural network model in production environment	• Install model in mill with on-line inputs • Collect predicted vs laboratory value data set • Compare predicted with laboratory values and revise model if necessary • Repeat steps 2 and 3 until satisfactory performance is achieved.
Develop wet end chemistry control decisions component of system	• Decide how to integrate neural network input pertaining to input parameter variability, mill practice, and wet end chemistry knowledge into decision-making strategies • Decide how to address interactive response variables (e.g. what happens to brightness and color if you make a change to improve opacity?) • Interview mill personnel regarding wet end chemistry control practices pertaining to the problem at hand • Interview chemical suppliers regarding wet end chemistry control practices pertaining to the problem at hand • Define software selection criteria • Evaluate candidate software packages • Select software • Enter knowledge into acquired program and do necessary coding • Test prototype expert system by itself
Interface prototype expert system with neural network model to produce integrate prototype WECCA system	
Test integrated prototype WECCA system	
Modify WECCA system	
Implement "product" WECCA system.	
Evaluate performance of WECCA system	• Define success criteria • Define performance measurement parameters • Collect base-line database • Collect WECCA database • Evaluate data and draw conclusions pertaining to success (effectiveness) of system • Define steps for system improvement

First year budget

A budget is being developed for the project at this time. It will be presented for discussion at the meeting.

References

1. Renault, X.; Cuny, L. *User-Friendly System Involving a Developing Database [an Expert System] Created by and for the Operators, to Help Diagnose Malfunctions on the Paper Machine.* Rev. ATIP 51, no. 1: 28-30 (January/February 1997).
2. Maltais, D. *Continuous expert system for the optimization of the performance of a paper machine.* Pretires de la Conference Technologique Estivale 1997 (CPPA): 127-130 (1997; CPPA).
3. Basri, H.; Stentiford, E. I. *Expert System for Environmental Monitoring of Sanitary Landfills.* 1997 International Environmental Conference (TAPPI, CPPA Technical Section, and USDA Forest Service): 381-384 (May 4, 1997; TAPPI Press)
4. Morin, F.; Coderre, A. *Mill Experiences with "In-House" Expert Systems.* Control Systems '96 Preprints (CPPA), Session: Forum on Industry: 221-228 (1996; CPPA).
5. Fadum, O. *Expert Systems in Action* Process, Quality, and Information Control in the Worldwide Pulp and Paper Industry (Pulp & Paper): 23-34 (1996; Miller Freeman Inc.).
6. Fadum, O. *Constructing and Implementing Successful Expert Systems.* Process, Quality, and Information Control in the Worldwide Pulp and Paper Industry (Pulp & Paper): 18-22 (1996; Miller Freeman Inc.).
7. Fadum, O. *Introduction to Artificial Intelligence* Process, Quality, and Information Control in the Worldwide Pulp and Paper Industry (Pulp & Paper): 16-17 (1996; Miller Freeman Inc.).
8. Nault, G.; Maltais, D. *Application of an On-Line Expert System to Optimize Dryers and Press Section at Domtar [Fine Papers Inc.] Windsor.* 82e Congres annuel de la Section technique de l'Association canadienne des pates et papiers: Faconner aujourd'hui l'environnement de demain: Textes a etre presentees les mardi et mercredi, 30-31 janvier 1996, les Palais des Congres de Montreal, Montreal, Quebec: Pretires A (CPPA): A339-342 (January 30-31, 1996; CPPA).
9. Woollard, R.; Jury, J.; Clark, C. *Expert System Advises Operators on Process-Control Conditions* Tappi J. 79, no. 4: 137-141 (April 1996).
10. Amyot, R., Wyulie, R., Henzell, R., Futcher, J., Coderre, A., Henzell, P. Vadas, O. *Steam and condensate diagnostic expert system.* Pulp Paper. Can. 97(2): 18-20(January 1995).
11. Vercelli, E. *Optimization of recycling productivity and quality with advanced process control.* Ind. Carta 33, no. 1: 15-21 (January 1995).
12. Sedgwick, G.; White, J.; Woolley, J.; Wojcik, P.; Steinback, B.; Lyka, W.; Denton, R. *Control of Biological Effluent Treatment for Mechanical Pulp Mills* Environment Conference Proceedings (CPPA Technical Section): 69-74 (1995; CPPA Technical Section).
13. Racine, J. P.; Borsje, H. J.; Reinschmidt, K. F.; Leroueil, P. *Recovery-Boiler Expert-System Software at Weyerhaeuser [Co.]'s Longview [WA] Mill.* PaperAge 111, no. 10: 18-19 (October 1995).

14. Spence, M.; Danielson, K.; Ying, Y.; Rao, M. *On-Line Advisory Expert System Development at Daishowa [Canada Co. Ltd.'s] Peace River Pulp [Peace River, Alberta].* Pulp Pap. Can. 96, no. 7: 24-27 (July 1995).

15. Hagemoen, S. W. *Expert System Application for Lime Kiln Automation.* Res. In Biodeterioration of Wood, 1987-1992, 2: Diagnosis of Decay and In-Place Treatments: 91-97(1994).

16. Amyot, R.; Gowing, J.; Wylie, R.; Henzell, R.; Futcher, J.; Reinsborough, J.; Coderre, A.; Henzell, P.; Vadas, O. *Steam and Condensate Diagnostic Expert System*: 81e Congres annuel de la Section technique de l'Association canadienne des pates et papiers: Les textes a etre presentees les mardi et mercredi, 31 janvier-1 fevrier 1995, Le Palais des Congres de Montreal, Montreal, Quebec: Pretires "A" (CPPA): A41-44 (January 31-February 1, 1995; CPPA).

17. Viljakainen, E.; Hynninen, P.; Krogerus, M. *Biological Treatment-Plant Optimization with a Knowledge-Based Control.* 1995 International Environmental Conference: Proceedings (TAPPI): 499-508 (May 7, 1995; TAPPI Press).

18. : Mikkonen, J.; Koskinen, J.; Hanhinen, J. *Fuzzy Control in the Recovery Boiler* Pap. Puu 76, no. 5: 314-317 (May 24, 1994).

19. Allen, L. H.; Bouchard, D.; Lapointe, C. L.; Larin, Y.; Vadas, O.; Kowalski, A *Kraft Pitch Expert System; Knowledge-Based System for Pitch Control.* 1993 Spring Conference: Preprints (CPPA), Session: 3A, Paper No. 2: 4 p. (May 30, 1993; CPPA).

20. Harvey, D. M *Application of Expert System to Supervisory Control.* Annual Meeting (80th CPPA): B141 (Feb. 3-4, 1994).

21. Edel, A.; Springer, J. *Why Expert Systems?* Annual Meeting (80th CPPA): B31-34 (Feb. 3-4, 1994)

22. Amyot, R.; Vadas, O.; Jayatilaka, R.; Reinsborough, J.; Cook, D. *Steam and Condensate Advisor* Annual Meeting (80th CPPA): B51-54 (Feb. 3-4, 1994).

23. *Papermakers Act on Expert Advice* Pulp Pap. Int. 35, no. 12: 28-30, 32, 37 (Dec. 1993).

24. Gutierrez Chamorro, J. *Expert Systems Based on Fuzzy Logic.* El Papel no. 31: 35-38 (Oct./Nov. 1992)

25. Walker, R. *Artificial Intelligence [Papermaking Applications].* Am. Papermaker 56, no. 3: 24-26 (March 1993).

26. Fadum, O.; Harvey, D. M.; Herdman, P. T.; Wiltshire, S. P.; Ruiz, J.; Pascal, S.; Asunmaa, P.; Rantakokko, J.; Ahman, T.; Curtis, S. *Expert Systems in Action.* Pulp Pap. 67, no. 4: 86-99 (April 1993).

27. Fadum, O. *Constructing and Implementing Successful Expert Systems* Pulp Pap. 67, no. 3: 87-90, 92 (March 1993).

28. Ritala, R. K. *Knowledge-Based Diagnostics and Process Development on Paper Machines* Paper-Machine Diagnostics Sem. PB/103/CM/134 (Leatherhead), Paper no. 1: 17p. Pira; March 19-20, 1991

29. Herdman, P. T. *Expert-System Application* Paper-Machine Diagnostics Sem. PB/103/CM/134 (Leatherhead), Paper no. 12: 9 p. Pira; March 19-20, 1991

30. Spence, M.; Danielson, K.; Ying, Y.; Rao, M. *On-Line Advisory Expert System Development at Daishowa [Canada Co. Ltd.'s] Peace River Pulp [Peace River, Alberta]* CPPA Annu. Mtg. (Montreal) Preprints Vol. 79A: 143-148 (Jan. 26-29, 1993).

31. Williamson P. N. *Pitch Expert Saves Money for Canada's Kraft Mills.* Pulp Pap. Can. 93, no. 11: 12-13 (Nov. 1992).

32. Grace, T. *Recognizing Smelt/Water Emergencies.* PIMA 74, no. 6: 55-56 (June 1992).

33. Brooks, T. R.; Edwards, L. L. Real-Time, Model-Based Expert System for Multiple-Effect Evaporators. : Tappi J. 75, no. 11: 131-135 (Nov. 1992).

34. Evans, S.; Nuyan, S.; Amyot, J. R.. Expert System Diagnosis in CD [Cross-Directional] Weight Control. Pulp Pap. Can. 93, no. 6: 49-52 (June 1992).

35. Controlling the Future Pulp Mill. Pulp Pap. (Editorial Suppl.): 17-22 (1992). Engl.

36. Racine, J. P.; Borsje, H. J. Expert Systems for Detecting Leaks in Recovery-Boiler Tubes Tappi J. 75, no. 6: 147-152 (June 1992).

37. Schaafstal, A.; Bogers, H. *Knowledge-Based Systems for PM [Paper Machine] Diagnostics* Pap. Technol. 33, no. 2: 13-18 (Feb. 1992)

38. Frerichs, D. K. *Artificial Intelligence for Supervisory Control and Operator Decision Support* Tappi J. 75, no. 6: 138-141 (June 1992).

39. Rao, M.; Corbin, J *Intelligent System for Batch Digester Operation* CPPA Ann. Mtg. (Montreal) Preprints 78B: B81-85 (Jan. 30-31, 1992).

40. Risto, L.; Jorma, P *Computer-Based Expert Systems in the Process Upgrading of Waste-Water Treatment Plants in the Pulp and Paper Industry* EUCEPA 24th Conf. Proc. (Stockholm), Control, Maintenance, & Environ.: 447-453 (May 8-11, 1990).

41. Racine, J. P.; Borsje, H. J. *Use of Expert Systems for Recovery-Boiler Tube-Leak Detection* Process Control Conf. (Atlanta) Notes: 49-58 (TAPPI; March 3-5, 1992).

42. Smith, D. B.; Edwards, L. L.; Damon, R. A *Development and Application of a Real-Time Recovery-Boiler Expert System* Tappi J. 74, no. 11: 93-96 (Nov. 1991).

43. Duever, T. A.; McIlwraith, G. D.; Hrymak, A. N.; Taylor, P. A.; Whiting, P.; Read, E. W *Application of Expert Systems to TMP Refiner Control* CPPA Ann. Mtg. (Montreal) Preprints 77B: B259-267 (Jan. 31-Feb. 1, 1991).

44. Ritala, R *Knowledge-Based Diagnostics on Paper Machines pap. Technol. 32, No. 9:21-24(1991).*

45. Windon, D. R., Jr.; Cook, D. F.; Massey, J. G. *Integrating the Art and Science of Papermaking in an Expert System* Tappi J. 74, no. 9: 85-89 (Sept. 1991).

46. Grigoriu, M. M.; Clemett, A. *Expert Systems Increase Paper-Industry Competitiveness* TAPPI Papermakers Conf. (Seattle) Proc.: 19 (April 8-10, 1991).

47. Tyagi R. D. and Du, Y. G. Operational determination of the activated sludge process using neural networks. Water Sci. Technol. 26, no. 9-11: 2461-2464(1992).

48. Schweiger, C. A. and Rudd, J. B. Prediction and control of paper-machine parameters using adaptive technologies in process modeling. TAPPI Process Control Symposium (New Orleans) Proceedings: 145-154 (TAPPI; Feb. 7-10, 1994).

49. Sasaki, T. XIV IMEKO World Congress: New Measurements – Challenges and Visions, XB: Actuator Systems in Paper Machine: 139-144 (1997).

50. Haataja, K., Leiviska, K., and Suinen, R. XIV IMEKO World Congress: New Measurements – Challenges and Visions, XB: Actuator Systems in Paper Machine: 139-144 (1997).

51. Baines, G. H., Hayes, R. L., Stabell, J. L. "Predicting boiler emissions with neural networks" Tappi J. 80, no. 5: 57-61, 87, 95, 103(1997).

52. Briggs, S., Stapper, B., Drow, W. Predictive emissions monitoring system (PEMS) for a paper mill power boiler 1997 International Environmental Conference: 599-606, May 4, 1997.

53. Broeren, L. A., Smith, B. A., Conte, T. O, Stapley, C. Wastepaper VI Conference Proceedings (Paper Recycler, Pulp and Paper, Miller Freeman Inc.) Session: 2B, Paper No. 14: 25 p. (1995 Miller Freeman Inc.)

54. H. Wang and B Ohebande. On the application of neural networks modeling to a wet end chemical process in papermaking". Proceedings of IEEE Conference, 1995, pp. 657-662.

55. "Modeling of a papermaking process via genetic neural networks and first principle approaches". Wang, H., Borairi, M., Roberts, J. C. and H Xiao. Proceedings of 1997 IEEE International Conference on Intelligent Processing Systems, October 28-31, Beijing, China, pp. 584-588.

56. Neural networks in web break diagnosis of a newsprint machine". Miyanishi, T. and H. Shimada. Proceedings of 1997 TAPPI Papermakers Conference, Nashville TN, 605-612, (October 6-9, 1997.)

57. "Neural network model for a paper forming process". Scharcanski, J. and Dodson, C. Conference Record of the 1996 Annual Pulp and Paper Industry Technical Conference (IEEE Pulp and Paper Industry Committee), Paper No. 27:236-255(1996).

58. "Neural networks, expert systems, and simulation; some powerful tools at the service of the pulp and paper industry". Laperriere, L. Pretires de la Conference Technologique Estivale 1997, (CPPA), 121-125 (1997, CPPA). Fr.

59. "Achieving results in control methods." Kosunen, J.; Van Fleet, R.; Forslund, O. Paper Asia 13, no. 3: 26-28 (March 1997).

60. "Innovation at the interface: best of man and machine" J. Roberts. Pulp Paper Europe 1, No. 10:19-21 (Dec. 1996-Jan 1997).

61. "Introduction to artificial intelligence". O. Fadum. Process, quality, and information control in the worldwide pulp and paper industry (Pulp and Paper): 16-17 (1996; Miller Freeman, Inc.)

62. "Software for process analysis". Powell, R. E. 1996 Engineering Conference Proceedings: 617-620(September 16, 1996).

63. "Control of wood chip refining using neural networks". Kooi, S. B. L., Khorasani, K. Tappi J. no. 6:156-0162 (June 1992).

64. Rudd and Schweiger. Tappi J. 77, no. 11:201-208(November, 1994.)

65. "Application of feedforward neural networks and partial least squares regression for modeling kappa number in a continuous Kamyr digester". Dayal, B. S., MacGregor, J. F., Taylor, P. A., Kildaw, R., Marcikic, S. Pulp Paper. Can. 95, no. 1:26-32(January 1994).